

LITHUANIAN UNIVERSITY OF HEALTH SCIENCES
MEDICAL ACADEMY

Ingrida Pikūnienė

**VALUE OF MAGNETIC RESONANCE
IMAGING DEFINING EFFECT
OF DIFFERENT MODALITIES OF
NEOADJUVANT TREATMENT IN
PATIENTS WITH STAGE II AND III
RECTAL CANCER**

Doctoral Dissertation
Medical and Health Sciences,
Medicine (M 001)

Kaunas, 2025

The dissertation was prepared at the Department of Radiology, Faculty of Medicine, Medical Academy, Lithuanian University of Health Sciences, during the period of 2015–2024.

The dissertation is defended extramurally.

Scientific Consultant

Prof. Dr. Žilvinas Saladžinskas (Lithuanian University of Health Sciences, Medical and Health Sciences, Medicine – M 001).

The dissertation is defended at the Medical Research Council of the Lithuanian University of Health Sciences:

Chairperson

Prof. Dr. Giedrius Barauskas (Lithuanian University of Health Sciences, Medical and Health Sciences, Medicine – M 001).

Members:

Assoc. Prof. Dr. Inga Zaborienė (Lithuanian University of Health Sciences, Medical and Health Sciences, Medicine – M 001);

Prof. Dr. Kristina Žvinienė (Lithuanian University of Health Sciences, Medical and Health Sciences, Medicine – M 001);

Assoc. Prof. Dr. Jonas Jurgaitis (Klaipėda University, Medical and Health Sciences, Medicine – M 001);

Assoc. Prof. Dr. Mindaugas Račkauskas (Florida University, Medical and Health Sciences, Medicine – M 001).

The dissertation will be defended at the open session of the Medical Research Council of the Lithuanian University of Health Sciences on the 7th of February 2025 at 12 a.m. in the auditorium No. A-202 of the Centre for the Advanced Pharmaceutical and Health Technologies of the Lithuanian University of Health Sciences.

Address: Sukilėlių 13, LT-50162 Kaunas, Lithuania.

LIETUVOS SVEIKATOS MOKSLŲ UNIVERSITETAS
MEDICINOS AKADEMIJA

Ingrida Pikūnienė

**MAGNETINIO REZONANSO
TOMOGRAFIJOS VERTĖ NUSTATANT
SKIRTINGŲ NEOADJUVANTINIO
GYDYMO METODŲ EFEKTĄ II IR III
STADIJOS TIESIOSIOS ŽARNOS VĖŽIU
SERGANTIEMS PACIENTAMS**

Daktaro disertacija
Medicinos ir sveikatos mokslai,
medicina (M 001)

Kaunas, 2025

Disertacija rengta 2015–2024 metais Lietuvos sveikatos mokslų universiteto Medicinos akademijos Medicinos fakulteto Radiologijos klinikoje.

Disertacija ginama eksternu.

Mokslinis konsultantas

prof. dr. Žilvinas Saladžinskas (Lietuvos sveikatos mokslų universitetas, medicinos ir sveikatos mokslai, medicina – M 001).

Disertacija ginama Lietuvos sveikatos mokslų universiteto Medicinos mokslo krypties taryboje:

Pirmininkas

prof. dr. Giedrius Barauskas (Lietuvos sveikatos mokslų universitetas, medicinos ir sveikatos mokslai, medicina – M 001).

Nariai:

doc. dr. Inga Zaborienė (Lietuvos sveikatos mokslų universitetas, medicinos ir sveikatos mokslai, medicina – M 001);

prof. dr. Kristina Žvinienė (Lietuvos sveikatos mokslų universitetas, medicinos ir sveikatos mokslai, medicina – M 001);

doc. dr. Jonas Jurgaitis (Klaipėdos universitetas, medicinos ir sveikatos mokslai, medicina – M 001);

doc. dr. Mindaugas Račkauskas (Floridos universitetas, medicinos ir sveikatos mokslai, medicina – M 001).

Disertacija bus ginama viešame Lietuvos sveikatos mokslų universiteto Medicinos mokslo krypties tarybos posėdyje 2025 m. vasario 7 d. 12 val. Lietuvos sveikatos mokslų universiteto Naujausių farmacijos ir sveikatos technologijų centro A-202 auditorijoje.

Disertacijos gynimo vietos adresas: Sukilėlių pr. 13, LT-50162 Kaunas, Lietuva.

CONTENTS

ABBREVIATIONS	7
INTRODUCTION.....	9
The aim of the study.....	11
The objectives of the study.....	11
The novelty of the study.....	11
1. LITERATURE REVIEW.....	13
1.1. Epidemiology and incidence	13
1.2. Etiology and risk factors for colorectal cancer.....	15
1.3. Diagnosis of rectal cancer	16
1.3.1. Conventional magnetic resonance imaging.....	18
1.3.2. Functional magnetic resonance imaging	21
1.3.2.1 Diffusion-weighted magnetic resonance imaging and apparent diffusion coefficient.....	22
1.3.2.2. Dynamic contrast-enhanced magnetic resonance imaging	23
1.4. The role of multidisciplinary team in management of patients with colorectal cancer.....	23
1.5. Staging of rectal cancer	25
1.5.1. T staging	26
1.5.2. N staging.....	27
1.6. Prognostic factors for rectal cancer.....	28
1.6.1. Mesorectal fascia and circumferential resection margin	28
1.6.2. Extramural vascular invasion	29
1.7. Restaging after neoadjuvant treatment.....	31
1.8. Response assessment after neoadjuvant treatment.....	33
1.8.1. Magnetic resonance imaging volumetry and tumor volume reduction rate	33
1.8.2. Magnetic resonance imaging-assessed tumor regression grade	34
1.9. Interpretation of magnetic resonance imaging and structured reporting.....	36
1.10. Treatment of rectal cancer	37
2. METHODS	42
2.1. Ethics	42
2.2. Study population and design	42
2.3. Inclusion and exclusion criteria of the study population.....	43
2.4. Diagnosis and treatment	43
2.4.1. Magnetic resonance imaging protocol.....	43
2.4.2. Interpretation of magnetic resonance images	45
2.4.2.1. Tumor location, size, and morphology.....	45
2.4.2.2. Relationship to the mesorectal fascia	47
2.4.2.3. Relationship to the anterior peritoneal reflection	48
2.4.2.4. T staging	50
2.4.2.5. Extramural vascular invasion	52
2.4.2.6. Lymph nodes and tumor deposits.....	52

2.4.2.7. Evaluation and measurement of apparent diffusion coefficient by magnetic resonance imaging	54
2.4.2.8. Magnetic resonance imaging volumetry and tumor volume reduction rate	56
2.4.2.9. Magnetic resonance imaging-assessed tumor regression grading	57
2.5. Statistical analysis	58
3. RESULTS.....	60
3.1. Characteristics of the study population	60
3.2. Location of the tumor	60
3.3. Characteristics of the tumor stage	60
3.3.1. T and N stage	60
3.3.2. Associations of tumor T and N stage with pathological results.....	61
3.4. Involvement of mesorectal fascia and circumferential resection margin	63
3.5. Extramural vascular invasion and extramural vascular invasion score.....	64
3.6. Diffusion-weighted imaging and apparent diffusion coefficient.....	66
3.6.1. Apparent diffusion coefficient and T stage before treatment.....	66
3.6.2. Apparent diffusion coefficient and N stage before treatment.....	67
3.6.3. Apparent diffusion coefficient and T stage after treatment	69
3.6.4. Apparent diffusion coefficient and N stage after treatment.....	71
3.6.5. Associations between apparent diffusion coefficient and extramural vascular invasion	73
3.7. Magnetic resonance imaging volumetry and tumor volume reduction rate.....	74
3.8. Magnetic resonance imaging-assessed tumor regression grade.....	77
3.9. Magnetic resonance imaging volumetry and tumor volume reduction rate between good and bad responders.....	77
4. DISCUSSION.....	80
4.1. T and N staging and restaging in rectal cancer.....	80
4.2. Diffusion-weighted magnetic resonance imaging for evaluating rectal cancer and locoregional lymph nodes.....	81
4.3. Mesorectal fascia as a prognostic indicator.....	82
4.4. Extramural vascular invasion as a prognostic indicator	83
4.5. Interplay between magnetic resonance imaging volumetry, tumor volume reduction rate, and tumor regression grade	84
CONCLUSIONS	87
LIMITATIONS OF THE STUDY.....	88
PRACTICAL RECOMMENDATIONS	89
SANTRAUKA.....	90
REFERENCES	114
LIST OF SCIENTIFIC PUBLICATIONS	130
LIST OF PRESENTATIONS IN SCIENTIFIC CONFERENCES.....	132
APPENDICES	134
CURRICULUM VITAE	142
PADĚKA	143

ABBREVIATIONS

ADC	– apparent diffusion coefficient
AJCC	– American Joint Committee on Cancer
AUC	– area under the curve
CEA	– carcinoembryonic antigen
CRC	– colorectal cancer
cCR	– complete clinical response
CRM	– circumferential resection margin
CT	– computed tomography
CTx	– chemotherapy
CRT	– chemoradiotherapy
DCE	– dynamic contrast-enhanced
DRE	– digital rectal examination
DWI	– diffusion-weighted imaging
ERUS	– endoscopic rectal ultrasound
EMVI	– extramural vascular invasion
ESGAR	– European Society of Gastrointestinal and Abdominal Radiology
ESMO	– European Society for Medical Oncology
FOV	– field of view
FOLFOX	– fluorouracil, leucovorin, and oxaliplatin
HDI	– Human Development Index
ICD-O	– International Classification of Diseases for Oncology
IV	– intravenous
LVI	– lymphovascular invasion
M	– distant metastasis
MDT	– multidisciplinary team
MR	– magnetic resonance
MRI	– magnetic resonance imaging
MRF	– mesorectal fascia
mrT	– MRI-assessed T stage before treatment
mrN	– MRI-assessed N stage before treatment
mrTRG	– MRI-assessed tumor regression grade
N	– lymph node/nodal stage
NPV	– negative predictive value
OS	– overall survival
PET	– positron emission tomography

PET-CT	– positron emission tomography-computed tomography
pLVI	– pathological lymphovascular invasion
pTRG	– pathological tumor regression grade
pCRM	– pathological circumferential resection margin
pCR	– pathological complete response
PPV	– positive predictive value
ROC	– receiver operating characteristic curve
ROI	– region of interest
RT	– radiotherapy
RSNA	– Radiological Society of North America
SAR	– Society of Abdominal Radiology
ymrT	– MRI-assessed T stage after treatment
ymrN	– MRI-assessed N stage after treatment
yMRF	– MRI-assessed mesorectal fascia after treatment
ypT	– pathological T stage after treatment
ypN	– pathological N stage after treatment
T	– tumor T stage
T1W	– T1 weighted
T2W	– T2 weighted
TE	– echo time
TEM	– transanal endoscopic microsurgery
TNM	– Tumor Node Metastasis classification system
TME	– total mesorectal excision
TR	– repetition time
TVRR	– tumor volume reduction rate
UICC	– Union for International Cancer Control

INTRODUCTION

Colorectal cancer (CRC) is a major global health problem with a high rate of incidence and mortality. As the third most common cancer globally and the second in terms of cancer-related deaths, it substantially burdens healthcare systems and society [1]. It ranks second among cancers in women and third among cancers in males. There were more than 1.9 million new cases of CRC in 2022 worldwide [2]; meanwhile, in Europe, there were more than 538,000 new CRC cases [3]. In Europe, CRC ranks among the top cancer types, affecting both men and women, making it a critical health issue for the region.

Magnetic resonance imaging (MRI) has become known as the primary diagnostic technique for the early stage of rectal cancer and is essential for precise diagnosis and treatment planning. It is essential to categorize patients based upon their risk levels and treatment requirements. This can be done by finding important factors that could cause a local recurrence and figuring out if neoadjuvant therapy is needed. The importance of MRI in precise disease staging has been emphasized by numerous studies, which have also highlighted key prognostic factors for evaluating and presenting findings [5–7].

Initial MRI has emerged as the primary staging method for surgical planning and categorization of patient groups to facilitate more effective neoadjuvant therapy [6, 8]. Its principal objectives in rectal cancer diagnosis encompass localizing the tumor, assessing its invasion beyond the bowel wall, and evaluating its involvement in significant anatomical structures such as the mesorectal fascia (MRF), peritoneum, and pelvic organs [8]. MRI is also essential for identifying significant prognostic factors such as lymph node metastases, MRF involvement and extramural vascular invasion (EMVI) [9]. This thorough assessment offers a complete prognostic profile for malignancies, allowing clinicians to classify patients into low-, intermediate-, or high-risk categories. This evaluation guides treatment choices, from surgery exclusively for low-risk tumors to neoadjuvant radiation or chemoradiotherapy (CRT) for aggressive high-risk cases [5, 7, 10].

As the treatment for rectal cancer has become increasingly personalized, the role of radiologists has grown in significance. The heightened focus on organ preservation has placed a greater responsibility on radiologists to monitor patients undergoing neoadjuvant treatment. MRI, along with endoscopy, is crucial for assessing local tumor response to neoadjuvant therapy. The restaging process determines whether patients need conventional surgical intervention or can be treated with conservative methods, such as a “watch-and-wait” strategy [11, 12].

Various imaging techniques, reporting requirements, and staging templates have been created to assist radiologists in this essential job [13]. Moreover, new diagnostic grading systems have been created to assist radiologists in assessing local tumor response following neoadjuvant therapy [13, 14]. The main objective of these templates and grading systems is to enhance consistency in radiological reporting, therefore ensuring a consistent and evidence-based methodology for patient management. However, challenges and pitfalls exist regarding the application and clinical implementation [15, 16].

Research indicates that the experience level of a radiologist significantly affects diagnostic performance, which in turn influences multidisciplinary team (MDT) decisions and treatment outcomes [17]. Many new diagnostic methods, such as response-grading systems, have been tested by only small groups of expert radiologists before being included in the guidelines [13, 18, 19]. The reproducibility and accuracy of these tools in everyday clinical practice among a broader group of radiologists still need to be studied further. Furthermore, there is limited information on how effectively staging guides and templates, such as those released by the European Society of Gastrointestinal and Abdominal Radiology (ESGAR), are integrated into routine clinical practice, their clinical effectiveness, and any practical limitations that warrant further investigation [20, 21].

Adequate local tumor staging is essential for guiding treatment and assisting surgeons in planning effective resection strategies. MRI gives surgeons crucial information about tumor characteristics, enabling radiation oncologists to define target areas for radiotherapy, which can significantly influence treatment outcomes [22]. It is still difficult to provide accuracy and precision in the radiological reporting of rectal cancer, even with progress in imaging technology [23]. In response to these issues, several leading radiography organizations, such as the ESGAR, the Society of Abdominal Radiography (SAR), and the Radiological Society of North America (RSNA), have created standardized reporting templates [24, 25]. These templates guarantee the systematic and consistent performance of the essential aspects of staging. They align with the tumor node metastasis (TNM) classification system established by the American Joint Committee on Cancer (AJCC) and the Union for International Cancer Control (UICC) [24, 25]. Although the TNM system categorizes patients based on local tumor stage, lymph node involvement, and distant metastases, it was initially created from a pathological perspective. Consequently, radiologists cannot forget the use of TNM concepts in imaging interpretation and reporting.

Recent advancements in rectal cancer staging have introduced innovative concepts, such as EMVI or sigmoid take-off [26]. Nonetheless, achieving

consistent application of these concepts in clinical reporting is problematic, affected by the complex anatomy of the rectum and the dynamic nature of clinical recommendations.

Improving the quality and consistency of radiological reporting is essential for accurate diagnosis and effective treatment of rectal cancer [27, 28]. Healthcare professionals can more effectively address the critical issue of CRC through ongoing education and the standardization of reporting practices [29, 30]. The improvement of imaging techniques and reporting methodologies may significantly enhance patient outcomes and resolve the challenges presented by this widespread disease.

The aim of the study

The aim of the study was to determine changes in magnetic resonance imaging parameters and their diagnostic value in patients with stage II and III rectal cancer treated with different neoadjuvant treatment regimens: chemotherapy with FOLFOX without radiation and standard chemoradiotherapy treatment.

The objectives of the study

1. To evaluate the role of magnetic resonance imaging in downstaging tumor (T) and lymph nodes (N) after neoadjuvant treatment in the chemotherapy and chemoradiotherapy groups.
2. To estimate the apparent diffusion coefficient value of diffusion-weighted MRI in rectal tumor and pathological lymph nodes, and to evaluate if this parameter is of value in determining response to treatment.
3. To evaluate changes in mesorectal fascia involvement and extramural vascular invasion after treatment in the chemotherapy and chemoradiotherapy groups, and to estimate the value of these parameters as noninvasive prognostic factors.
4. To analyze changes in the tumor volume reduction rate and magnetic resonance imaging-assessed tumor regression grade before and after treatment in the chemotherapy and chemoradiotherapy groups, and to estimate their value as noninvasive prognostic factors.

The novelty of the study

According to the literature, MRI, over the last two decades, became a highly effective method for staging patients with rectal cancer. As a result, MRI is now considered the gold standard for both local and regional staging

and restaging in rectal cancer according to major international guidelines. MRI-assessed factors such as tumor stage, lymph node involvement, and surgical resection area extension classify patients as low, intermediate, or high risk. This guides decisions on immediate surgery or the need for neoadjuvant radiation and CTx to decrease the tumor size. A meta-analysis has reported that MRI has an overall sensitivity and specificity of 94 % and 85 %, respectively, for determining the T stage of rectal cancer. However, MRI accuracy in N staging is more limited, with sensitivity and specificity ranging from 58 % to 77 % and from 62 % to 74 %, respectively [31]. New research suggests that DWI might be better than regular MRI at detecting tumors and certain differences in the histopathology of cells and microvasculature [32].

This prospective study involved patients diagnosed with stage II and III rectal cancer based on radiological examinations seeking to evaluate tumor and nodal downstaging in two neoadjuvant treatment groups: FOLFOX CTx and standard CRT. In addition to the tumor-node-metastasis (TNM) system staging and restaging, it was assessed the significance of the ADC in functional MRI DWI sequences and compared results between the neoadjuvant treatment groups [33]. The study also investigated the independence of ADC values for tumors and lymph nodes and the differentiation between healthy and involved lymph nodes. The study also aimed to determine the ability of DWI to reflect specific histopathological differences between metastatic and non-metastatic lymph nodes. To assess the effectiveness of both CTx and CRT groups, MRI metrics were compared by measuring tumor volume, TVRR, and examining the correlation between MRI-assessed tumor regression grade (mrTRG) and pathological tumor regression grade (pTRG). Finally, EMVI was evaluated, exploring its positivity, score, and downstaging in both treatment groups.

Understanding metrics such as tumor volume, tumor volume reduction rate, and magnetic resonance tumor regression grade is essential for effective rectal cancer care, enabling a multidisciplinary approach that enhances collaboration among radiologists, surgeons, medical oncologists, radiation oncologists, and pathologists. With a comprehensive understanding of tumor characteristics and its response to treatment, each specialist can make more informed decisions.

1. LITERATURE REVIEW

1.1. Epidemiology and incidence

CRC, positioned as the third most prevalent and the second most lethal cancer globally, accounted for approximately 1.9 million new cases and 900,000 deaths in 2022 [2]. The occurrence of CRC is more frequent in highly developed nations and is on the rise in countries with lower and middle incomes, partly due to changes in lifestyle and diet. However, by adopting healthy behaviors, individuals can significantly reduce their risk of developing CRC. Additionally, there is an increasing trend in the incidence of CRC in younger populations [34]. The substantial number of CRC cases worldwide represents a significant challenge to global public health. Enhancing awareness about CRC is vital for fostering healthy behaviors, developing innovative CRC treatment approaches, and establishing widespread screening initiatives, all essential for diminishing the future health burden and mortality associated with CRC. CRC is a diverse condition, with various subtypes affecting prognosis and treatment effectiveness. Therefore, precisely classifying CRC subtypes is crucial for fundamental research and clinical outcomes.

Analyses of the incidence and mortality rates from CRC frequently summarize statistics from colon, rectal, and occasionally anal cancers. These are categorized under codes C18–C21 by the International Classification of Diseases for Oncology (ICD-O) [35].

Globally, the prevalence of CRC has been escalating at a concerning pace. In 2022, an estimated 1.99 million new cases of CRC and 0.97 million deaths due to CRC were reported, constituting 9.6 % of all new cancer cases (19.97 million) and 9.3 % of cancer-related deaths (9.04 million). CRC is the third leading cause of cancer-related mortality in both sexes, with an estimated 1 069,446 deaths in males and 856,979 in females in 2022 [3].

According to estimates from GLOBOCAN 2022 [3], in Europe, there were 538,262 CRC cases in 2022, both sexes, 289,049 males and 249,213 females. New rectal cancer cases accounted for 181,701, and deaths accounted for 83,466 cases in 2022. Within the Lithuanian population, in 2022, an estimated 1506 new cases of CRC and 938 deaths due to CRC were reported, constituting 16,413 of all new cancer cases (Fig. 1.1.1) [3].

	Males	Females	Both sexes
Population	1 231 601	1 430 103	2 661 704
Incidence*			
Number of new cancer cases	9 245	7 168	16 413
Age-standardized incidence rate	391.3	224.0	287.9
Risk of developing cancer before the age of 75 years (cum. risk %)	38.8	22.2	29.3
Top 3 leading cancers (ranked by cases) [†]	Prostate Lung Colorectum	Breast Colorectum Corpus uteri	Prostate Breast Colorectum
Mortality[‡]			
Number of cancer deaths	4 639	3 710	8 349
Age-standardized mortality rate	181.6	88.7	125.0
Risk of dying from cancer before the age of 75 years (cum. risk %)	19.7	9.7	13.9
Top 3 leading cancers (ranked by deaths) [†]	Lung Prostate Colorectum	Breast Colorectum Lung	Lung Colorectum Stomach
Prevalence*			
5-year prevalent cases	28 314	22 582	50 896



Top 5 most frequent cancers**

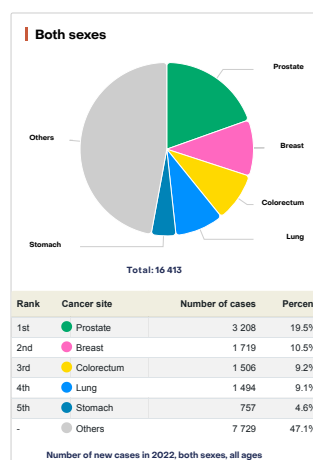
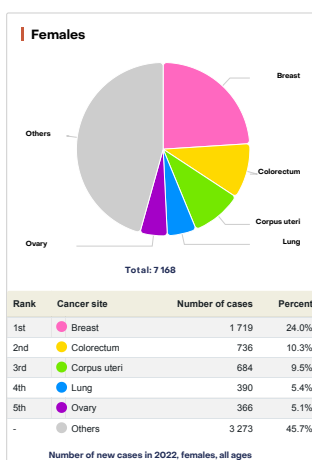
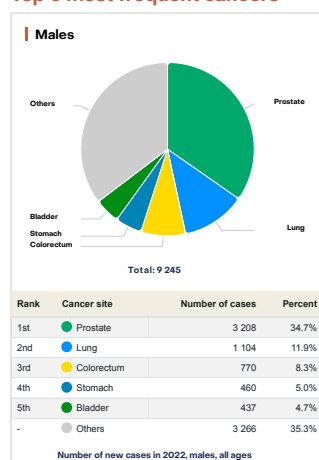


Fig. 1.1.1. Source: Globocan 2022. Number of new cancer cases in 2022 in Lithuania [3].

This figure is adapted from a review by GLOBOCAN, 2022 [3].

The distribution of CRC cases based on anatomical location shows that the rectum and sigmoid colon rank first. In 2022, there were a significant number of new cases of colon and rectal cancer reported worldwide. This information is illustrated in Fig. 1.1.2.

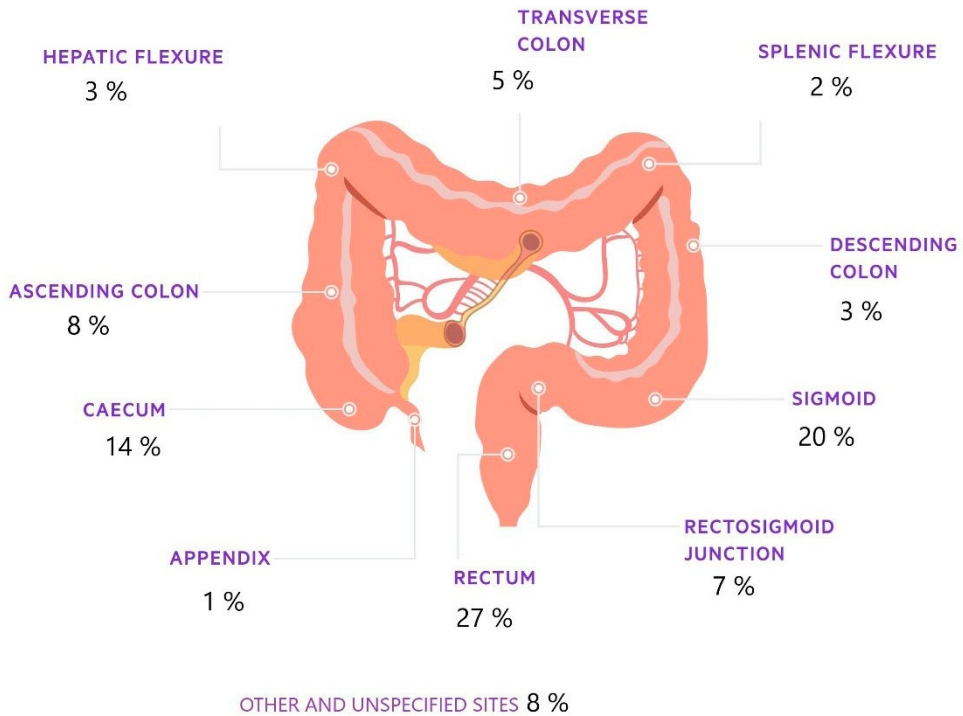


Fig. 1.1.2. Distribution of colorectal cancer cases based on the location of the anatomy. World new cases of colon and rectum cancer in 2022 [3].

CRC is associated with countries with higher incomes and socioeconomic progress. This association is obvious in the high incidence rates followed in North America, Western Europe, and Australia. Conversely, Africa and Central America have the lowest incidence rates [3, 37]. These incidence rate variations mirror the adverse dietary and lifestyle habits prevalent in areas with a higher Human Development Index (HDI) [38]. An increasing trend is observed in CRC incidence rates in previously low-HDI and economically disadvantaged countries, including parts of Eastern Europe. This increase is simultaneous with wide-spreading Western lifestyles and diets in these areas [34, 38].

1.2. Etiology and risk factors for colorectal cancer

The majority of CRC cases, including rectal cancer, are sporadic, making up about 70 % of diagnoses, with an average age of diagnosis at 50 years or older. A small percentage of patients (10 %) show an actual genetic agreement, setting a higher risk for those diagnosed before age 50, while 20 % exhibit familial clustering without an apparent inherited syndrome [39].

Approximately 5 % of CRC cases are associated with familial adenomatous polyposis and Lynch syndrome (hereditary non-polyposis CRC), the most recognized cancer syndromes [39, 40]. Risk factors include personal or family history of CRC [41], adenomatous polyps [42], and particular types of dysplasia, which significantly increase the risk of synchronous or metachronous cancers and warrant close monitoring. Inflammatory bowel disease, especially ulcerative colitis, raises cancer risk, with an incidence of 0.5 % per year occurring 10 to 20 years after diagnosis, increasing to 1 % per year subsequently; by the fourth decade, the probability of developing CRC may reach 30 % [43]. Epidemiological analyses indicate that environmental and lifestyle factors play a significant role in strongly influencing CRC risk, with obesity, red and processed meat consumption, and tobacco use linked to colon cancer. In contrast, protective factors include a healthy diet, physical workouts, and some medications, such as aspirin and nonsteroidal anti-inflammatory drugs [44, 45].

In addition to these factors, gender also influences CRC risk and presentation. Men tend to have higher mortality rates from CRC compared to women [46]. Modifiable lifestyle and dietary choices are crucial in reducing the risk of CRC. The supervision of a healthy weight, regular workouts, tobacco avoidance, alcohol consumption limitations, and a nutritious diet are all essential practices for prevention. Encouraging these healthy habits is essential for reducing the risk of CRC and managing the disease, emphasizing a significant influence of lifestyle choices on overall health [47].

1.3. Diagnosis of rectal cancer

Rectal cancer poses a significant public health challenge, primarily due to its high incidence and mortality rates [3]. However, the role of MRI in early detection is a beacon of hope for improving patient outcomes. Advanced imaging techniques, with MRI at the forefront, are crucial in this process [48, 49]. MRI is a key tool for the diagnosis, staging, and treatment planning of CRC, particularly in cases involving rectal tumors [5, 6, 20, 50].

MRI has become a gold standard for locoregional staging in rectal cancer, providing highly detailed images of soft tissues [4, 6]. This precision allows for an accurate assessment of tumor characteristics, including the depth of invasion and relationship to adjacent structures. Such precise locoregional staging is fundamental as it significantly impacts treatment decisions and potential surgical options [6, 8, 51]. MRI precision is particularly valuable in evaluating the expansion of rectal tumors, aiding in the differentiation between layers of the intestinal wall and determining whether the cancer has spread to surrounding tissues and organs.

In the diagnostic way for CRC, MRI is often used next to other imaging modalities. While initial diagnoses usually involve endoscopic examinations, including rigid sigmoidoscopy and colonoscopy, MRI can provide additional information that is decisive for staging and surgical planning (Fig. 1.3.1) [52–54]. For rectal cancer cases, mainly, MRI is mandatory as it helps in identifying candidates for specific surgical approaches such as transanal endoscopic microsurgery (TEM). TEM is a minimally invasive method that can be employed when the tumor is localized, making accurate pre-surgical staging via MRI essential. MRI can identify the size and location of the tumor, as well as any potential spread, which is crucial for determining if the patient is a suitable candidate for this less invasive surgical approach [55].

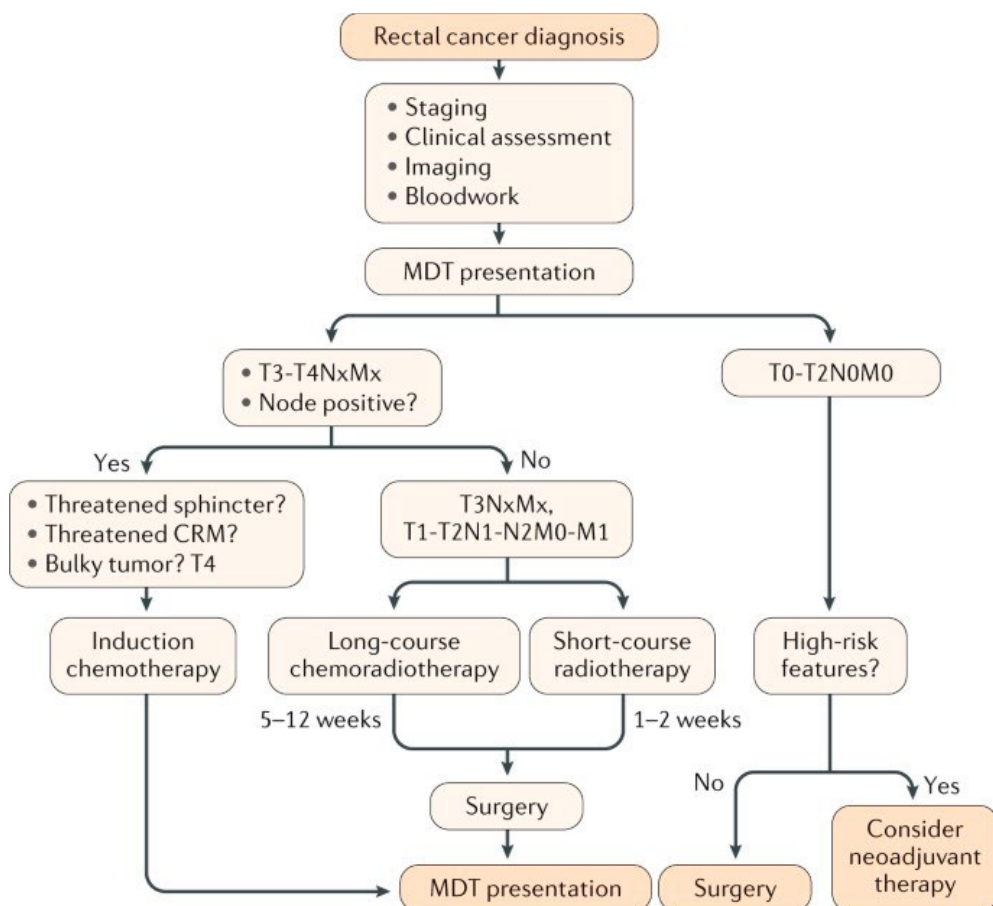


Fig. 1.3.1. Rectal cancer diagnosis [52, 53].

This figure is adapted from a review by European Society for Medical Oncology (ESMO) Guidelines, 2020 [62].

Additionally, MRI ability to visualize lymph nodes and evaluate for metastases is the main point in determining the overall prognosis and treatment strategy for patients [9, 56]. By offering a non-invasive method to gather critical information about tumor spread, MRI aids clinicians in making informed decisions regarding CTx, radiation therapy, and surgical interventions.

By implementing MRI in the diagnostic and staging processes, we are aligning with the guidelines set by the UICC [24, 25]. These guidelines rely on the TNM classification system, where the depth of primary tumor invasion (T), lymph node involvement (N), and distant metastasis (M) are critical components in accurately staging the cancer. MRI plays a crucial role in evaluating the T stage, assessing how far the cancer has invaded the rectal wall and indicating whether it has extended to adjacent organs [57, 58]. This alignment with global best practices should instill confidence in our approach.

As the rate of CRC continues to increase, especially among younger populations, the demand for reliable diagnostic methods like MRI becomes even more critical [39, 59]. Increased awareness of rectal symptoms and the importance of timely imaging can lead to earlier diagnoses and improved prognoses [59, 60].

1.3.1. Conventional magnetic resonance imaging

MRI is progressively recognized as the gold standard imaging technique for staging rectal cancer, which is pivotal in guiding patient management and treatment pathways [4–6, 8]. This advanced imaging modality provides unparalleled detail and clearness, enabling precise assessment of the tumor size, location, extent, and relationship to surrounding structures [4, 8, 21]. High-resolution MRI images allow clinicians to develop a more targeted and individualized view of patient care, significantly influencing decisions regarding surgery, CTx, and radiation therapy. As such, the accuracy and detail provided by MRI are invaluable in optimizing patient outcomes and adaptive treatment plans to the specific characteristics of each tumor [61, 62].

Understanding the normal anatomy of the rectal region is essential for accurate cancer staging (Table 1.3.1.1). Knowledge of the intricate details of pelvic anatomy, including the various layers of the rectal wall, surrounding tissues, and adjacent organs, is crucial for identifying the precise location and extent of cancerous lesions [58, 62, 63]. Familiarity with the terms used in rectal cancer staging, such as T (tumor), N (nodes), and M (metastases), along with the definitions of local invasion and lymph node involvement, is vital for interpreting MRI findings correctly. This understanding aids in distinguishing between different stages of the disease, assessing the likelihood of successful surgical resection, and predicting patient prognosis [9, 54, 64].

Table 1.3.1.1. Rectal and perirectal structures

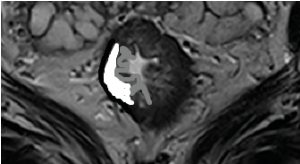
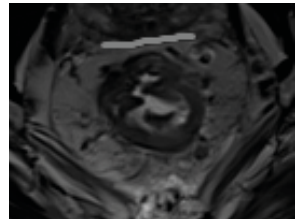


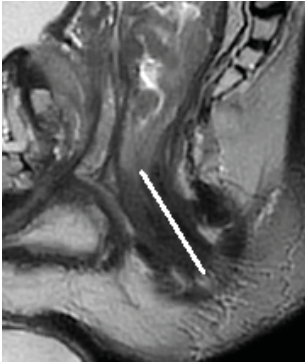
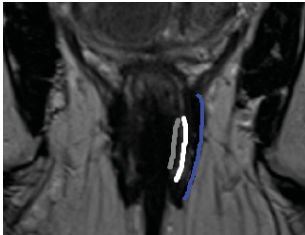
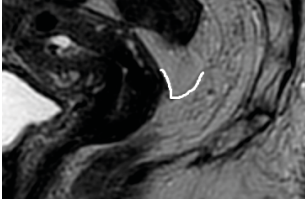
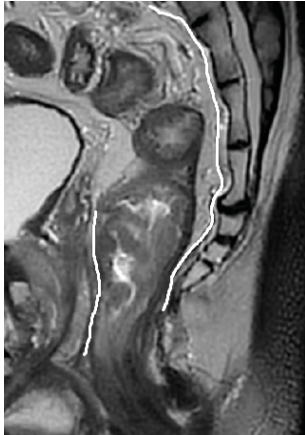
Term	Definition	Representative figure
Rectal wall	<p>The muscularis mucosae layer is the fine innermost low signal intensity layer (grey area)</p> <p>The submucosal layer is deeper to the mucosa, is thicker, with higher SI internal structure (white area)</p> <p>The muscularis propria is the outer, low signal intensity layer (black area)</p>	
Denonvilliers' /rectoprostatic /rectovaginal fascia	<p>Anteroinferior component of the MRF (in men, it lies between the mesorectum and the prostate; in women, it is named the rectovaginal fascia and lies between the vagina and the rectum).</p> <p>The rectal wall frequently touches the Denonvilliers' fascia (grey line).</p>	
Anal verge	<p>Distal end of the anal canal (white line)</p>	
Anorectal junction	<p>The junction between the anal canal and the rectum (grey line)</p> <p>On MRI, the anorectal junction is identified as the area where the internal sphincter thickens and intensifies in signal on T2W imaging.</p> <p>This change, along with a noticeable shift in the rectum orientation due to the puborectalis muscle, marks the junction.</p> <p>If visualization is challenging, drawing an imaginary line between the lower margins of the sacral and pubic bones can help locate the anorectal junction.</p>	

Table 1.3.1.1 cont.

Term	Definition	Representative figure
Anal canal	<p>The lower section of the gastrointestinal track, which typically spans 3 to 5 cm in length (white line).</p> <p>There are two perspectives on defining the anal canal: from an anatomical standpoint, it stretches from the dentate line to the anal verge; surgically, it is considered to extend from the anorectal junction down to the anal verge.</p>	
Anal sphincter complex	<p>The inner circular sphincter consists of the internal sphincter smooth muscle and part of the rectum muscle in the anal canal (grey line).</p> <p>The intersphincteric space, filled with fat, divides the internal and external sphincters (white line).</p> <p>The external anal sphincter includes puborectalis and its own muscle fibers, facilitating anal control (blue line).</p>	
Anterior peritoneal reflection	<p>The anterior peritoneal reflection is a thin peritoneum layer that attaches to the front of the middle rectum. It separates the intra- and extraperitoneal sections of the rectum. Visually, at the point where the rectum lining meets the front, it forms a V-shape or gull-wing appearance. Sagittally, it can extend up to 1 cm below the seminal vesicles in men or 1 cm below the posterior vaginal fornix insertion to the cervix in women. It can be highly variable (white line).</p>	
Mesorectal fascia	<p>The mesorectal fascia is a thin T2W hypointense fascial layer surrounding the extraperitoneal portion of the rectum and its mesorectal fat. It is crucial for surgical planning as it defines the surgical plane for total mesorectal excision. This fascia merges anteriorly with the Denonvilliers' fascia and posteriorly with the presacral fascia. Superiorly, the mesorectal fascia ends at the anterior peritoneal reflection but extends posterolaterally to around the S2 level (white line).</p>	

Consistent reporting plays a vital role in improving the accuracy and consistency of radiology reports for MRI scans of rectal cancer. Using standardized terms, radiologists can guarantee that all essential information is reliably passed on to the physicians providing treatment. This includes details such as tumor size, location, depth of invasion, involvement of surrounding tissues, and presence of lymph nodes or distant metastases [13, 14, 54]. Standardized reports ease clear and efficient communication among the MDT members, including surgeons, oncologists, and radiation therapists [17]. Furthermore, this uniformity helps compare patient data over time and across different institutions, contributing to improved outcomes and more systematic research and analysis [65].

1.3.2. Functional magnetic resonance imaging

Functional MRI has transformed the evaluation of biological characteristics of tumors, marking significant progress in oncological imaging that could improve treatment effectiveness [66, 67]. The variety of biological factors within tumors can affect treatment responses. Cell density, blood supply, oxygen levels, and the extracellular matrix microenvironment all have critical roles to play. Unlike traditional volume measurements from conventional anatomical MRI T2W images, functional MRI provides a comprehensive “whole tumor biopsy.” This capability allows for detailed insights into the variability within a tumor, helps tailor treatment plans to match the patient’s specific tumor characteristics. Additionally, traditional MRI alterations frequently become apparent too late to guide early treatment decisions adequately. Conversely, functional MRI techniques have the potential to predict treatment outcomes in locally advanced rectal cancer, emphasizing the need for additional studies evaluating tumor diversity to predict early response to treatment [68].

As time progresses, there is an urgent need for more accurate imaging biomarkers to predict and assess responses to neoadjuvant CRT [66]. Such biomarkers allow better classification of patients into prognostic groups, facilitate an individualized treatment approach and potentially allow organ-sparing procedures that reduce surgical morbidity. Techniques like DWI and dynamic contrast-enhanced (DCE) MRI (DCE-MRI) are being explored for their ability to predict treatment responses while providing a deeper understanding of tumor biology compared to standard MRI sequences [33, 69, 70]. Ongoing research is actively investigating the clinical utility of functional MRI in predicting CRT outcomes and characterizing rectal cancer metabolically through *ex vivo* high-field MR spectroscopy. Ultimately, these efforts aim to enhance individualized treatment strategies, improve therapeutic outcomes, and minimize treatment toxicity for patients with rectal cancer.

1.3.2.1 Diffusion-weighted magnetic resonance imaging and apparent diffusion coefficient

DWI is a specialized MRI technique that tracks the movement of water molecules within tissues. The ADC, derived from DWI-MRI, inversely reflects tissue cellularity. In living tumor cells, water movement is restricted, resulting in reduced diffusion, while in dead or necrotic cells, water can move more freely. Therefore, higher cell density and alterations in the extracellular structure lead to a lower ADC, which correlates with the tumor density and malignancy level [32, 33, 69]. Radiotherapy causes tissue destruction that can be detected shortly after treatment begins, and the ADC ability to differentiate between viable tumor tissue and areas of inflammation or necrosis indicates its utility in monitoring the immediate effects of radiotherapy [71]. The ADC is a potential prognostic imaging marker in rectal cancer [72]. ADC values are usually represented as the mean ADC, which can be acquired from a single tumor slice, sample measurements, or by outlining the entire tumor volume on diffusion-weighted images. The latter method is preferred and yields the most reproducible results, becoming the standard for tumor ADC measurements. However, it is labor-intensive and time-consuming, hindering the transition of quantitative ADC measures from research to clinical practice [73].

Several studies have explored the role of DWI in evaluating the response to CRT in locally advanced rectal cancer, demonstrating ADC effectiveness in predicting and determining the pathological response to CRT [74, 75]. However, the ADC thresholds for establishing response have been set arbitrarily and require formal validation.

DWI in rectal cancer is a rapidly evolving area of research that is increasingly being integrated into clinical practice. Over the past decade, DWI has transitioned from qualitative visual interpretation to more sophisticated quantitative analysis methods. Current evidence supports DWI use in assessing tumor response to neoadjuvant treatment, particularly for visualizing residual tumors in post-radiation fibrosis [33, 76, 77]. While promising results for quantitative DWI analysis – especially regarding ADC – have emerged for predicting treatment responses and overall tumor prognosis, standardization of protocols is still needed [69, 78]. Until such standardization occurs, clinical evaluations of DWI should emphasize qualitative assessments, as its role in tumor and nodal staging remains less defined. Additionally, novel methods and new post-processing tools for DWI continue to be developed, and their clinical applicability will need to be established in the coming years.

1.3.2.2. Dynamic contrast-enhanced magnetic resonance imaging

DCE-MRI provides valuable insights into the characteristics of microvessels within tissues, including parameters such as blood flow, vessel wall permeability, and the composition of the extracellular space surrounding blood vessels. By targeting specific areas, DCE-MRI can effectively monitor the rate and extent of contrast agent absorption and elimination by the tissues. This capability reveals unique and distinctive patterns associated with cancerous tumors, characterized by a more rapid and pronounced uptake and release of contrast material, along with a higher signal intensity compared to healthy tissues [79]. These unique patterns underscore the impressive diagnostic capabilities of DCE-MRI.

The Ktrans parameter, derived from the Tofts pharmacokinetic model, quantitatively captures the rate of contrast agent influx, known as “wash-in”. Initial research has established a connection between DCE-MRI metrics and the extent of tumor vascularization, as indicated by measures such as microvessel density and the presence of vascular endothelial growth factor, a key player in blood vessel formation [80]. Several studies suggest that DCE-MRI metrics may also predict the tumor treatment response, particularly in shrinkage or downstaging [80–82]. Furthermore, DCE-MRI plays a crucial role in evaluating the tumor vascular environment, providing valuable insights into its biological aspects and potentially influencing how it reacts to radiation therapy. This emphasis on the role of DCE-MRI in cancer research keeps the audience informed and knowledgeable about the latest advancements in the field.

1.4. The role of multidisciplinary team in management of patients with colorectal cancer

The conception of MDT discussions in patient care has been a fundamental component of routine medical practice for several decades. This attitude has been applied across multiple clinical areas, emphasizing the integration of various specialties and additional services to improve patient outcomes [83]. Specifically in oncology, MDTs began as broad meetings that allowed for the review and discussion of cancer patients to optimize treatment strategies. Over time, as clinical practice evolved and became more specialized, these tumor boards were directed toward disease-specific discussions.

A specialized MDT is essential for effectively managing patients with CRC. The team should consist of critical professionals, including radiologists, gastroenterologists, surgeons, radiation oncologists, medical oncologists, and pathologists [84]. Regular meetings are important for reviewing all relevant

patient cases to ensure critical members are present when their expertise is needed. The MDT coordinator is essential in organizing these meetings and facilitating decision-making based on clinical guidelines. Furthermore, the team should lead audits to ensure the implementation of their decisions and review patient outcomes through standardized quality assurance measures.

For each patient, a comprehensive evaluation is necessary, which should include a careful history and physical examination, a digital rectal examination (DRE), complete blood count, liver and renal function tests, serum carcinoembryonic antigen (CEA) levels, and a computed tomography (CT) scan of the thorax and abdomen. This assessment helps determine the patient's functional status and identify any metastases. While positron emission tomography (PET) scans can provide further insights into the disease spread beyond the pelvis, current evidence does not support their routine use in every patient due to variable effectiveness (Table 1.4.1) [6, 54, 85, 86].

In older patients, factors such as increasing age, existing comorbidities, and reduced functional supplies are associated with a higher risk of early postoperative mortality and adverse reactions to radiotherapy (RT) and CTx. Therefore, realizing a formal geriatric assessment or utilizing screening tools to evaluate weakness in patients aged more than 70 years is advisable before proceeding with treatment plans [87, 88].

Diagnostic procedures such as rigid rectoscopy and preoperative colonoscopy up to the cecal pole are important for checking for synchronous colorectal tumors. A virtual colonoscopy or MR-enterocolonography should be performed when the obstruction prevents a routine colonoscopy. Suppose a preoperative colonoscopy has not been performed; it is recommended to complete the colonoscopy within six months following surgery to ensure a thorough evaluation and management of the patient's condition [89].

Endoscopic rectal ultrasound (ERUS) can be instrumental in determining treatment strategies for early-stage rectal cancer, particularly for T1 tumors suitable for TEM, by assessing whether the cancer is confined to the mucosa or submucosa. However, ERUS is less beneficial for more advanced stages [6, 54, 64].

For initial staging, PET-CT is not recommended as a standard procedure. However, it can be helpful alongside liver MRI and contrast-enhanced CT scans of the thorax, abdomen, and pelvis for identifying characteristics indicative of a higher metastasis risk, such as significant EMVI seen in MRI or elevated levels of CEA. While the effectiveness of PET-CT in evaluating the primary tumor and lymph nodes remains unconfirmed, it can help determine the goals of radiation therapy. Bone scans and brain imaging should be reserved for cases where symptoms indicate their need.

Table 1.4.1. Diagnostic work-up in rectal cancer [54]

Parameter	Method of choice
Location (distance from anal verge)	DRE/palpation Rigid sigmoidoscopy, flexible endoscopy
Morphological verification	Biopsy
cT stage Early Intermediate/advanced	ERUS, MRI MRI
Sphincter infiltration	MRI
cN stage	MRI (CT)
M stage	CT, MRI of the abdomen CT of the thorax PET-CT if extensive EMVI for other sites
Evaluation for all patients	MDT discussion

CT, computed tomography; DRE, digital rectal examination; EMVI, extramural vascular invasion; ERUS, endoscopic rectal ultrasound; EUA, examination under anesthesia; MDT, multidisciplinary team; MRI, magnetic resonance imaging; PET, positron emission tomography.

1.5. Staging of rectal cancer

MRI is recognized as the most precise method for the initial and follow-up staging of rectal cancer [5, 9, 21, 25, 31, 57, 58, 63]. The findings from the initial MRI (“primary staging”) play a crucial role in guiding clinical decisions, including whether to initiate neoadjuvant CRT or short-course radiotherapy before surgical intervention [20, 25]. The post-treatment MRI (“restaging”) is essential for determining the surgical approach or alternative options, such as the “watch-and-wait” approach [9, 25, 80, 91].

The ESGAR and the SAR have recently issued consensus statements advocating for the implementation of “structured reporting” for rectal MRI, providing templates for reporting both primary staging and restaging [6, 92].

The MDT managing rectal cancer should utilize, document, and consistently update the latest version of the TNM staging classification (8th edition) as per the guidelines of the UICC (Appendix 1, Appendix 2 and Appendix 3). Following these guidelines ensures consistency and accuracy in cancer staging and treatment planning. Moreover, high-quality MRI allows for further subclassification of cT3 tumors, which is vital for developing personalized treatment strategies. A robust understanding of the MRI anatomy of the rectum and its surrounding structures elevates the diagnostic evaluation and reporting processes.

From a surgical oncology perspective, rectal cancers pose a unique challenge among colorectal tumors. Key MRI findings for rectal carcinoma involve not only tumor size, extramural spread (T stage), the peritoneal reflection, and lymph node involvement; at the same time, MRI evaluation provides EMVI and the presence of bone metastases [93, 94].

1.5.1. T staging

Using radiologists' standardized terminology is essential for delivering relevant reports to referring clinicians. MRI is the preferred imaging technique for staging rectal cancer, mainly because it effectively defines the extent of the primary tumor. The T stage classification is based on whether the tumor extends beyond the muscularis propria and its involvement with the MRF. Rectal cancer MRI reporting emphasizes the importance of detailing the tumor location (high, middle, low rectum), morphology, size, and proximity to the anorectal junction, including circumferential positioning [5, 9, 21, 25, 58, 63, 91]. The distance from the anorectal junction, particularly concerning the involvement of anal sphincter muscles and surgical margins, is critical. Historical margins of 1 cm for T1–T2 tumors and 2 cm for T3–T4 tumors are being reevaluated in light of surgical expertise and evolving evidence [95]. Several studies have shown the prognostic significance of minimal distal margins, with a ≤ 1 mm margin linked to increased local recurrence and reduced disease-free survival. However, adjuvant therapy can improve outcomes for those with positive margins [96, 97].

For MRI, Tx, primary tumor cannot be assessed; T0, no evidence of primary tumor; Tis, carcinoma in situ: invasion of lamina propria; T1, tumor invades submucosa; T2, tumor invades muscularis propria; T3, tumor invades subserosa or into non-peritonealized pericolic or perirectal tissues (T3 tumors are divided into substages as follows: T3a < 1 mm; T3b: 1–5 mm; T3c: 5–15 mm; and T3d > 15 mm); T4, tumor infiltrates/invades the peritoneal reflection (T4a) or other pelvic organs and structures (T4b). MRI frequently cannot distinguish between T1 and T2 tumors.

MRI capability to accurately identify T3 stage indicators, T4 stage signs, and pathological lymph nodes underscores its value [98]. Early identification of advanced stages (T3 cd/T4, N2, M0) is vital due to their high recurrence risk without neoadjuvant treatment, while tumors like T3ab and N0 show good outcomes with surgery alone [99]. The tumor proximity to the MRF and its shortest distance are crucial prognostic factors impacting survival and recurrence predictions [100].

Lastly, careful examination of the tumor relationship to the peritoneal reflection, the iliococcygeus and puborectalis muscles, and the external

sphincter and pelvic wall involvement is imperative. These details influence T-stage categorization and inform surgical and treatment planning, reflecting the nuanced and comprehensive approach required in rectal cancer management [101].

1.5.2. N staging

MRI effectiveness in staging lymph nodes for rectal cancer is still limited by moderate sensitivity and specificity, often leading to an overestimation of nodal involvement compared to histopathological findings [4, 31, 102]. The lymph node size is not assumed to be a very useful criterion in determining metastatic involvement, as studies indicate that up to 40 % of nodes measuring less than 5 mm may contain tumors [103]. The most reliable indicators of nodal involvement on MRI include a combination of signal heterogeneity, irregular contour, round shape, and size. Nodes that exceed 9 mm in short axis diameter are considered suspicious for metastasis. For nodes measuring between 5 and 9 mm, at least two features must be present: signal heterogeneity, irregular contour, or round shape; nodes smaller than 5 mm must exhibit all three characteristics [90, 104]. In a restaging context, nodes larger than 5 mm are considered as remaining involved or suspicious.

The nodal classification system includes the following categories: Nx: Regional nodes cannot be assessed; N0: No regional lymph node metastases. N1: Metastasis in 1 to 3 regional (perirectal) lymph nodes; N1a: Metastasis in 1 regional lymph node; N1b: Metastasis in 2 to 3 regional lymph nodes; N1c: Tumor deposit(s) in the subserosa, mesentery, or non-peritonealized pericolic or perirectal tissues without regional nodal metastasis; N2: Metastasis in 4 or more regional lymph nodes; N2a: Metastasis in 4–6 regional lymph nodes; N2b: Metastasis in 7 or more regional lymph nodes.

It is important to note that mesorectal, inferior mesenteric, and superior rectal nodes, as well as internal iliac and obturator lymph nodes, are considered locoregional lymph nodes in the setting of rectal cancer. In contrast, all other lymph nodes, including inguinal, external iliac, common iliac, and paraaortic nodes, are considered non-locoregional / distant lymph nodes (metastatic disease, M1) in the setting of rectal cancer.

A multicenter study indicated that lateral nodes exceeding 7 mm are associated with a higher likelihood of recurrence when treatment consists solely of CRT and rectal cancer surgery without pelvic sidewall dissection. In restaging, internal iliac nodes larger than 4 mm and obturator nodes larger than 6 mm are considered as remaining involved [105, 106].

Another area of contention is the classification of tumor deposits (TD), defined as cancer nodules in the mesorectum without lymph node architecture,

distinct from EMVI. The distinction between tumor deposits and metastatic lymph nodes is crucial, as tumor deposits (stage N1c) often indicate a worse prognosis than metastatic lymph nodes, a differentiation not yet reflected in the TNM classification [107–109]. Radiologists are advised to denote tumor deposits as N1c in MRI reports, although this classification may not fully represent their prognostic significance [110]. When tumor deposits are the sole finding, they should be reported as N1C; if combined with nodal involvement, the notation should include the nodal stage plus tumor deposits (e.g., N1b + TD). Future updates to the AJCC classification may revise these reporting standards [111].

While nomograms have been proposed to predict lymph node involvement, their accuracy has yet to be confirmed. Eventually, evaluating the tumor proximity to the MRF is more vital for clinical decision-making than the status of lymph nodes.

1.6. Prognostic factors for rectal cancer

1.6.1. Mesorectal fascia and circumferential resection margin

The rectum and the surrounding mesorectal fat, known as the mesorectum, are surrounded by the MRF, which is attached to the sacrum by the presacral fascia of Waldeyer. The MRF is a thin fibrous structure that is the expected resection plane when performing a total mesorectal excision (TME). The term MRF is sometimes incorrectly used interchangeably with the circumferential resection margin (CRM), and this must be revised. The MRF is an anatomical structure, while the CRM is a technical term that refers to the margin created by the surgeon during resection and the distance reported by pathologists between the tumor and the outer edge of the resected specimen [9, 90, 112]. Therefore, radiologists should avoid using the term CRM and instead describe the tumor relationship to the MRF.

Whether performing a low anterior resection, an intersphincteric resection, or an abdominoperineal resection, TME entails the complete removal of the mesorectum in relation to the MRF [112, 113]. The involvement of the MRF by tumor (positive MRF) is the most significant predictor of local recurrence and disease-free survival [9, 21, 58].

Research suggests that MRF involvement, identified when cancer is within 1 mm of the MRF – including the primary tumor, extramural vascular invasion, and cancer deposits – poses significant risks [4, 20, 63]. Meanwhile, distances between 1 and 2 mm are classified as “threatened” MRF. A negative MRF, indicating no cancer cells within 1 mm of the margin, correlates with a decreased risk of local recurrence and enhanced survival outcomes. However,

the role of lymph nodes near the MRF remains debated. Studies indicate that MRF involvement by metastatic lymph nodes alone is uncommon, with a small percentage of cases showing MRF positivity due to metastatic nodes [115].

In locally advanced rectal cancers, particularly T3c tumors, neoadjuvant CRT is beneficial before reassessment for surgical resection, with MRI playing a pivotal role in this evaluation. The MRF is described in MRI reports as a thin hypointense line. Distances measured from the MRF to the tumor margin should always be included in reports for T3 tumors, as they correlate with the likelihood of recurrence and guide treatment decisions [9, 20, 68].

Distance measurements to the MRF are generally not applied to lower rectal tumors near the levator ani, where the mesorectum significantly narrows as it approaches the anal sphincter complex. The proximity of these structures increases the risk of MRF involvement. For lower rectal tumors, it is essential to measure the distance from the tumor lower extent to the upper margin of the anal sphincter, which is important for planning a low anterior resection LAR, and to assess the involvement of the intersphincteric space or external anal sphincter to guide the surgical approach [57, 116].

1.6.2. Extramural vascular invasion

EMVI is defined as a direct tumor invasion into a blood vessel (usually a vein). Preoperative identification of EMVI is linked to an increased likelihood of local recurrence, both synchronous and metachronous distant metastases, and higher overall mortality rates [9, 93]. Consequently, EMVI is often recommended as a criterion for initiating neoadjuvant CRT in various international guidelines [94, 117].

On MRI, EMVI manifests as replacing the typical dark vascular flow void seen in T2-weighted imaging with an intermediate signal intensity that resembles that of the primary rectal tumor. More advanced tumor invasion can lead to vessel expansion and irregularity or nodularity of the vessels. In cases of primarily mucinous tumors, EMVI appears significantly hyperintense on T2-weighted images, similar to the primary tumor. The MRI-based EMVI scoring system has been developed by Smith et al. [118], focusing on the tumor growth pattern, the primary tumor location about visible penetrating vessels, the diameter and shape of the vessel, and the intraluminal signal intensity to assign a likelihood score (Table 1.6.2.1) [118].

Table 1.6.2.1. Five-point scoring system for MRI-detected extramural vascular invasion [118]



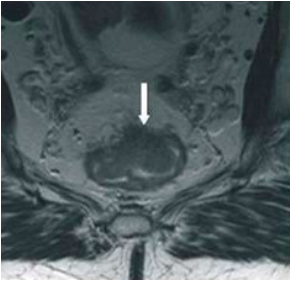

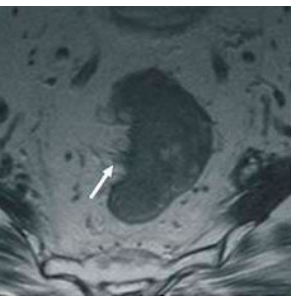



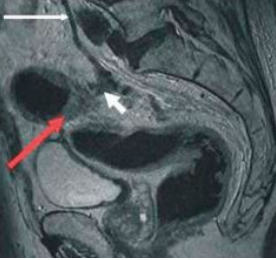
MRI-EMVI score	Predicted EMVI status	Typical imaging features	Schematic illustration	Representative MRI figure
0	Negative	Definitely negative (no vessels adjacent to areas of tumor penetration)		
1	Negative	Probably negative (minimal extramural stranding/nodular extension, but not in the vicinity of any vascular structure)		
2	Negative	Possibly negative (stranding demonstrated in the vicinity of extramural vessels, but these are of normal caliber, and no definite tumor signal in vessel)		
3	Positive	Probably positive (intermediate signal intensity apparent within the vessels, although contour and caliber of these vessels are only slightly expanded)		

Table 1.6.2.1 cont.

MRI-EMVI score	Predicted EMVI status	Typical imaging features	Schematic illustration	Representative MRI figure
4	Positive	Definitely positive (obvious irregular vessel contour or nodular expansion of vessel by definite tumor signal)		

(1) Rectal tumor with an anterior infiltrating border. Nodular tumor extension is demonstrated beyond the bowel wall (arrow), but not extending into adjacent vascular structures. MRI-EMVI score 1. (2) Polypoidal rectal tumor with an infiltrating medial margin (arrow). Normal-caliber perirectal vessels of low signal intensity are shown, but the intermediate tumor signal intensity does not extend to these vessels. MRI-EMVI score 2. (3) Low rectal tumor with an anterior infiltrating border. There is nodular extension beyond the rectal wall and tumor signal intensity is seen expanding the origin of an extramural vessel (arrow). MRI-EMVI score 3. (4) Tumor signal is seen expanding the origin of the superior rectal vein (short white arrow) adjacent to a rectosigmoid cancer (red arrow). A normal-caliber vein with low signal intensity is seen extending cranially beyond the expanded origin (long white arrow). MRI-EMVI score 4.

1.7. Restaging after neoadjuvant treatment

Precise restaging of tumors is essential to determine the most appropriate surgical treatment for patients with locally advanced rectal cancer undergoing neoadjuvant therapy. This process aims to prevent both poor oncological outcomes and overtreatment, heavily relying on the expertise of radiologists. The recommended modalities for local tumor restaging include a digital rectal examination, endoscopy, and pelvic MRI, while chest and abdominal CT are used to assess distant disease [9, 119, 120]. The optimal interval between neoadjuvant treatment and restaging, regarding oncological safety and the clinical effectiveness of treatment, remains uncertain or controversial, particularly for patients undergoing extended total neoadjuvant therapy [120–122]. Locally advanced rectal cancers typically undergo neoadjuvant chemoradiation therapy, followed by MRI approximately 6–8 weeks post-treatment, prior to surgery, to evaluate the response to therapy [8, 62, 122]. Radiologists play a significant role in this phase by determining the extent of tumor reduction, assessing the level of mesorectal involvement and extramural

vascular invasion, and identifying any potential residual tumor areas that may indicate an incomplete treatment response.

Timely identification of radioresistant patients at risk for disease progression creates significant challenges. However, there is hope with the use of MRI, which is critical for initial staging and has become a vital tool in evaluating the response to neoadjuvant treatment. The insights obtained from restaging MRIs can greatly influence surgical decisions, especially in cases where patients show a near-complete or complete response. This potential for near-complete/complete response opens the door to organ-preserving strategies, such as the “watch-and-wait” approach [12, 114, 121].

When a residual tumor is visible on T2-weighted images, the degree of response should be quantified, particularly regarding tumor size reduction. However, distinguishing between treatment response and radiation therapy-induced fibrosis remains challenging. This is because fibrosis, a common side effect of radiation therapy, can appear similar to residual tumor tissue on imaging, leading to potential misinterpretation. Fibrosis can obscure small remaining areas of the tumor, making it difficult to accurately assess the extent of treatment response [124].

DWI has been introduced as an innovative technique that explores the movement of water molecules to non-invasively gauge cellular density. While its application in initial staging remains under debate, its significance in reassessment following neo-adjuvant therapy is increasingly recognized, with studies confirming its utility in enhancing MRI accuracy. DWI aids in identifying either the presence of hyperintense foci, suggesting residual tumor or the absence thereof, indicating a complete response. However, interpreting DWI findings demands experience, as several factors, such as the T2 shine-through effect or artifacts from fibrosis, could mislead less experienced radiologists [71, 119, 120, 125]. Mucinous tumors are assessed separately due to their unique DWI signal characteristics resulting from their mucin content [126]. Additionally, ADC maps, which provide quantitative data, have been explored as potential biomarkers for predicting treatment outcomes. Despite revealing significant ADC differences between responders and non-responders, inconsistencies in study results have led to a hesitance in recommending routine ADC quantification.

Post-treatment lymph node evaluation should be compared against pre-treatment findings, focusing on changes in size, signal intensity, and morphology [9, 114, 120]. Recent research suggests that nodal size is a more reliable indicator of metastatic involvement. For instance, a reduction in nodal size by 70 % or more typically indicates no residual nodal disease (ypN0) with high accuracy [127]. Nodal reassessment after chemoradiation has proven more accurate than initial staging, primarily due to a decrease in

malignant nodes and the disappearance of smaller nodes following treatment. Consequently, the absence of detectable nodes on restaging DWI is considered a strong indicator of a complete response to neoadjuvant therapy.

1.8. Response assessment after neoadjuvant treatment

Currently, the most effective methods for evaluating the extent of rectal tumor response to neoadjuvant treatments involve a combination of digital rectal exams, endoscopy, and MRI imaging that takes T2-weighted and DWI sequences [128]. The response is classified into near-complete or possible complete response when there is a detected standard rectal wall or only fibrosis, good response with predominant fibrosis but suspicion of small tumor remnant within the fibrosis on T2-weighted MRI or DWI and poor response with predominantly solid tumor remnant [8, 15, 75]. Despite continuous improvements in rectal cancer assessment tools, there is still a relatively high rate of local recurrence, which highlights the challenges of identifying microscopic residual disease mixed with treatment-related fibrosis. Innovations in advanced imaging techniques and computational data processing, combined with more sensitive biomarkers for low-volume residual disease, may improve the ability to differentiate between fibrotic tissue and an incomplete response to neoadjuvant treatments [129, 130].

Following CRT, rectal tumors usually decrease in size and stand out with a fibrotic change, which is reflected by a significant reduction in signal intensity of the tumor on T2-weighted MRI images.

1.8.1. Magnetic resonance imaging volumetry and tumor volume reduction rate

Although treatment options for rectal cancer have improved, patient outcomes still vary widely and depend on factors such as the initial size and how quickly it decreases in size and volume during treatment. MRI provides important information regarding clinical prognosis and preoperative evaluation [131]. Measuring tumor volume and tumor volume reduction over time are key indicators that can enhance treatment strategies and patient care [132, 133].

The initial tumor volume evaluation is vital for improving surgical techniques in rectal cancer. It gives surgeons essential information about the tumor size and extent, enabling them to choose the best surgical technique – laparoscopic, robotic, minimally invasive or open surgery [134–136]. The rate of volume reduction can also influence the time of surgery – patients who respond quickly to treatment may be able to have surgery sooner. At the same time, those with slower responses might benefit from additional rounds of

chemotherapy or radiation before surgery. This evaluation is also important for identifying patients who may qualify for conservative treatment modes, such as organ-preserving methods or the “watch-and-wait” strategy [12, 114, 121, 137].

Additionally, the tumor location in relation to important structures induces surgical decisions. Knowing the tumor volume and volume reduction rates helps predict possible postoperative complications, like longer recovery times and risks of issues such as anastomotic leaks, bleeding, or infections. This information is relevant for preparing patients and guiding their expectations about recovery and potential bowel function changes after surgery [137, 138].

Furthermore, TVRR after neoadjuvant therapy indicates how the tumor behaves biologically. A significant decrease in size following treatment is typically a positive sign, suggesting that the tumor responds well to therapy, which may allow for less invasive surgical options [138, 139].

1.8.2. Magnetic resonance imaging-assessed tumor regression grade

Following therapy, as tumor volume and tumor volume reduction rates have already been identified as pivotal prognostic tools that promise to improve treatment planning and patient care strategies, one more prognostic factor can be added next to them. It is a mrTRG. The mrTRG classification is derived from the methodology developed by the MERCURY study group (Table 1.8.2.1) [140]. This scoring system evaluates the presence of residual tumor and fibrosis as observed on T2-weighted MRI images. By classifying the extent of these features, the mrTRG classification provides valuable insights into tumor response to treatment. This systematic evaluation is crucial for guiding clinical decision-making and adapting future therapeutic approaches for patients with rectal cancer. Ultimately, the mrTRG classification helps to improve the predictive accuracy of treatment outcomes based on imaging findings. The purpose of the MRI is to assess the level of tumor decrease in comparison to the histopathological assessment of tumor regression (known as pathological tumor regression grade, pTRG), which serves as the reference (Table 1.8.2.2). The treatment response in mrTRG is categorized on a scale from TRG-1 (visible fibrosis only, likely a complete response) to TRG-5 (no fibrosis, predominantly residual disease). It is essential to recognize that, in contrast to the remarkable precision of the initial pre-treatment MRI, the reliability of interpreting post-treatment results significantly diminishes, as distinguishing between the signals of therapy-induced fibrosis and active tumor cells can often be challenging or even unfeasible.

Table 1.8.2.1. Magnetic resonance imaging-assessed tumor regression grade [140]

Grade	Response	
mrTRG1	Complete radiologic response	Complete regression (absence of tumor signal and barely visible treatment related scar)
mrTRG2	Good response	Good regression (predominant low signal intensity fibrosis with no obvious residual tumor signal)
mrTRG3	Moderate response	Moderate regression (low signal intensity fibrosis predominates, but there are obvious areas of intermediate signal intensity)
mrTRG4	Slight response	Slight regression (little areas of low signal intensity fibrosis or mucin but mostly tumor)
mrTRG5	No response	No regression (intermediate signal intensity, same appearances as original tumor)

mrTRG, MRI-assessed tumor regression grade.

Table 1.8.2.2. Tumor regression grade [141, 142]

Grade	Response	
TRG0	No response	No regression
TRG1	Minimal response	Dominant tumor mass with obvious fibrosis and/or vasculopathy
TRG2	Partial response	Dominantly fibrotic changes with tumor cells or groups (easy to find)
TRG3	Near complete response	Very few (difficult to find microscopically) tumor cells in fibrotic tissue with or without mucous substance
TRG4	Complete response	No tumor cells, only fibrotic mass (total regression or response)

TRG, tumor regression grade.

Although the limitations and compliance between mrTRG and pTRG are still being explored, mrTRG is acquiring recognition for its potential to monitor treatment responses and guide therapeutic interventions closely. This emerging interest highlights the importance of incorporating imaging findings into clinical practice, as it may improve decision-making processes for patient management. By showing its effectiveness in assessing tumor response, mrTRG could be important in optimizing treatment strategies and improving patient outcomes.

Despite its importance, the agreement between mrTRG and pTRG is still limited and controversial. As a result, mrTRG cannot replace pTRG in clinical assessments. There is an increasing demand for additional research to improve the utility of mrTRG in identifying patients who may qualify for

non-surgical treatment approaches and to support pTRG in providing more detailed post-operative risk assessments.

Due to the widespread adoption of the AJCC TNM staging system, the AJCC Tumor Regression Grade (TRG) system was employed to maintain data uniformity, despite the existence of various TRG systems [141, 142]. The AJCC-TRG system categorizes tumor response to treatment into four levels:

The TVRR and mrTRG are important tools that help surgeons discuss long-term outcomes with their patients. Studies suggest in cases where tumor volume reduces significantly, are likely to have a more conducive prognosis, which is essential for developing post-operative care and monitoring plans [4, 20, 140]. Nonetheless, accepting TVRR and mrTRG as standard prognostic indicators in the treatment of rectal cancer presents several challenges. These include variability in measurement practices, the timing of evaluations, and differences in interpretation among different radiologists, which can affect the reliability and consistency of these assessments. Furthermore, the underlying biological reasons why certain tumors respond better to treatment than others remain still largely unclear.

1.9. Interpretation of magnetic resonance imaging and structured reporting

In clinical practice, free-text reporting is used for MRI reports. However, recent recommendations from the ESGAR and the SAR advocate for the adoption of “structured reporting” specifically for rectal MRI [6]. These organizations have developed standardized templates for MRI reports related to the primary staging and restaging of rectal cancer to enhance clarity and consistency in reporting.

According to these guidelines, the existing free-text MRI reports should be revised to follow the structured reporting approach for rectal cancer staging (Appendix 4) and for restaging (Appendix 5). This shift is intended to ensure that clinicians receive all essential information about the tumor. The use of structured reporting makes better communication among healthcare providers and aids in clinical decision-making by clearly outlining critical tumor characteristics, treatment recommendations, and expected outcomes. Overall, this move towards structured reporting marks a significant advancement in improving the quality and effectiveness of radiological assessment in rectal cancer management.

1.10. Treatment of rectal cancer

The staging and treatment of rectal cancer have progressed significantly over the past several decades, resulting in a notable decrease in locoregional recurrences [143, 144]. However, overall survival rates have not significantly improved as the risks of systemic recurrence remain largely unchanged.

For patients with rectal cancer that are advanced enough to necessitate neoadjuvant treatment for improved outcomes, it may be beneficial to postpone surgery if the tumor shows a complete clinical response (cCR) and allows for inclusion in the “watch-and-wait” approach [12, 114, 121]. While the optimal treatment method for achieving this needs to be clearly defined, the specific treatment used is less critical as long as cCR is achieved. The initial evaluation should occur early, around 5 to 6 weeks, to avoid unnecessary delays in surgery if the tumor has not responded adequately. Further delay offers no advantage for tumors that do not respond sufficiently and may even be harmful [5, 10, 15, 143, 144]. Conversely, if a near-complete response is observed, a safe extension of another 6 to 7 weeks is reasonable, and the “watch-and-wait” approach can be considered if cCR or an adequate response for local surgery or boost radiation therapy is indicated. The decision to initiate intentional organ preservation in early or intermediate-risk tumors should involve a thorough discussion between the patient and the physician, weighing the advantages and disadvantages appropriately [145, 146].

For patients with tumors at high risk for recurrence, particularly systemic recurrences, total neoadjuvant therapy is a logical approach [99, 147, 149]. This strategy could reduce the risk of distant metastasis, potentially leading to a cure for more patients. While randomized trials have demonstrated some benefits, these benefits are negligible. The ideal candidates or tumors for this treatment remain unidentified; thus, it should not be universally applied to all patients classified as having locally advanced rectal cancer as this may result in overtreatment for many individuals [149]. MRI-based N-positivity, including N2-positivity, is not a reliable criterion for selecting patients for total neoadjuvant therapy [150]. Much work is still needed to optimize treatment regimens and identify the best schedules, with the most pressing need for improvement relating to systemic therapy.

According to “Rectal cancer: ESMO Clinical Practice Guidelines for diagnosis, treatment and follow-up” [54], the treatment recommendations for rectal cancer are summarized in Fig. 1.10.1 and recommended treatment options for primary rectal cancer without distant metastases are summarized in Table 1.10.1.

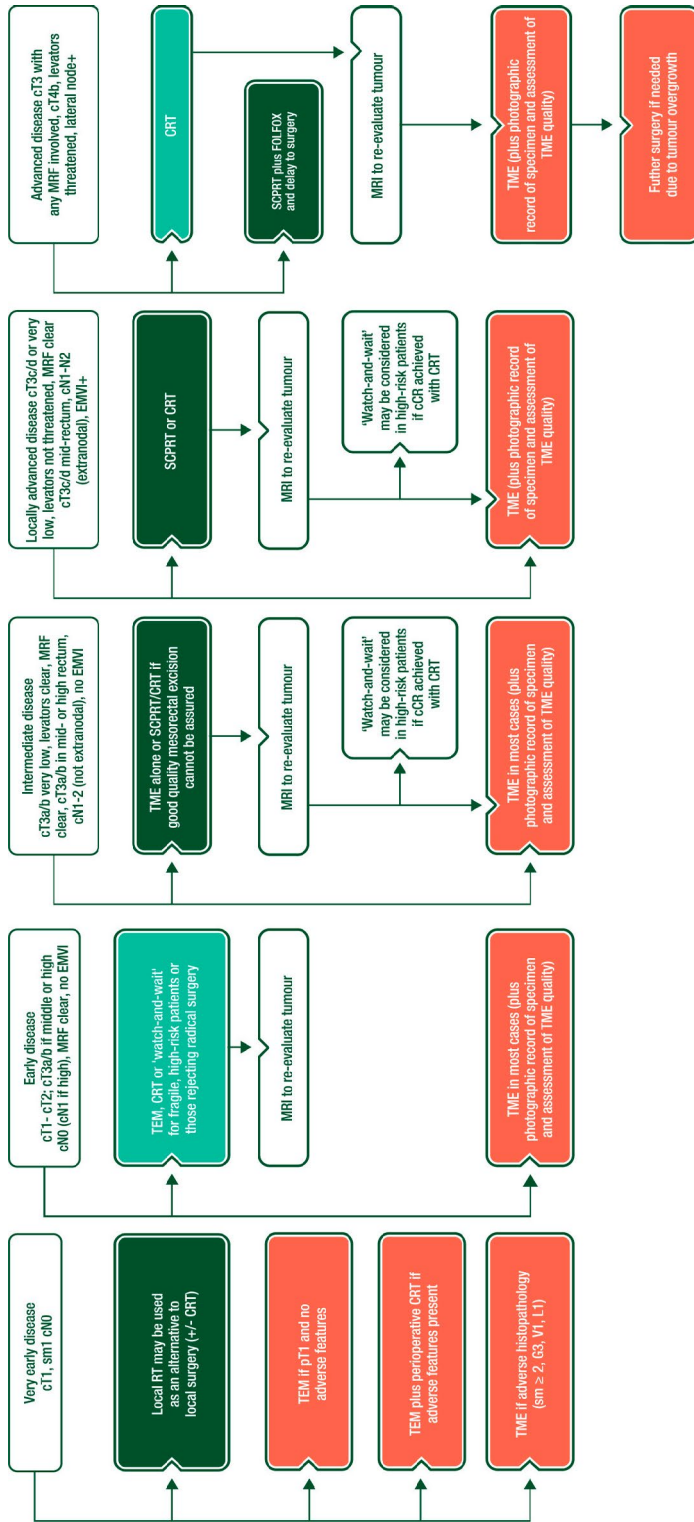


Fig. 1.10.1. Rectal cancer treatment

cCR, complete clinical response; CRT, chemoradiotherapy; EMVI, extramural vascular invasion; FOLFOX, leucovorin/fluorouracil/oxaliplatin; MRF, mesorectal fascia; MRI, magnetic resonance imaging; RT, radiotherapy; sm, submucosa; SCRPRT, short-course preoperative radiotherapy; TEM, transanal endoscopic microsurgery; TME, total mesorectal excision.

Table 1.10.1. Recommended choice of treatment options within TNM risk category of primary rectal cancer without distant metastases [54]

Risk group	TN substage	Possible therapeutic options	Further considerations
Very early	cT1 sm1 N0 (on ERUS and MRI)	Local excision (TEM) If pT1 and no adverse features, TEM is sufficient If adverse histopathology (submucosa ≥ 2 , G3, V1, L1) requires radical resection (TME) as standard	Alternatively, in the case of adverse features on pathology, TEM plus salvage (or adjuvant) CRT in perioperative high-risk patients (but unproven benefit—with high risk of local recurrence for pT2)
Early (Good)	cT1–cT2; cT3a/b if middle or high, N0 (or also cN1 if high), MRF clear, no EMVI	Surgery (TME) alone is standard. If unexpected poor prognostic signs on histopathology (CRM+, extranodal/N2), consider postoperative CRT/CT	For fragile, high-risk patients or those rejecting radical surgery (CRT with evaluation, local excision or if achieving cCR, “watch-and-wait”, organ preservation)
Intermediate	cT3a/b very low, levators clear, MRF clear or cT3a/b in mid- or high rectum, cN1–2 (not extranodal), no EMVI	Surgery (TME) alone is a standard only if good-quality mesorectal resection assured (and local recurrence $\leq 0.5\%$ or, if not, preoperative SCPRT (5×5 Gy) or CRT followed by TME	If CRT is given and cCR is achieved, a “watch-and-wait” approach in high-risk patients for surgery may be considered
Bad	cT3c/d or very low localization levators threatened, MRF clear cT3c/d mid-rectum, cN1–N2 (extranodal), EMVI+, limited cT4aN0	Preoperative SCPRT (5×5 Gy) or CRT followed by TME, depending on need for regression	If CRT and cCR achieved, a “watch-and-wait” approach in high-risk patients may be considered
Advanced (Ugly)	cT3 with any MRF involved, any cT4a/b, lateral node+	Preoperative CRT followed by surgery (TME and more extended surgery if needed due to tumor overgrowth), or preoperative SCPRT (5×5 Gy) plus FOLFOX and delay to surgery	Alternatively, 5×5 Gy alone with a delay to surgery in fragile/elderly or in patients with severe comorbidity who cannot tolerate CRT

Local recurrence is less common when high-quality TME is performed alongside preoperative radiotherapy (RT) or CRT. However, a recurrent pelvic tumor can lead to significant pain, often necessitating the use of

both opioid and non-opioid pain relief. In addition to pain, patients may experience troublesome symptoms, including offensive mucinous discharge and incontinence. According to the ESMO Clinical Practice Guidelines, the management of local recurrence is summarized in Fig. 1.10.2.

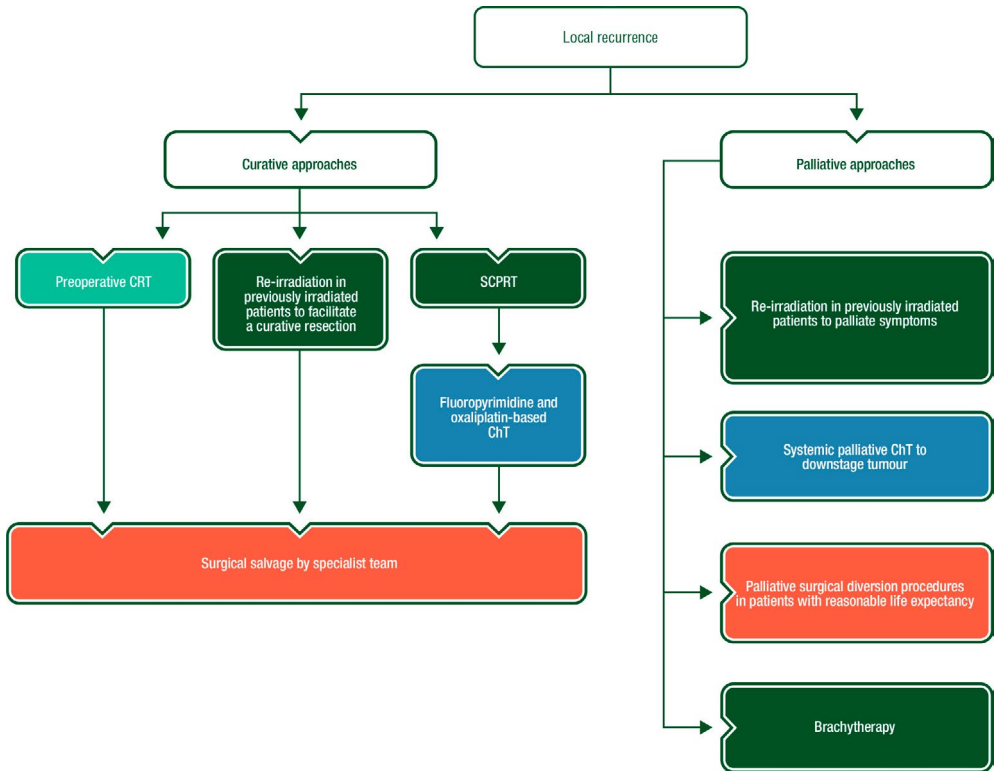


Fig. 1.10.2. Rectal cancer treatment of local recurrence

ChT, chemotherapy; CRT, chemoradiotherapy; RT, radiotherapy; SCPRT, short-course pre-operative radiotherapy.

The stages of metastatic rectal cancer are addressed in the ESMO consensus guidelines for metastatic CRC. These stages are designed to align with the overarching goals of treatment, which include considerations of tumor- and disease-related characteristics, as well as patient-related factors such as comorbidities, socioeconomic status, and the patient’s expectations. Additionally, treatment-related factors, including the potential for toxicity, play an important role in guiding treatment decisions. Management of advanced/metastatic disease is summarized in Fig. 1.10.3.

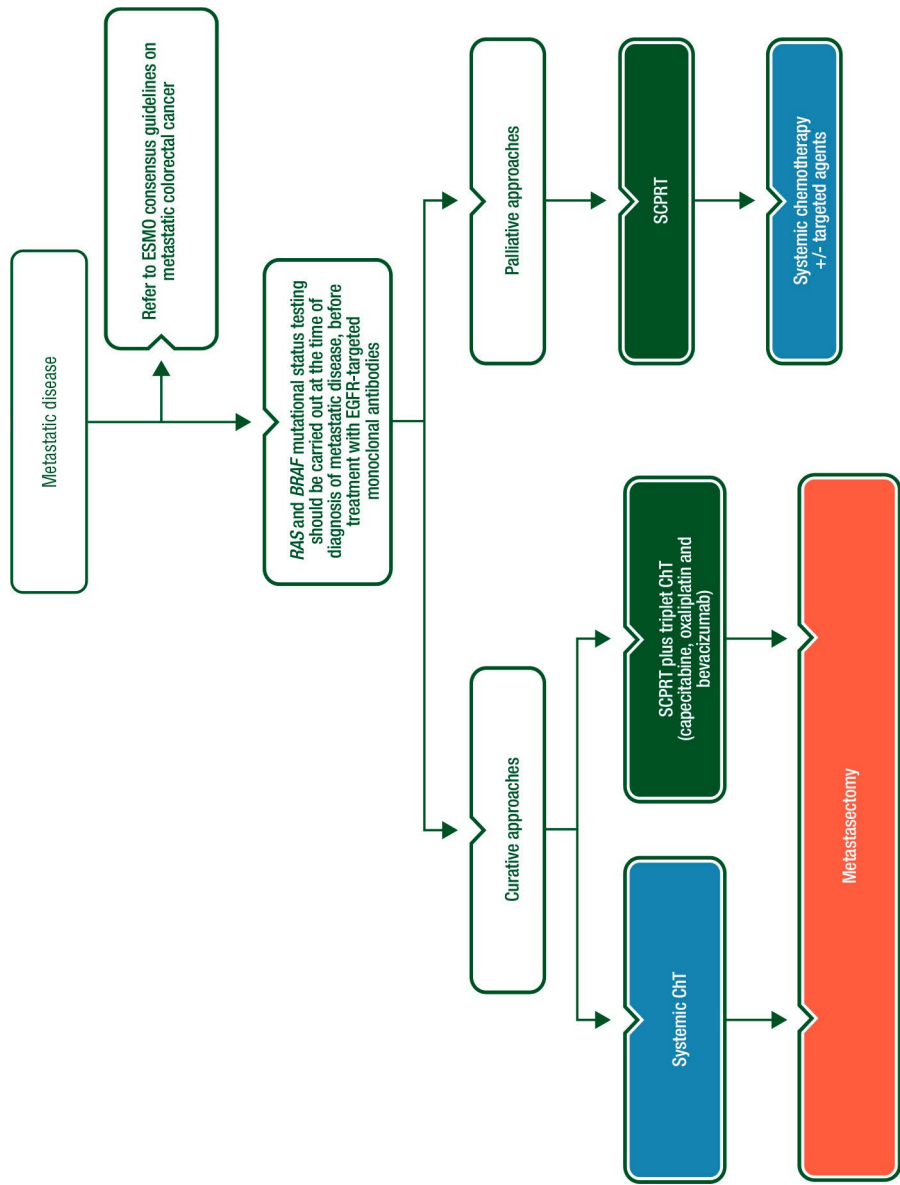


Fig. 1.10.3. Rectal cancer treatment of metastatic disease

ChT, chemotherapy; EGFR, epidermal growth factor receptor; ESMO, European Society for Medical Oncology; SCPRT, short-course preoperative radiotherapy.

2. METHODS

2.1. Ethics

Kaunas Regional Biomedical Research Ethics Committee approved the study (No. BE-2-32, dated July 17, 2015). All patients signed an informed consent form before inclusion.

2.2. Study population and design

We performed a single-center study in the Radiology, Surgery and Oncology and Hematology Departments at the Hospital of Lithuanian University of Health Sciences Kauno klinikos during 2015–2023. This was a prospective clinical study. Patients diagnosed with stage II and III rectal cancer based on radiological examinations (chest and abdominal CT, pelvic MRI) were included. Initially, all patients were stratified by tumor resectability. Participants were divided into two treatment groups at a 1:1 ratio (Appendix 6). The first chemotherapy group (CTx) received a new standard preoperative chemotherapy regimen FOLFOX4, for a total of 8 cycles. The effectiveness of the treatment was assessed using radiological methods (pelvic MRI), evaluating cancer marker dynamics, and the possibility of performing radical surgery (aiming for R0 resection). If a T4 size tumor or N(+) remained, as assessed by TNM, additional fractionated radiation therapy (50 Gy/25 fr) to the tumor was administered during the preoperative period, along with 2 cycles of chemotherapy with 5-Fu/Lv (MAYO regimen). Patients underwent surgery if there was a decrease in tumor size (T1–3, N0). Postoperatively, chemotherapy with the FOLFOX4 regimen continued for 4 cycles (up to 6 months of total systemic treatment), if R0 resection was achieved. The second, CRT group, received standard chemoradiation treatment in the preoperative period. After surgery, the degree of tumor regression was assessed. If the tumor significantly decreased post-chemoradiation (pT0N0 or pT1–2N0), the standard treatment was continued – 4 cycles of chemotherapy with 5 Fu/Lv. For remaining stage pII or pIII tumors, adjuvant chemotherapy with the FOLFOX regimen was planned, a total of 8 cycles.

The preoperative assessment of rectal cancer involved standard instrumental examination - MRI. Evaluations were based on the rectal cancer primary diagnosis and restaging protocol, established following the recommendations made at the 2012 ESGAR congress.

2.3. Inclusion and exclusion criteria of the study population

The inclusion criteria were as follows:

1. Age: patients 18 years and older;
2. Diagnosed with rectal adenocarcinoma;
3. Radiologically measurable tumor size;
4. Clinically (as determined by pelvic MRI) diagnosed as stage II or III rectal cancer;
5. Absence of distant disease spread (confirmed by radiological examinations, including chest and abdominal CT scans);
6. During preoperative proctoscopy, the tumor is identified at 0–15 cm from the anal verge;
7. Signed informed consent form.

The exclusion criteria were as follows:

1. Patients with signs of intestinal obstruction at the beginning of treatment;
2. Previous radiation therapy in the lower abdominal area;
3. Other malignant conditions within 5 years;
4. Pregnant or breastfeeding women;
5. Concurrent patient illnesses that would make the patient unsuitable for this study or significantly interfere with the assessment of safety and toxicity.

2.4. Diagnosis and treatment

Standard diagnostic methods were applied: radiological (pelvic MRI before the planned treatment and to assess treatment effect; chest CT and abdominal organ CT to assess distant disease spread), laboratory (cancer markers such as CEA, CA 19-9), and pathological (examination of tumor tissue for gene expression). Applied treatment: conventional neoadjuvant CRT (5-FU/Lv and radiation therapy 50 Gy) or new standard preoperative chemotherapy (more intensive, FOLFOX4 regimen) and surgery. Histopathological analysis was performed at the Department of Pathology, Medical Academy, Lithuanian University of Health Sciences, on a routine basis.

2.4.1. Magnetic resonance imaging protocol

The applied rectal cancer MRI protocol included pre-examination fasting for 4–6 h and micro-enema before MRI scanning. A small enema before MR imaging may minimize sensitivity from bowel air [6]. Upon arrival to the study, the patient filled out standard MRI consent form (Appendix 7, patient survey form for MRI). The person was informed about the progress of the investigation. All subjects changed their clothes to special clothing.

MRI examination was performed using a Siemens 1.5 T Magnetom Avanto scanner with surface coils (Tables 2.4.1.1 and 2.4.1.2). In the supine position, patients received pelvic MRI for initial cancer staging and again 6–8 weeks after treatment for response evaluation.

Table 2.4.1.1. Imaging sequences at 1.5 T

Parameter	TR/TE (ms)	FOV (mm)	Matrix (%)	Signal Averages	In Plane Resolution	Slice Thickness/Gap (mm)	Time (Min:Sec)
Axial T2W (TSE)	4000/110	360	448 × 358 (80)	1	1.0 × 0.8	5.5/1.1	1:38
Sagittal T2W (TSE)	4380/99	200	320 × 266 (83)	2	0.66 × 0.63	3.0/0.3	4:37
HR oblique axial T2W (TSE)	4750/95	180	320 × 256 (80)	4	0.56 × 0.56	3.0/0.3	5:10
HR oblique coronal T2W	6420/106	180	320 × 256 (80)	4	0.56 × 0.56	3.0/0.3	5:16
DWI b0, 500, 800	4500/66	230	128 × 109 (85)	b0–1 b400–6 b800–8	1.8 × 1.8	3.5/0	3:47

TR, repetition time; TE, echo time; FOV, field of view; HR, high-resolution; TSE, turbo spin echo; T2W, T2 weighted imaging; DWI, diffusion-weighted imaging.

Table 2.4.1.2. The protocol of MRI for the detection and evaluation of rectal cancer before treatment and with gadolinium injection after treatment/before surgery

Pelvic MRI for initial cancer staging	Pelvic MRI restaging
Patient fasted overnight	Patient fasted overnight
Micro-enema before MRI	Micro-enema before MRI
Patient placed in the supine position in an MR scanner	Patient placed in the supine position in an MR scanner
Buscopan injection	Buscopan injection
MRI scan: T2 sag T2 ax – perpendicular to the main tumor axis T2 cor – perpendicular to the axial images T2 small FOV – perpendicular to the main tumor axis DWI/ADC – the same as T2W inclination, high b value (≥ 800 mm ² /s)	MRI scan: T2 sag T2 ax – perpendicular to the main tumor axis T2 cor – perpendicular to the axial images T2 small FOV – perpendicular to the main tumor axis DWI/ADC – the same as T2W inclination, high b value (≥ 800 mm ² /s)
	MRI scan + T1 ax + contrast

Butylscopolamine (20 mg IV) was administered to reduce bowel movement and improve image quality [6,149]. A single dose of (0.2 mg/kg) IV gadolinium-based contrast media (Magnevist Bayer Schering Pharma, Berlin Germany) was injected into an arm vein at 2 mL/s. One radiology technologist conducted the examination, and a radiologist supervised the procedure. MRI protocol involved T2-weighted sagittal, axial and coronal planes, small FOV T2 axial through tumor and DWI/ADC axial planes.

For restaging after chemotherapy alone or CRT prior to surgery, contrast-enhanced sequences were added to evaluate local recurrences (Table 2.4.1.2) and to stage locally advanced rectal cancers, where the involvement of other pelvic structures is a critical factor in determining the surgical approach [152].

2.4.2. Interpretation of magnetic resonance images

MRI images were evaluated on the picture archiving and communication system (PACS, Syngo.via, Siemens Healthineers) workstation by a radiologist with 7-year experience in rectal cancer imaging.

2.4.2.1. Tumor location, size, and morphology

Accurately identifying the tumor location and position relative to specific anatomical points is essential for planning surgical intervention and anticipating surgical margins, also influence the need for neoadjuvant treatment [153].

- The location of the tumor was defined by measuring the distance from the lowest point of the anal canal (referred to as the “anal verge”) and from the highest point (known as the “anorectal junction”) to the lowest point of the tumor (Fig. 2.4.2.1.1).
 - The measurement from the anal verge was used to categorize the tumor location into the upper, middle, and lower sections of the rectum:
 - Low rectum < 5 cm from the anal verge;
 - Mid rectum > 5–10 cm from the anal verge;
 - Upper rectum > 10–15 cm from the anal verge.

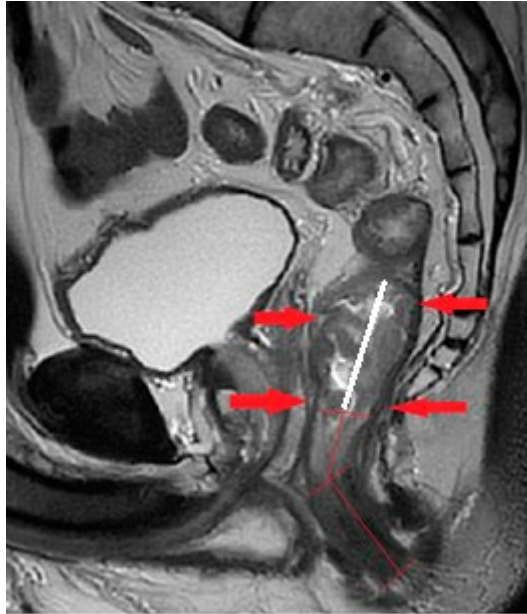


Fig. 2.4.2.1.1. *Measurement of tumor height using magnetic resonance imaging*

The location of the rectal cancer (red arrows) and the tumor height were measured from the anal verge to the lowest margin of the cancer along the luminal center of the anorectum in the midsagittal plane (red lines). The craniocaudal dimension was measured as white line.

- The circumferential position of the tumor was indicated (for example, from 10 o'clock to 3 o'clock, Fig. 2.4.2.1.2).
- The dimensions were reported at the craniocaudal dimension and the maximal wall thickness of the tumor (Figs. 2.4.2.1.1 and 2.4.2.1.2).
- Tumor morphology was described as polypoid, circumferential, or partly circumferential. While morphology does not affect the T stage, research indicates that polypoid tumors tend to correlate with lower pathologic T and N stages [154].
- The invasive border refers to the part of the tumor exhibiting the deepest level of invasion, typically found at the center of the lesion.

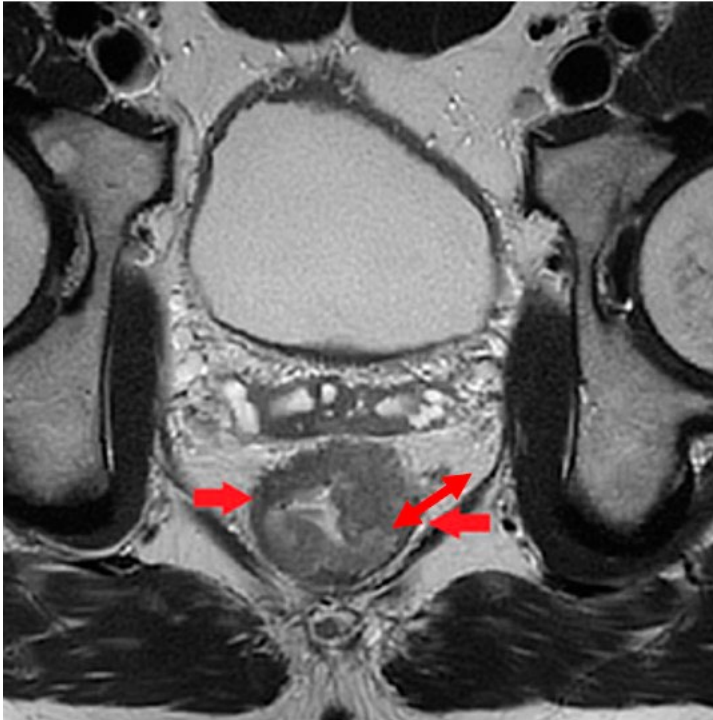


Fig. 2.4.2.1.2. Measurement of tumor circumferential position using magnetic resonance imaging

The position of the rectal cancer was noted according to o'clock hours (red arrows), and the maximal wall thickness of tumor was measured along the thickest portion of tumor (red double-headed arrow).

2.4.2.2. Relationship to the mesorectal fascia

Tumor association and the distance to the MRF play a crucial role in evaluating the potential CRM. A suspected or definitely involved MRF intensifies the need for neoadjuvant treatment to decrease local recurrence rates [9, 155].

- The distance to the MRF was measured as follows (Fig. 2.4.2.2.1) [156]:
 - The minimum linear distance between the tumor and the MRF was generally assessed using T2W/anatomical images, which helped evaluate their relationship.
 - distance of less than 1 mm signifies an involved MRF;
 - distance is less than 2 mm, indicated a threatened MRF.

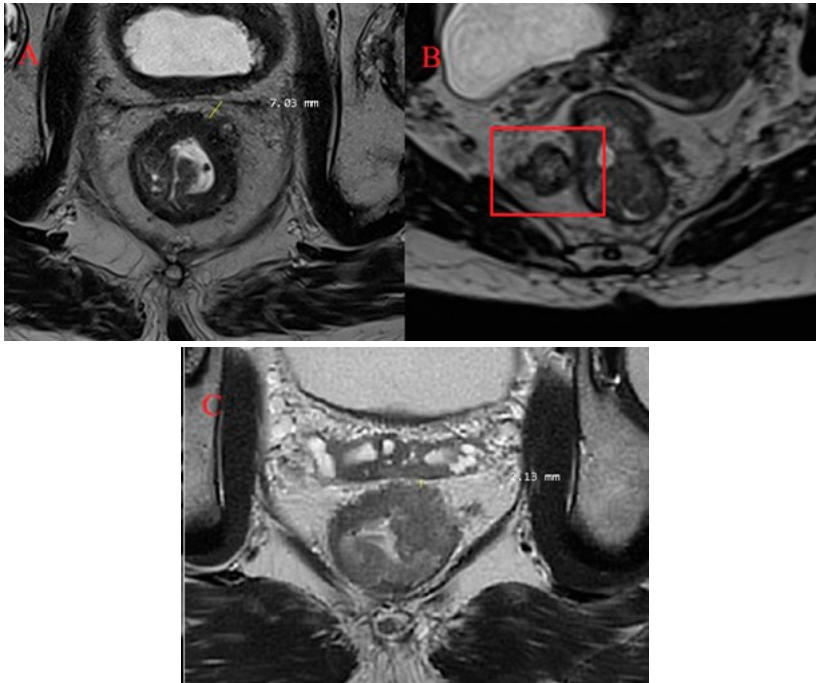


Fig. 2.4.2.2.1. Representative MRI scans showing the involvement of the mesorectal fascia

(A) Mesorectal fascia was not involved – the distance between tumor and MRF was approximately 7 mm; (B) The tumor node involved the right lateral part of mesorectal fascia; (C) A threatened MRF was suspected, when the distance was measured approximately 2 mm.

2.4.2.3. Relationship to the anterior peritoneal reflection

The anterior peritoneal reflection is a landmark seen on MR that helps determine the peritonealized and nonperitonealized portions of the rectum. Important to delineate the relationship between high and mid-rectal tumors [157].

- Tumor involvement of the anterior peritoneal reflection represents a T4a tumor and may be at risk for seeding and intraperitoneal recurrence in rectovesical space [158];
- The anterior peritoneal reflection is variable in location but typically at the level of the seminal vesicles in males and at the cervical-vaginal junction in females (Fig. 2.4.2.3.1);
- Seagull sign: the anterior peritoneal reflection on axial images is reminiscent of a seagull.

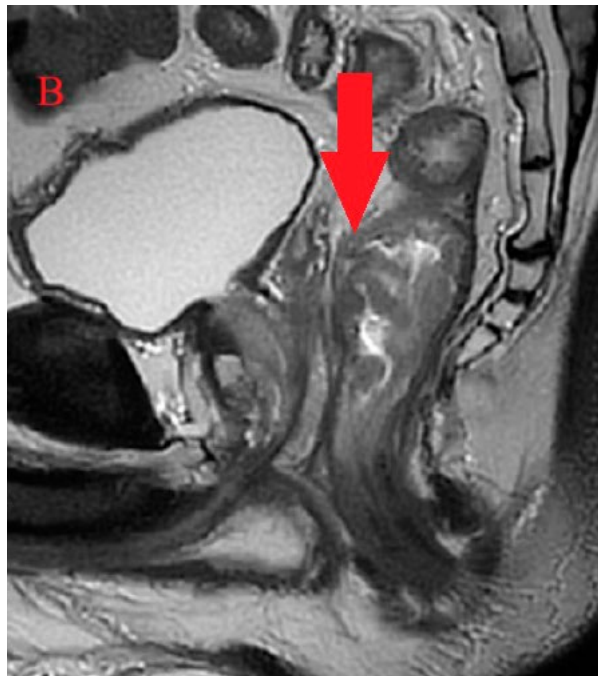
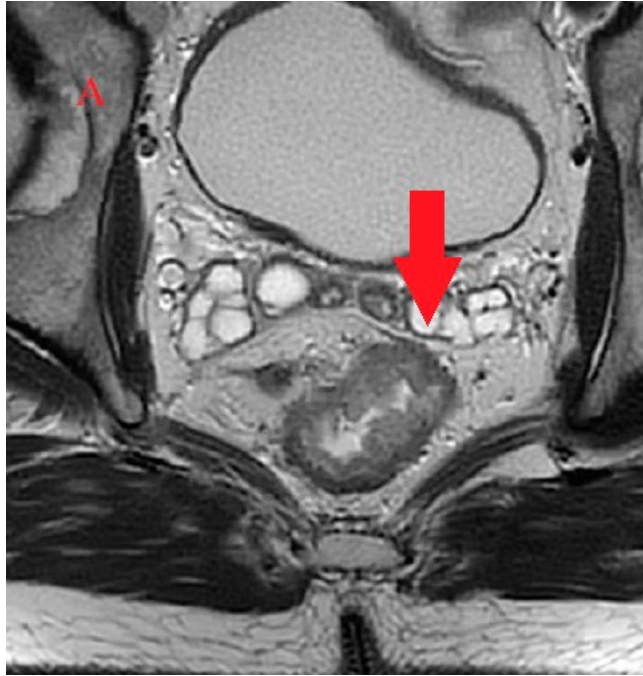


Fig. 2.4.2.3.1. Representative MRI scans showing the involvement of the anterior peritoneal reflection

(A) Axial image (near red line); (B) sagittal image (near red line).

2.4.2.4. T staging

The depth of tumor involvement in the rectal wall directly affects the available treatment options.

- High-resolution T2-weighted (T2W) imaging, oriented perpendicular to the long axis of the tumor, is essential for T staging due to its ability to provide intricate details of the rectal wall layers [7, 159];
 - Extramural depth invasion of rectal cancer tumors was measured as follows:
 - Measure the distance between the outermost edge of tumor and the outer edge of muscularis propria/MP (or expected outer edge of the MP if not present due to replacement by tumor);
 - Spicules were not included in the measurement.
 - According to the UICC TNM staging (8th edition) system, depending on the depth of invasion beyond the muscularis propria (in mm), T3 was subdivided into (Fig. 2.4.2.4.1) [141]:
 - T3a < 1 mm;
 - T3b 1– 5 mm;
 - T3c 5–15 mm;
 - T3d > 15 mm.
- DWI is useful in identifying small primary tumors, which generally showed high signal intensity on high b value images.
- Relationship to the anal canal evaluation: sphincter invasions and extension to upper/mid/distal 1/3 part of the anal canal.

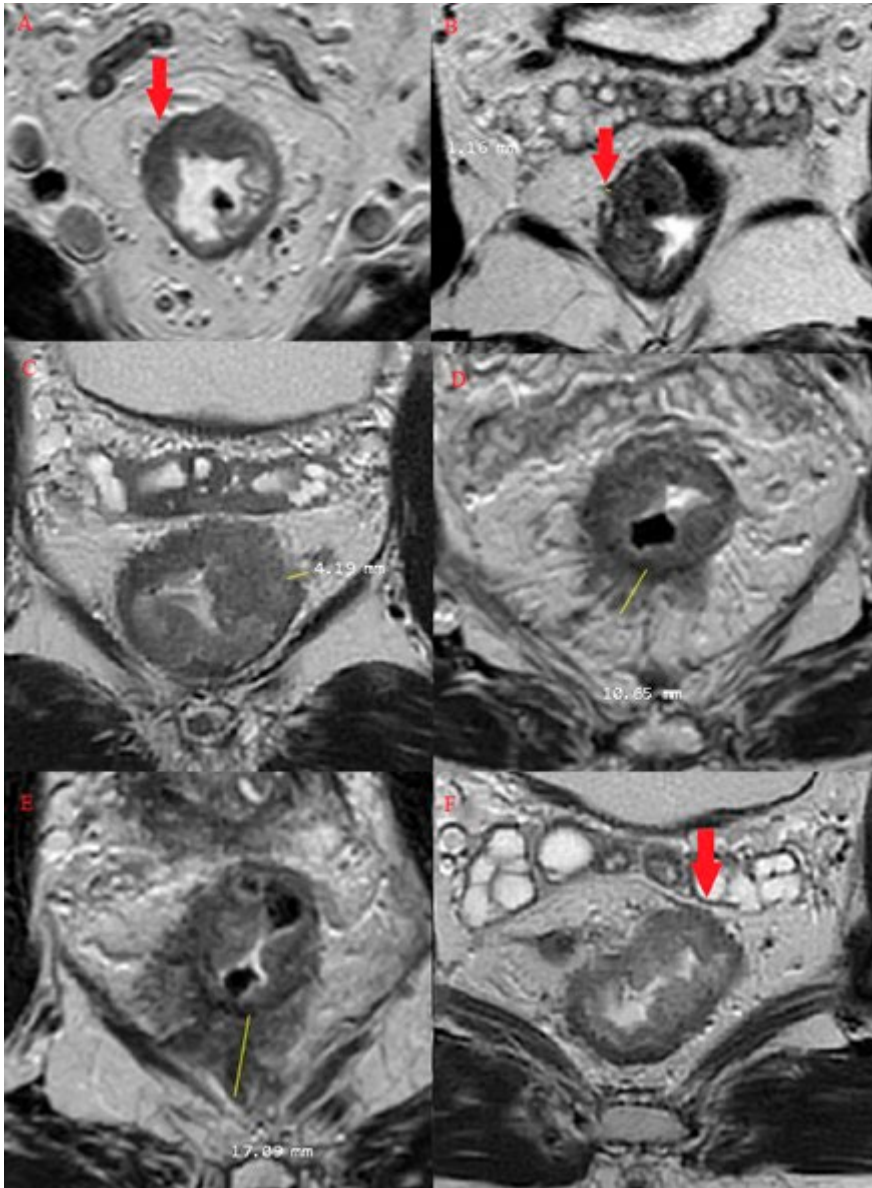


Fig. 2.4.2.4.1. Representative MRI scans showing different invasion of the tumor into muscularis propria and beyond it

(A) T2 tumor invaded muscularis propria, but not beyond (red arrow); (B) T3a tumor invaded through muscularis propria into perirectal tissues not more than 1 mm (red arrow); (C) T3b tumor invaded through muscularis propria into perirectal tissues 1–5 mm; (D) T3c tumor invaded through muscularis propria into perirectal tissues 5–15 mm; (E) T3d tumor invaded through muscularis propria into perirectal tissues more than 15 mm; (F) T4a tumor invaded peritoneal reflection/ visceral peritoneum (red arrow).

2.4.2.5. Extramural vascular invasion

- EMVI indicates the presence of tumor cells within vessels situated outside the muscularis propria of the rectum [9, 93, 94, 160];
- According to definitions, the presence of EMVI categorized the rectal tumor as a T3 lesion;
- It is essential to examine any vessels present in the mesorectal fat that appear tubular or serpiginous and are extending from the tumor; a nodular contour and expansion of the lumen with tumor signal are suspicious for vessel involvement and EMVI.
- The mrEMVI score is a five-point grading system that is derived by comparing the morphological features in MRI with histopathological references and is used to evaluate the severity of vascular invasion [9, 94, 161, 162]. The scoring system ranges from 0 to 4:
 - 0-1-2 mrEMVI negative (0, definitely not present; 1, probably not present; 2, equivocal);
 - 3-4 mrEMVI positive (3, probably present; 4, definitely present).

2.4.2.6. Lymph nodes and tumor deposits

- Locoregional lymph nodes
 - Mesorectal, superior rectal, inferior mesenteric, internal iliac and obturator lymph nodes;
 - If the tumor extended below the dentate line, inguinal lymph nodes are also considered locoregional lymph nodes.
- For the locoregional (mesorectal, superior rectal, and inferior mesenteric lymph nodes) lymph nodes initial staging, the Dutch Criteria have been adopted by both the ESGAR and the SAR Colorectal and Anal Cancer DFP (Fig. 2.4.2.6.1) [90].
 - These criteria included the short-axis dimension and morphologic characteristics as round shape (A), internal heterogenous architecture (B), irregular border (C) (Fig. 2.4.2.6.2)
 - Suspicious for positive LN:
 - > 9 mm in short axis or greater;
 - 5–8 mm in short axis + 2 morphologic criteria;
 - < 5 mm in short axis + 3 morphologic criteria.

TME (mesorectal, superior, rectal)
<ul style="list-style-type: none"> • Size (short axis) <ul style="list-style-type: none"> • < 5 mm: 3 • 5-9 mm: 2 • >9 mm: suspicious
Internal iliac:
<ul style="list-style-type: none"> • > 7 mm
Obturator
<ul style="list-style-type: none"> • > 7 mm
M1 (inguinal, external iliac, common iliac, retroperitoneal)
<ul style="list-style-type: none"> • > 10 mm

Fig. 2.4.2.6.1. *Criteria for suspicious lymph nodes on initial staging [90]*

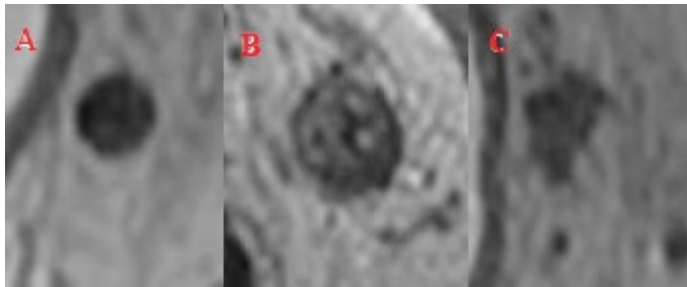


Fig. 2.4.2.6.2. *Morphologic SAR criteria for a positive lymph node*

(A) round; (B) internal heterogenous architecture; (C) irregular border [90].

- Initial staging criteria for suspicious locoregional lateral pelvic side (internal iliac and obturator) lymph nodes:
 - > 7 mm in short axis or greater.
- Restaging criteria after neoadjuvant therapy for suspicious locoregional lymph nodes (Fig. 2.4.2.6.3):
 - The Dutch criteria are no longer applicable;
 - Suspicious for positive LN:
 - mesorectal, superior rectal or inferior mesenteric lymph node measures > 5 mm in the short axis;
 - internal iliac lymph node > 4 mm or an obturator lymph node is > 6 mm in the short axis.

TME (mesorectal, superior, rectal)
• >5 mm
Internal iliac:
• > 4 mm
Obturator
• > 6 mm
M1 (inguinal, external iliac, common iliac, retroperitoneal)
• > 10 mm

Fig. 2.4.2.6.3. *Criteria for suspicious lymph nodes on initial staging [90]*

- Non-locoregional/distant lymph nodes (metastatic disease/M1):
 - External iliac, common iliac, paraaortic, and inguinal lymph nodes;
 - > 10 mm in the short axis – suspicious;
 - malignant features such as parenchymal signal abnormality, abnormal lymph node border, asymmetry and spherical shape.
- Tumor deposit MRI features [88, 109, 111, 159]:
 - contiguity with vein on two orthogonal planes;
 - tumor tissue tapering into the vein (comet tail appearance);
 - irregularity in shape.

2.4.2.7. Evaluation and measurement of apparent diffusion coefficient by magnetic resonance imaging

A radiologist manually marked the regions of interest (ROIs) on consecutive ADC map tumor slices ($b = 1000 \text{ mm}^2/\text{s}$). The average ADC of the rectal mass was determined by selecting three different regions within the tumor across the images. These regions were identified as restricted areas on the ADC map that aligned with their isotropic DWI, enabling the calculation the average ADC value. T2W sequences were utilized to identify the primary tumor and lymph nodes. Each ROI was defined according to the maximum cross-sectional area of the tumor on the ADC map, effectively minimizing the T2W shine-through effect. This approach clearly differentiated the tumor and surrounding normal tissue (Fig. 2.4.2.7.1).

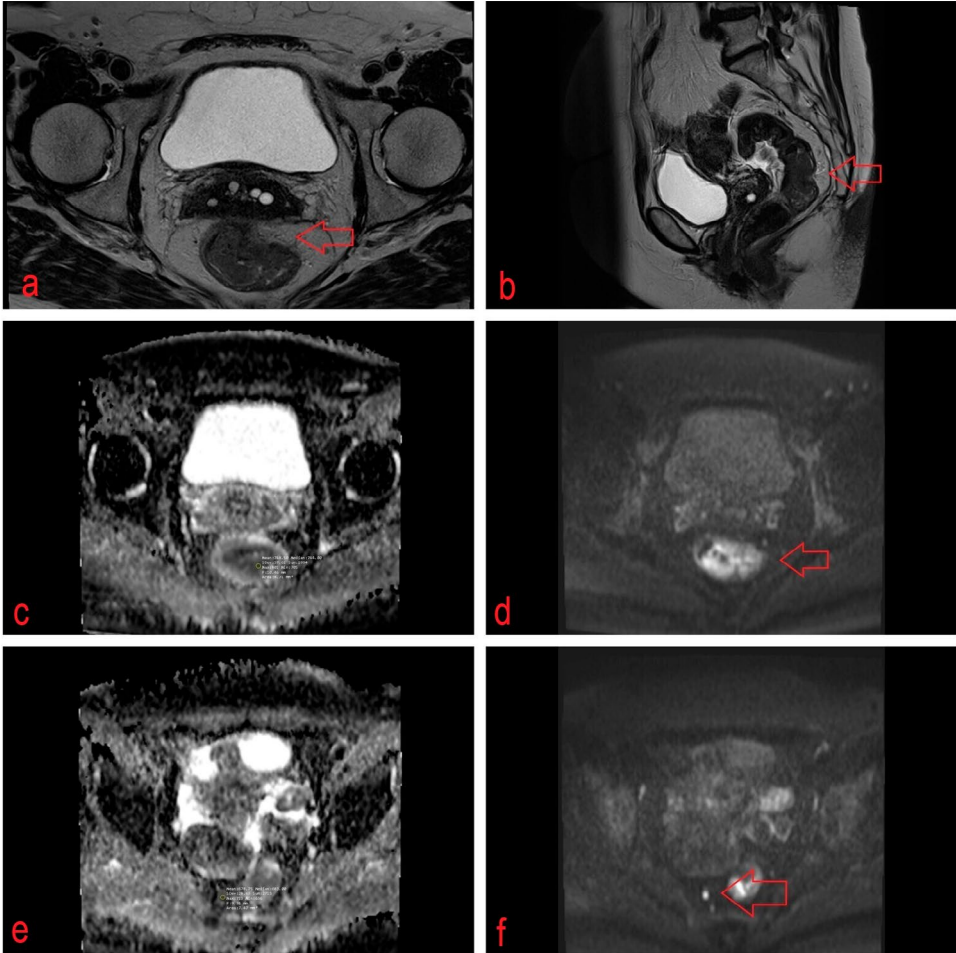


Fig. 2.4.2.7.1. MRI scans of rectal cancer, staged as T3bN2, involving the mesorectal fascia and multiple enlarged mesorectal lymph nodes

The ADC value of rectal cancer was $748 \times 10^{-3} \text{ mm}^2/\text{s}$; the ADC value of a suspicious lymph node was $678 \times 10^{-3} \text{ mm}^2/\text{s}$. (a) Axial T2 (red arrow); (b) Sag T2 (red arrow); (c) rectal cancer ADC map; (e) lymph node ADC map; (d) rectal cancer high-b value ($b = 1000 \text{ s}/\text{mm}^2$) DWI image (red arrow) and (f) lymph node high-b value ($b = 1000 \text{ s}/\text{mm}^2$) DWI image (red arrow).

2.4.2.8. Magnetic resonance imaging volumetry and tumor volume reduction rate

Rectal tumor volume before and after neoadjuvant (CTx or CRT) treatment and TVRR after treatment were evaluated as follows [163]:

- Using T2W axial images, the tumor area in square centimeters (cm²) was measured. This was achieved by manually tracing the tumor boundaries on each image slice to define an irregular ROI (Fig. 2.4.2.8.1).
- This area was multiplied by the slice interval (0.3 cm) to calculate the tumor volume.
- The process was repeated for every tumor slice, and the volumes were added together.
- To determine the extent of tumor reduction after treatment, the TVRR was calculated as follows:

$$\text{TVRR}\% = \frac{\text{Volume 1} - \text{Volume 2}}{\text{Volume 1}} \times 100\%$$

Where Volume 1 indicates the tumor volume measured before treatment, and Volume 2, the tumor volume after treatment.

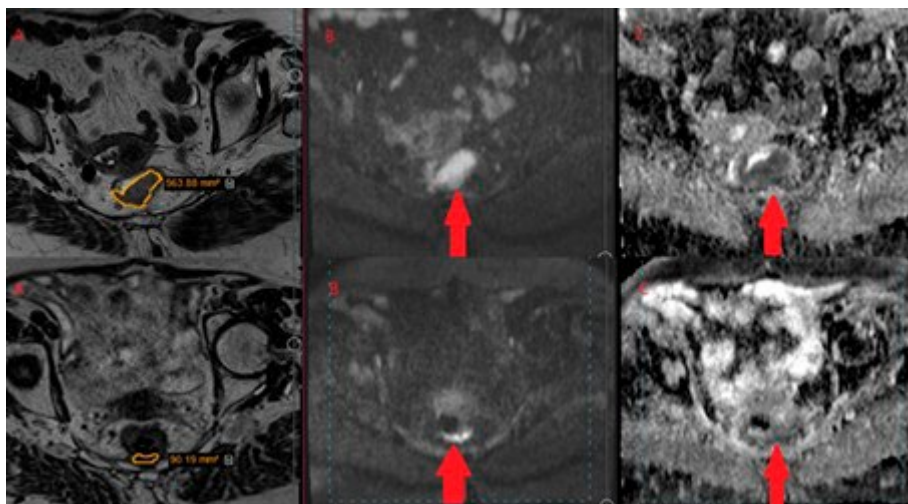


Fig. 2.4.2.8.1. Representative MRI scans of rectal cancer before (upper panel) and after treatment (lower panel) in the same transverse section

(A) T2W image; (B) DWI image; (C) ADC map image. On T2W images, the region of interest is contoured (orange); red arrows show the tumor on DWI images and ADC map images.

2.4.2.9. Magnetic resonance imaging-assessed tumor regression grading

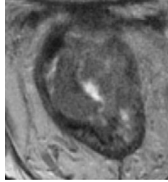
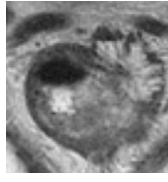
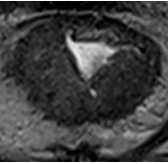
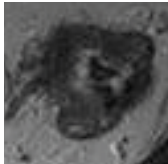
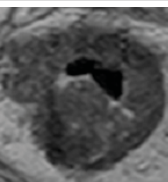
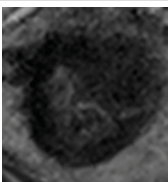
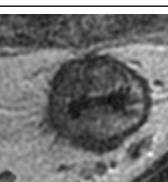

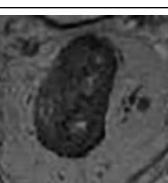
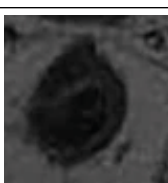
The effectiveness of CTx or CRT in treating rectal cancer was evaluated using the mrTRG classification derived from the methodology employed by the MERCURY study group [137]. This scoring system evaluates the presence of residual tumor and fibrosis as observed on T2-weighted MRI. Furthermore, actual tumor samples were analyzed by certified pathologists who employed the Dworak regression scale to measure the success of the neoadjuvant chemotherapy [164] (Table 2.4.2.9.1). Patients were divided into two groups based on their varying tumor responses, as shown in the MRI results. A score of mrTRG1-2 indicated a good response, while scores of mrTRG3-4-5 indicated a poor response (Table 2.4.2.9.2). This classification was also applied to the responses observed in surgical pathology, where stage pTRG3-4 was classified as a good responder, and pTRG0-1-2 was regarded as a poor responder [165].

Table 2.4.2.9.1. *Magnetic resonance imaging-assessed and pathological tumor regression grade*

MRI Terms	mrTRG	Response	pTRG	Pathology
No regression (intermediate signal intensity, same appearances as original tumor)	mrTRG5	No response	pTRG0	No regression
Slight regression (little areas of low signal intensity fibrosis or mucin but mostly tumor)	mrTRG4	Slight/minimal response	pTRG1	Dominant tumor mass with obvious fibrosis and/or vasculopathy
Moderate regression (low signal intensity fibrosis predominates, but there are obvious areas of intermediate signal intensity)	mrTRG3	Moderate/partial response	pTRG2	Dominantly fibrotic changes with tumor cells or groups (easy to find)
Good regression (predominant low signal intensity fibrosis with no obvious residual tumor signal)	mrTRG2	Near complete response	pTRG3	Very few (difficult to find microscopically) tumor cells in fibrotic tissue with or without mucous substance
Complete regression (absence of tumor signal and barely visible treatment related scar)	mrTRG1	Complete response	pTRG4	No tumor cells, only fibrotic mass (total regression or response)

mrTRG, MRI-assessed tumor regression grade; pTRG, pathological tumor regression grade.

Table 2.4.2.9.2. *Magnetic resonance imaging-assessed tumor regression grade*

Grade	Response	Initial MR staging	Restaging
mrTRG5	No regression (0 % fibrosis)		
mrTRG4	Slight regression (25 % fibrosis)		
mrTRG3	Moderate regression (50 % fibrosis)		
mrTRG2	Good regression (75 % fibrosis)		
mrTRG1	Complete regression (100 % fibrosis)		

mrTRG, MRI-assessed tumor regression grade.

2.5. Statistical analysis

Statistical analysis was performed using ©SPSS for Windows 23.0™ software and ©Microsoft Excel 16™. The Shapiro–Wilk test was used to check continuous data distribution. Data that were found to be normally distributed were expressed as mean with standard deviation (SD) and compared with the Student’s t test (parametric test). Nonnormally distributed continuous data were expressed as median with interquartile range (IQR) and compared with the Mann–Whitney U test (nonparametric test). Categorical data were

provided as number with percentage, and the chi-square (χ^2) criterion was used to compare such data. To compare continuous data of more than two groups, one-way ANOVA was used. The coincidence rate was calculated as follows:

$$\text{Coincidence rate \%} = \frac{\text{Total number of observations}}{\text{Number of agreements}} \times 100\%$$

Receiver operating characteristic (ROC) curves were generated to determine optimal cut-off values yielding best areas under the curves (AUC), specificity, and sensitivity. Moreover, a positive predictive value (PPV) and a negative predictive value (NPV) were calculated. Sensitivity and specificity were computed according to the following formulas:

$$\text{Sensitivity \%} = \frac{a}{a + c} \times 100\%$$

$$\text{Specificity \%} = \frac{d}{b + d} \times 100\%$$

where a is the number of true-positive cases; b, number of false-positive cases; c, the number of false-negative cases; d, the number of true-negative cases. *P* values less than 0.05 were considered to be statistically significant.

The required minimum number of patients to get statistically reliable conclusions was calculated using the formula:

$$n = \frac{z^2 \nu(1-\nu)}{\Delta^2}$$

ν – the frequency of the event; z – normal distribution $N(0,1)$ $\frac{1+P}{2}$ quantum; Δ – the probability assessment accuracy. The frequency of events was based on the European population study, and the disease incidence rate in the Eastern European centers was 12.7 %. The minimum number of patients to get reliable results was 85.

3. RESULTS

3.1. Characteristics of the study population

The study included 89 patients with rectal cancer. The overall age of the study population varied from 37 to 83 years, with a mean age of 64.26 years (SD 9.17). There were 67.4 % (n = 60) of men and 32.6 % (n = 29) of women. Table 3.1.1 shows the demographic characteristics of the patients by the groups. The CTx group consisted of 40 patients: 27 males (67.5 %) and 13 females (32.5 %). Meanwhile, the CRT group consisted of 49 patients: 33 (67.3 %) males and 16 (32.7 %) females. Both the groups were matched for age and sex (p > 0.05).

Table 3.1.1. Characteristics of patients in the chemotherapy and chemoradiotherapy groups

Characteristic	CTx group (n = 40)	CRT group (n = 49)	p
Age, mean (SD), years	61.58 (8.81)	66.45 (8.95)	0.36
Female	13 (32.5)	16 (32.7)	0.63
Male	27 (67.5)	33 (67.3)	

Values are number (percentage) unless stated otherwise. CTx, chemotherapy; CRT, chemoradiotherapy.

3.2. Location of the tumor

In the CTx group (n = 40), 12 patients (30 %) had rectal cancer in the lower third of the rectum; 13 (32.5 %), in the mid third of the rectum; and 15 (37.5 %), in the upper third of the rectum. Meanwhile, the corresponding distribution of 49 patients in the CRT group by the location of rectal cancer was as follows: 18 (36.73 %), 21 (42.86 %), and 10 (20.41 %), respectively. There were no significant differences in the distribution of patients by the location of rectal cancer between the CTx and CRT groups (p = 0.24).

3.3. Characteristics of the tumor stage

3.3.1. T and N stage

MRI scans of patients in the CTx group (n = 40) at the time of initial diagnosis classified 16 patients (40.0 %) as stage T3b and 5 patients (12.5 %) as stage T3d (Table 3.3.1.1). Significant changes in disease staging were observed after CTx. Specifically, 2 patients (5.0 %) showed no evidence of the disease and were classified as T0. Additionally, 19 patients (47.5 %)

were categorized as stage T3b. These changes were statistically significant ($p = 0.001$).

Table 3.3.1.1. *Distribution of patients by MRI-assessed T and N stages before and after treatment in the chemotherapy and chemoradiotherapy groups*

Stage	CTx group (n = 40)		p	CRT group (n = 49)		p
T stage	mrT	ymrT		mrT	ymrT	
T0	0	2 (5)	0.001	0	4 (8.2)	0.060
T1	0	0		0	0	
T2	0	6 (15)		3 (6.1)	0	
T3a	0	10 (25)		19 (38.8)	8 (16.3)	
T3b	16 (40)	19 (47.5)		14 (28.5)	37 (75.5)	
T3c	13 (32.5)	2 (5)		7 (14.3)	0	
T3d	5 (12.5)	1 (2.5)		6 (12.2)	0	
T4a	6 (15.0)	0		0	0	
N stage	mrN	ymrN	0.001	mrN	ymrN	0.001
N0	0	15 (37.5)		1 (2)	19 (38.8)	
N1	13 (32.5)	11 (27.5)		17 (34.7)	27 (55.1)	
N2	27 (67.5)	14 (35.0)		31 (63.3)	3 (6.1)	

Values are numbers (%). CTx; chemotherapy, CRT; chemoradiotherapy; mrT, MRI-assessed T stage before treatment; ymrT, MRI-assessed T stage after treatment; mrN, MRI-assessed N stage before treatment; ymrN, MRI-assessed N stage after treatment.

Initial MRI scans of patients in the CRT group (n = 49) classified 3 patients (6.1 %) as stage T2, while 19 patients (38.8 %) were categorized as T3a. After treatment, the results showed changes with 4 patients (8.2 %) classified as T0 and 37 patients (75.5 %) as stage T3b. However, these changes were not statistically significant ($p = 0.06$).

In the CTx group, initial nodal staging identified 32.5 % of patients as N1 and 67.5 % as N2. Following treatment, 37.5 % of the patients were classified as N0; 27.5 %, as N1; and 35.0 %, as N2 ($p = 0.001$). In the CRT group (n = 49), initial nodal staging classified 2.0 % of patients as N0, 34.7 % as N1, and 63.0 % as N2. Post-treatment results revealed significant changes, with 38.8 % of patients classified as N0; 55.1 %, as N1; and 6.1 %, as N2 ($p = 0.001$) (Table 3.3.1.1).

3.3.2. Associations of tumor T and N stage with pathological results

The results of pathological analysis differed in the CTx and CRT groups (Table 3.3.2.1). In the CTx group (n = 40), the pathologically confirmed tumor stages were as follows: 4 patients (10.0 %) were classified as T0, 1

patient (2.5 %) as T1, 8 patients (20.0 %) as T2, and 27 patients (67.5 %) as T3. Pathologically confirmed nodal staging showed 52.5 % of patients as N0, 37.5 % as N1, and 10.0 % as N2.

Table 3.3.2.1. *Distribution of patients by MRI-assessed T and N stages after treatment and pathologically confirmed T and N stages in the chemotherapy and chemoradiotherapy groups*

Stage	CTx group (n = 40)		p	CRT group (n = 49)		p		
	ymrT	pT		ymrT	pT			
T0	2 (5)	4 (10)	0.008	4 (8.2)	9 (18.4)	0.001		
T1	0	1 (2.5)		0	2 (4.1)			
T2	6 (15)	8 (20)		0	9 (18.4)			
T3a	10 (25)	27 (67.5)		8 (16.3)	29 (59.2)			
T3b	19 (47.5)			37 (75.5)				
T3c	2 (5)			0				
T3d	1 (2.5)			0				
T4a	0	0		0	0			
N stage	ymrN	pN			ymrN		pN	
N0	15 (37.5)	21 (52.5)		0.001	19 (38.8)		33 (67.3)	0.001
N1	11 (27.5)	15 (37.5)	27 (55.1)		12 (24.5)			
N2	14 (35.0)	4 (10.0)	3 (6.1)		4 (8.2)			

Values are numbers (%). CTx; chemotherapy, CRT; chemoradiotherapy; ymrT, MRI-assessed T stage after treatment; pT, pathological T stage; ymrN, MRI-assessed N stage after treatment; pN, pathological N stage.

In the CRT group (n = 49) pathological tumor stages were as follows: 9 patients (18.4 %) were classified as T0, 2 patients (4.1 %) as T1, 9 patients (18.4 %) as T2, and 29 patients (59.2 %) as T3. Pathologically confirmed nodal staging in this group revealed 67.3 % of patients as N0, 24.5 % as N1, and 8.2 % as N2.

The evaluation of treatment outcomes in patients with rectal cancer demonstrated significant reductions in T and N staging following treatment, though N staging showed inferior and limited results compared to T staging. In the CTx group, the coincidence rate between ymrT and pT was 77.5 % (p = 0.008), and the coincidence rate between ymrN and pN was 51.4 % (p = 0.001). In the CRT group, the coincidence rate between ymrT and pT was 79.4 % (p = 0.001), and the coincidence rate between ymrN and pN was 56.4 % (p = 0.001).

Sensitivity, specificity, PPV, and NPV between ymrT and pT as well as between ymrN and pN were calculated (Table 3.3.2.2).

Table 3.3.2.2. Diagnostic performance between MRI-assessed T stage after treatment and pathological T stage as well as MRI-assessed N stage after treatment and pathological N stage

Parameter	CTx group (n = 40)		CRT group (n = 49)		CTx + CRT group (n = 89)	
	ymrT vs. pT	ymrN vs. pN	ymrT vs. pT	ymrN vs. pN	ymrT vs. pT	ymrN vs. pN
Sensitivity, %	83.33	75.00	84.56	69.39	79.49	67.53
Specificity, %	83.00	68.80	87.20	76.00	80.00	71.65
PPV, %	80.00	75.00	83.20	69.39	80.00	72.00
NPV, %	85.71	73.00	77.00	70.56	80.00	73.65

CTx, chemotherapy; CRT, chemoradiotherapy; PPV, positive predictive value; NPV, negative predictive value; ymrT, MRI-assessed T stage after treatment; pT, pathological T stage; ymrN, MRI-assessed N stage after treatment; pN, pathological N stage.

3.4. Involvement of mesorectal fascia and circumferential resection margin

In the CTx group (n = 40), MRI identified 20 patients (50.0 %) as MRF-negative (MRF-) and 20 patients (50.0 %) as MRF-positive (MRF+). In the CRT group (n = 49), MRI staging revealed 20 patients (40.8 %) as MRF- and 29 patients (59.2 %), as MRF+ (Table 3.4.1). Pathological analysis revealed 35 patients (87.5 %) as CRM-negative (CRM-) and 5 patients (12.5 %) as CRM-positive (CRM+) in the CTx group. In the CRT group, there were 46 patients (93.9 %) identified as CRM- and 3 patients (6.1 %), as CRM+.

Table 3.4.1. Distribution of patients by the involvement of mesorectal fascia and circumferential resection margin in the chemotherapy and chemoradiotherapy groups

Status	CTx group (n = 40)		p	CRT group (n = 49)		p
	mrMRF	ymrMRF		mrMRF	ymrMRF	
Negative (-)	20 (50)	28 (70)	0.110	20 (40.8)	38 (77.6)	0.001
Positive (+)	20 (50)	12 (30)		29 (59.2)	11 (22.4)	
	ymrMRF	pCRM	0.101	ymrMRF	pCRM	0.043
Negative (-)	28 (70)	35 (87.5)		38 (77.6)	46 (93.9)	
Positive (+)	12 (30)	5 (12.5)		11 (22.4)	3 (6.1)	

Values are numbers (%). CTx, chemotherapy; CRT, chemoradiotherapy; mrMRF, MRI-assessed mesorectal fascia before treatment; ymrMRF, MRI-assessed mesorectal fascia after treatment; pCRM, pathological circumferential resection margin.

Both treatment groups demonstrated an increase in the percentage of patients classified as MRF-negative after treatment. However, only in the CRT

group a statistically significant improvement was observed ($p = 0.001$). The CTx group showed no statistically significant difference in the percentage of patients by MRI-assessed MRF status before and after treatment ($p = 0.110$). Pathological analysis indicated a higher proportion of CRM-negative patients in both groups after treatment. However, this difference was statistically significant only in the CRT group ($p = 0.043$), whereas the CTx group showed no significant difference between ymrMRF and pCRM ($p = 0.101$).

The overall coincidence rate between ymrMRF and pCRM status in the combined CTx and CRT group was 70.8 %. The corresponding coincidence rates in the CTx and CRT groups were 80.0 % and 63.3 %, respectively (Table 3.4.2). Sensitivity, specificity, PPV, and NPV for these parameters were calculated as well.

Table 3.4.2. *Coincidence rates and diagnostic performance between MRI-assessed mesorectal fascia and pathologically confirmed circumferential resection margin after treatment in the chemotherapy, chemoradiotherapy, and combined groups*

Parameter	CTx group (n = 40)	CRT group (n = 49)	Combined CTx + CRT group (n = 89)
Coincidence rate, %	80.0	63.3	70.8
Sensitivity, %	41.67	60.00	50.00
Specificity, %	83.33	88.37	85.56
PPV, %	41.67	54.55	47.83
NPV, %	83.33	90.48	86.96

Coincidence rate calculated between MRI-assessed mesorectal fascia after treatment and pathological circumferential resection margin. CTx, chemotherapy; CRT, chemoradiotherapy; PPV, positive predictive value; NPV, negative predictive value.

3.5. Extramural vascular invasion and extramural vascular invasion score

Following neoadjuvant treatment, the proportion of patients with negative EMVI status (evaluated by a radiologist) or lymphovascular invasion (LVI) (proven by a pathologist) increased in both the CTx and CRT groups (Table 3.5.1). However, this change was statistically significant in the CTx group ($p = 0.024$) but not significant in the CRT group ($p = 0.838$).

Pathological analysis after treatment revealed no significant differences in the proportions of patients by the EMVI status in both groups ($p = 0.482$ and $p = 1.00$ for the CTx and CRT groups, respectively). Both the CTx and CRT groups showed a significant decrease in the percentages of patients having greater EMVI scores after treatment ($p = 0.001$ for both groups).

Table 3.5.1. Distribution of patients by the status and score of extramural vascular invasion in the chemotherapy and chemoradiotherapy groups

Parameter	CTx group (n = 40)		p	CRT group (n = 49)		p
	mrEMVI	ymrEMVI		mrEMVI	ymrEMVI	
EMVI-	17 (42.5)	28 (70)	0.024	27 (55.1)	29 (59.2)	0.838
EMVI+	23 (57.5)	12 (30)		22 (44.9)	20 (40.8)	
	ymrEMVI	pLVI	0.482	ymrEMVI	pLVI	1.0
EMVI-	28 (70)	24 (60)		34 (69.4)	34 (69.4)	
EMVI+	12 (30)	16 (40)		15 (30.6)	15 (30.6)	
EMVI score	Before treatment	After treatment	0.001	Before treatment	After treatment	0.001
0	17 (42.5)	28 (70.0)		26 (53.1)	34 (69.4)	
1	0	0		2 (4.1)	0	
2	0	6 (15.0)		2 (4.1)	2 (4.1)	
3	13 (32.5)	5 (12.5)		10 (20.4)	9 (18.4)	
4	10 (25.0)	1 (2.5)		9 (18.4)	4 (8.2)	

Values are numbers (%). CTx, chemotherapy; CRT, chemoradiotherapy; mrEMVI, extramural vascular invasion before treatment; ymrEMVI, extramural vascular invasion after treatment; pLVI, pathological lymphovascular invasion.

The overall coincidence rate between ymrEMVI and pLVI status in the combined CTx and CRT group was 91.25 %, with high sensitivity (88.57 %), specificity (93.55 %), PPV (88.57 %), and NPV (93.55 %) observed (Table 3.5.2). The coincidence rate was 82.5 % in the CTx group and 100.00 % in the CRT group, reflecting superior accuracy in the CRT cohort.

Table 3.5.2. Coincidence rates and diagnostic performance between MRI-assessed extramural vascular invasion and pathologically confirmed lymphovascular invasion after treatment in the chemotherapy, chemoradiotherapy, and combined groups

Parameter	CTx group (n = 40)	CRT group (n = 49)	Combined CTx + CRT group (n = 89)
Coincidence rate, %	82.5	100.00	91.25
Sensitivity, %	80.00	100.00	88.57
Specificity, %	85.71	100.00	93.55
PPV, %	80.00	100.00	88.57
NPV, %	85.71	100.00	93.55

Coincidence rate calculated between MRI-assessed extramural vascular invasion and pathological lymphovascular invasion after treatment. CTx, chemotherapy; CRT, chemoradiotherapy; PPV, positive predictive value; NPV, negative predictive value.

3.6. Diffusion-weighted imaging and apparent diffusion coefficient

3.6.1. Apparent diffusion coefficient and T stage before treatment

In this study, the mean tumor ADC value before treatment was 699.75 (SD 95.35) $\times 10^{-3}$ mm²/s in the CTx group and 708.88 (SD 114.57) $\times 10^{-3}$ mm²/s in the CRT group. When considering both groups together, the mean tumor ADC value before treatment was 704.32 (SD 104.96) $\times 10^{-3}$ mm²/s. Table 3.6.1.1 shows the ADC_{min}, ADC_{mean}, and ADC_{max} values of tumors by the T stage in both the groups before treatment. No significant differences were found comparing ADC_{min}, ADC_{mean}, and ADC_{max} values separately by the T stage in both the groups.

Table 3.6.1.1. ADC_{min}, ADC_{mean}, and ADC_{max} values of tumors by the T stage before treatment in the chemotherapy and chemoradiotherapy groups

Stage	CTx group (n = 40)			CRT group (n = 49)		
	T ADC _{min}	T ADC _{mean}	T ADC _{max}	T ADC _{min}	T ADC _{mean}	T ADC _{max}
T0	–	–	–	–	–	–
T1	–	–	–	–	–	–
T2	–	–	–	709.64 (69.92)	775.16 (51.60)	940.67 (80.60)
T3a	–	–	–	691.21 (118.03)	847.18 (82.84)	1003.16 (111.91)
T3b	605.38 (29.44)	811.12 (84.36)	1016.88 (127.06)	665.14 (114.89)	843.53 (98.75)	1021.93 (155.42)
T3c	663.39 (17.95)	783.69 (40.00)	1004.00 (83.37)	656.43 (148.31)	835.35 (90.07)	1014.29 (92.40)
T3d	623.00 (35.38)	789.30 (93.94)	955.60 (121.52)	651.00 (92.45)	818.25 (55.13)	985.50 (116.09)
T4a	644.17 (36.01)	837.33 (61.17)	1030.50 (147.47)	–	–	–
p value	0.324	0.438	0.724	0.793	0.696	0.865
RV	1228.28 (124.82)			1219.80 (128.44)		

Values are mean (SD). CTx, chemotherapy; CRT, chemoradiotherapy; T ADC, tumor apparent diffusion coefficient before treatment; RV, “healthy” rectal wall.

The ROC curve analysis showed that an optimal cut-off ADC value to discriminate between the healthy and invaded rectal wall was 705 $\times 10^{-3}$ mm²/s (Fig. 3.6.1.1) with an AUC of 0.688 (p < 0.001), sensitivity of 75 %, and specificity of 73 %.

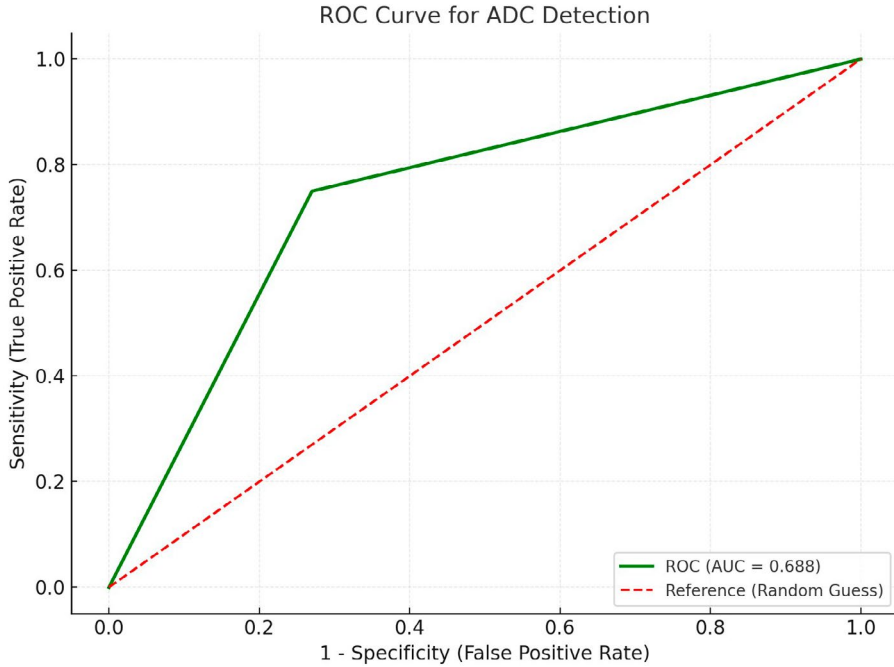


Fig. 3.6.1.1. *The receiver operating characteristic (ROC) curve for an optimal apparent diffusion coefficient (ADC) cut-off value to distinguish the healthy from the invaded rectal wall before treatment*

The optimal cut-off value was $705 \times 10^{-3} \text{ mm}^2/\text{s}$; the AUC was 0.688.

3.6.2. Apparent diffusion coefficient and N stage before treatment

Before treatment, the mean overall ADC values of lymph nodes in the CTx and CRT groups were similar (639.33 , $SD 71.83 \times 10^{-3} \text{ mm}^2/\text{s}$ and 654.39 , $SD 71.83 \times 10^{-3} \text{ mm}^2/\text{s}$, respectively). Table 3.6.2.1 shows the ADC_{\min} , ADC_{mean} , and ADC_{\max} values of lymph nodes by the N stage in both the groups before treatment. No significant differences were found comparing ADC_{\min} , ADC_{mean} , and ADC_{\max} values separately by the N stage in both the groups.

Table 3.6.2.1. ADC_{min} , ADC_{mean} , and ADC_{max} values of lymph nodes by the N stage before treatment in the chemotherapy and chemoradiotherapy groups

Stage	CTx group (n = 40)			CRT group (n = 49)		
	N ADC _{min}	N ADC _{mean}	N ADC _{max}	N ADC _{min}	N ADC _{mean}	N ADC _{max}
N0	–	–	–	779.00 (00.00)	950.50 (00.00)	922.00 (00.00)
N1	688.00 (106.51)	788.42 (67.51)	988.85 (107.59)	638.59 (132.30)	911.59 (86.77)	984.53 (122.17)
N2	605.41 (91.09)	810.63 (72.02)	1015.85 (118.69)	581.94 (102.80)	846.50 (79.29)	911.06 (119.51)
p value	0.595	0.358	0.492	0.290	0.149	0.476
ILN	844.05 (102.80)			858.05 (102.08)		

Values are mean (SD). CTx, chemotherapy; CRT, chemoradiotherapy; N ADC, lymph node apparent diffusion coefficient before treatment; ILN, “healthy” inguinal lymph node.

The ROC curve analysis revealed that an optimal cut-off ADC value allowing to distinguish benign from malignant lymph nodes was $655 \times 10^{-3} \text{ mm}^2/\text{s}$ (Fig. 3.6.2.1) with an AUC of 0.508 ($p < 0.001$), sensitivity of 58 % and a specificity of 60 %.

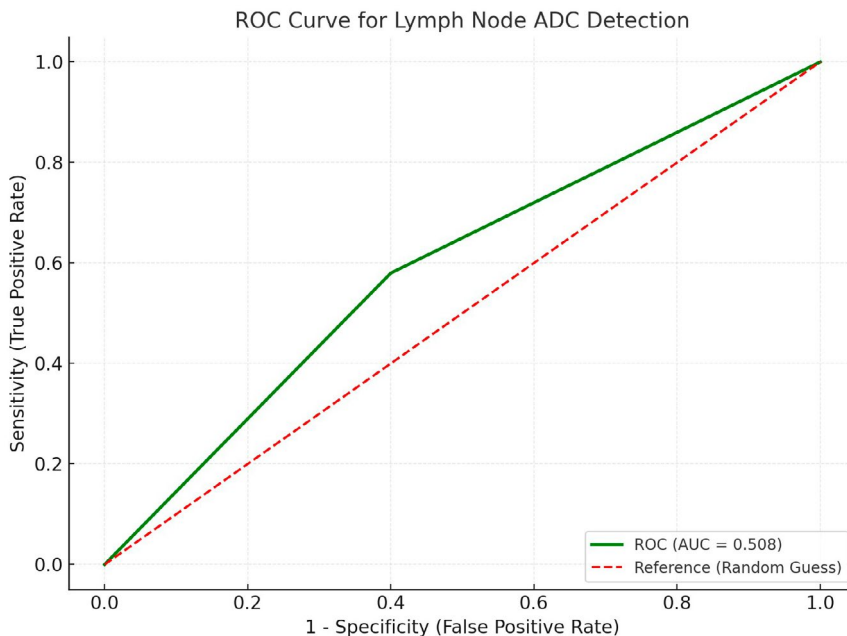


Figure 3.6.2.1. The receiver operating characteristic (ROC) curve for an optimal apparent diffusion coefficient (ADC) cut-off value to distinguish benign from malignant lymph nodes before treatment

The optimal cut-off value was $655 \times 10^{-3} \text{ mm}^2/\text{s}$; the AUC was 0.508.

3.6.3. Apparent diffusion coefficient and T stage after treatment

After treatment, the mean overall ADC values increased in both groups, reaching 890.35 (SD 105.81) $\times 10^{-3}$ mm²/s in the CTx group and 999.41 (SD 115.97) $\times 10^{-3}$ mm²/s in the CRT group. Table 3.6.3.1 shows the ADC_{min}, ADC_{mean}, and ADC_{max} values of tumors by the T stage in both the groups after treatment. No significant differences were found comparing ADC_{min}, ADC_{mean}, and ADC_{max} values separately by the T stage in both the groups.

Table 3.6.3.1. ADC_{min}, ADC_{mean}, and ADC_{max} values of tumors by the T stage after treatment in the chemotherapy and chemoradiotherapy groups

yT	CTx group (n = 40)			CRT group (n = 49)		
	yT ADC _{min}	yT ADC _{mean}	yT ADC _{max}	yT ADC _{min}	yT ADC _{mean}	yT ADC _{max}
T0	822.00 (32.52)	926.00 (0.70)	1030.00 (31.11)	874.25 (85.63)	969.62 (77.46)	1065.00 (102.12)
T1	–	–	–	–	–	–
T2	761.33 (137.00)	928.33 (124.59)	1095.33 (125.54)	–	–	–
T3a	7837.10 (75.44)	907.00 (85.65)	1076.90 (161.81)	840.38 (138.46)	940.25 (90.34)	1040.13 (114.45)
T3b	725.95 (108.41)	911.57 (87.47)	1097.21 (138.64)	804.08 (110.32)	948.40 (85.78)	1092.73 (149.59)
T3c	751.00 (72.12)	903.50 (1.00)	955.50 (74.24)	–	–	–
T3d	636.00 (00.00)	909.50 (00.00)	983.00 (00.00)	–	–	–
T4a	–	–	–	–	–	–
p value	0.256	0.217	0.559	0.150	0.855	0.619
RV	1227.67(169.29)			1219.80 (148.13)		

Values are mean (SD). CTx, chemotherapy; CRT, chemoradiotherapy; yT ADC, tumor apparent diffusion coefficient after treatment; RV, “healthy” rectal wall.

The ADC value after treatment was higher in the CRT group (Fig. 3.6.3.1).

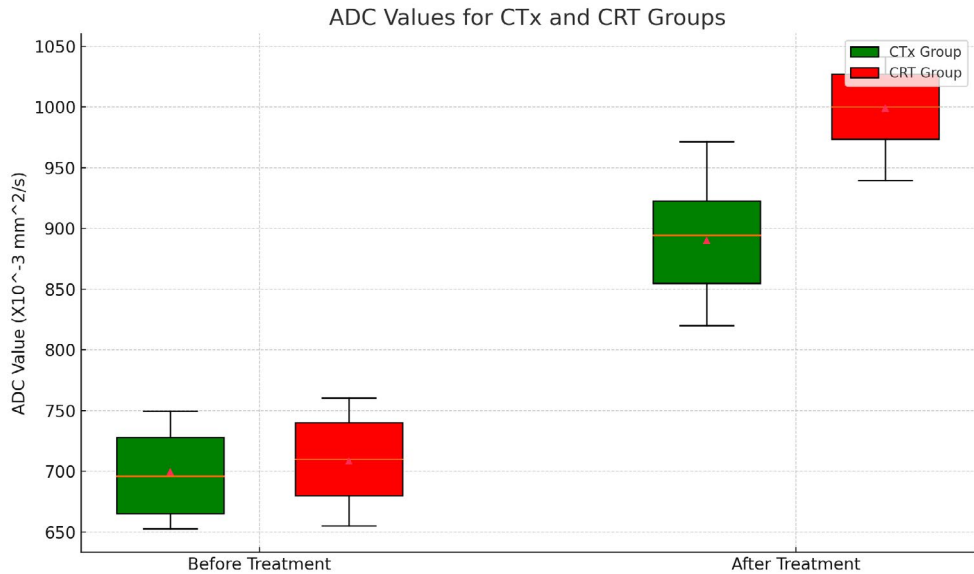


Fig. 3.6.3.1. *Boxplots showing tumor apparent diffusion coefficient values in both treatment groups before and after treatment*

ADC values are given $\times 10^{-3}$ mm²/s. CTx, chemotherapy; CRT, chemoradiotherapy; ADC, apparent diffusion coefficient.

The ROC curve analysis showed that an optimal cut-off ADC value after treatment to discriminate between the healthy and invaded rectal wall was 991×10^{-3} mm²/s (Fig. 3.6.3.2) with an AUC of 0.772 ($p < 0.001$), sensitivity of 75 %, and specificity of 73 %.

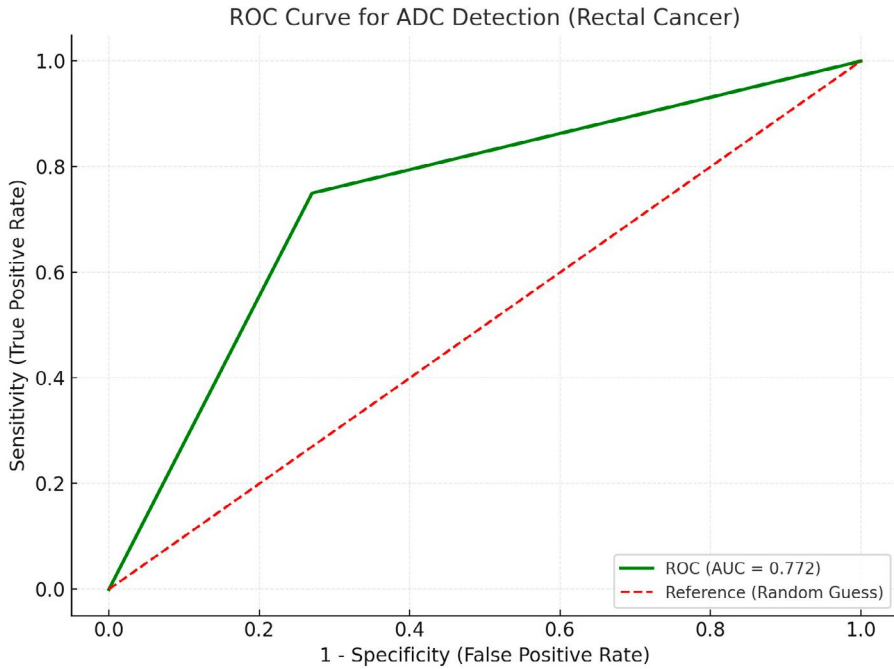


Fig. 3.6.3.2. The receiver operating characteristic (ROC) curve for an optimal apparent diffusion coefficient (ADC) cut-off value to distinguish the healthy from the invaded rectal wall after treatment

The optimal cut-off value was $991 \times 10^{-3} \text{ mm}^2/\text{s}$; the AUC was 0.772.

3.6.4. Apparent diffusion coefficient and N stage after treatment

After treatment, both groups significantly increased ADC values (Table 3.6.4.1). No significant differences were found comparing ADC_{\min} , ADC_{mean} , and ADC_{\max} values separately by the N stage in both the groups.

Table 3.6.4.1. ADC_{\min} , ADC_{mean} , and ADC_{\max} values of tumors by the N stage after treatment in the chemotherapy and chemoradiotherapy groups

yN	CTx group (n = 40)			CRT group (n = 49)		
	yN ADC_{\min}	yN ADC_{mean}	yN ADC_{\max}	yN ADC_{\min}	yN ADC_{mean}	yN ADC_{\max}
N0	849.80 (112.71)	923.96 (98.39)	1098.13 (134.06)	811.21 (125.37)	969.86 (68.60)	1128.53 (102.49)
N1	828.36 (117.74)	916.68 (96.49)	1105.00 (112.79)	888.96 (108.88)	933.96 (89.31)	1078.96 (158.80)
N2	811.07 (91.66)	891.78 (90.56)	1172.50 (166.09)	918.67 (154.37)	949.00 (133.92)	1079.33 (193.45)

Table 3.6.4.1 cont.

yN	CTx group (n = 40)			CRT group (n = 49)		
	yN ADC _{min}	yN ADC _{mean}	yN ADC _{max}	yN ADC _{min}	yN ADC _{mean}	yN ADC _{max}
p value	0.626	0.645	0.825	0.787	0.373	0.495
yILN	876.20 (70.19)			899.80 (71.92)		

Values are mean (SD). CTx, chemotherapy; CRT, chemoradiotherapy; yN ADC, lymph node apparent diffusion coefficient after treatment; yILN, “healthy” inguinal lymph node after treatment.

Specifically, the CTx group reported lymph nodes ADC value of 755.38 (SD 105.81) $\times 10^{-3}$ mm²/s, while the CRT group showed a slightly higher ADC value of 884.78 (SD 73.22) $\times 10^{-3}$ mm²/s (Fig. 3.6.4.1). The CRT group lymph nodes showed significantly higher ADC values than CTx lymph nodes ($p < 0.001$), and CTx lymph nodes were significantly lower than healthy inguinal lymph nodes ($p < 0.001$), while CRT lymph nodes demonstrated no significant difference from healthy lymph nodes ($p = 0.058$).

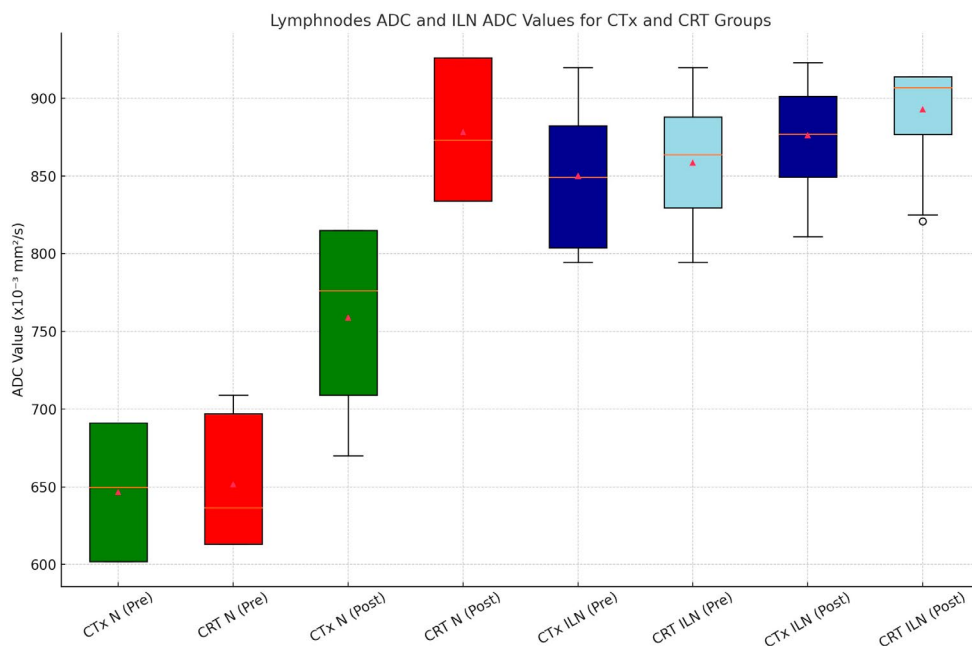


Fig. 3.6.4.1. Boxplots for the nodal ADC in the CTx and CRT group and “healthy” inguinal lymph nodes before and after treatment

ADC values are given $\times 10^{-3}$ mm²/s. CTx or CRT N_ADC Before – lymph nodes ADC mean before CTx or CRT, CTx or CRT N_ADC After – lymph nodes ADC mean after CTx or CRT, CTx or CRT ILN Before/After – “healthy” inguinal lymph nodes ADC mean before and after treatment.

The ROC curve analysis revealed that an optimal cut-off ADC value allowing to distinguish benign from malignant lymph nodes after treatment was $770 \times 10^{-3} \text{ mm}^2/\text{s}$ (Fig. 3.6.4.2) with an AUC of 0.609 ($p < 0.001$), sensitivity of 62 % and a specificity of 67 %.

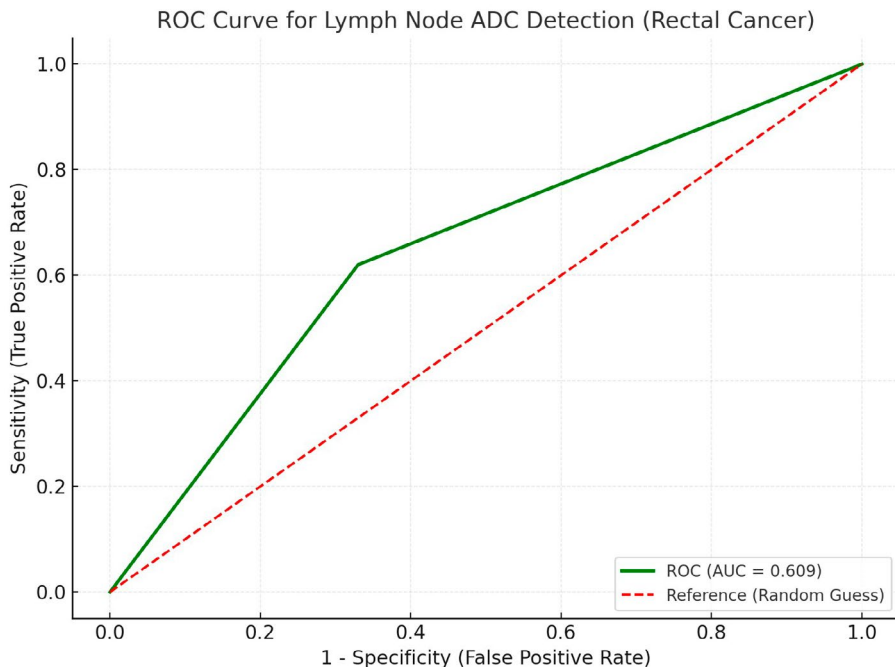


Fig. 3.6.4.2. The receiver operating characteristic (ROC) curve for an optimal apparent diffusion coefficient (ADC) cut-off value to distinguish benign from malignant lymph nodes after treatment

The optimal cut-off value was $770 \times 10^{-3} \text{ mm}^2/\text{s}$; the AUC was 0.609.

3.6.5. Associations between apparent diffusion coefficient and extramural vascular invasion

The study compared CTx and CRT groups, which were divided into two categories based on the presence or absence of EMVI (EMVI– and EMVI+). The measurements were related to the T ADC values, which were often used in imaging to assess tissue characteristics. Before treatment, the mean T ADC_{min}, ADC_{mean}, and ADC_{max} values were the same in both EMVI groups ($p = 0.974$, $p = 0.143$, $p = 0.074$ in the CTx group, and $p = 0.539$, $p = 0.801$, $p = 0.347$ in the CRT group, respectively). After treatment, despite the mean T ADC_{min}, ADC_{mean}, and ADC_{max} values increased, no significant differences

comparing the EMVI– and EMVI+ groups were found ($p = 0.773$, $p = 0.111$, $p = 0.051$ in the CTx group, and $p = 0.102$, $p = 0.620$, $p = 0.462$ in the CRT group, respectively) (Table 3.6.5.1). There were no significant changes in T ADC values between the CTx and CRT groups, regardless of EMVI status before or after treatment.

Table 3.6.5.1. Relationships between T ADC parameters and EMVI

Before treatment	CTx group (n = 40)		p	CRT group (n = 49)		p
	EMVI–	EMVI+		EMVI–	EMVI+	
T ADC _{min}	699.18 (103.24)	700.17 (91.45)	0.974	778.07 (120.25)	757.59 (108.90)	0.539
T ADC _{mean}	884.32 (68.06)	917.52 (70.38)	0.143	933.74 (87.74)	939.88 (80.19)	0.801
T ADC _{max}	1069.47 (87.66)	1134.87 (125.55)	0.074	1089.41 (118.41)	1122.18 (122.04)	0.347
After treatment	CTx group (n = 40)		p	CRT group (n = 49)		p
	EMVI–	EMVI+		EMVI–	EMVI+	
T ADC _{min}	833.57 (109.51)	822.83 (100.85)	0.773	917.41 (122.76)	858.60 (89.49)	0.102
T ADC _{mean}	1026.21 (98.18)	974.50 (74.21)	0.111	1052.83 (84.45)	1039.66 (86.67)	0.620
T ADC _{max}	1218.86 (136.68)	1126.17 (123.80)	0.051	1188.26 (142.48)	1220.73 (138.16)	0.462

Values are mean (SD). CTx, chemotherapy; CRT, chemoradiotherapy; ADC, apparent diffusion coefficient; EMVI, extramural vascular invasion.

3.7. Magnetic resonance imaging volumetry and tumor volume reduction rate

Analysis of the tumor volume and TVRR revealed that the median tumor volume before treatment was similar between the CTx and CRT groups, with no statistically significant difference ($p = 0.73$) (Table 3.7.1). However, a significant difference in tumor volumes was observed after treatment, with the CRT group having a lower median tumor volume compared to the CTx group (19.85 cm³, IQR 15.5–25.52 vs. 28.4 cm³, IQR 22.04–39.56; $p < 0.001$). Moreover, the TVRR was significantly higher in the CRT group, indicating a greater tumor volume reduction compared to the CTx group (53.3 %, IQR 41.9 %–67.5 % vs. 31.1 %, IQR 25.6 %–40.9 %; $p < 0.001$).

Table 3.7.1. Tumor volumes and tumor volume reduction rates before and after treatment in the chemotherapy and chemoradiotherapy groups

Parameter	CTx (n = 40)	CRT (n = 49)	p
Volume before treatment, cm ³	46.75 (34.74–59.81)	46.5 (34.0–57.1)	0.73
Volume after treatment, cm ³	28.4 (22.04–39.56)	19.85 (15.5–25.52)	< 0.001
TVRR, %	31.1 (25.6–40.9)	53.3 (41.9–67.5)	< 0.001

Values are median (interquartile range). CTx, chemotherapy; CRT, chemoradiotherapy, TVRR, tumor volume reduction rate.

The particular cut-off values for TVRR in the CTx and CRT groups were calculated using the ROC analysis to differentiate between the two treatment groups. Based on the ROC analysis, the area under the curve (AUC) for TVRR was outlined (Fig. 3.7.1).

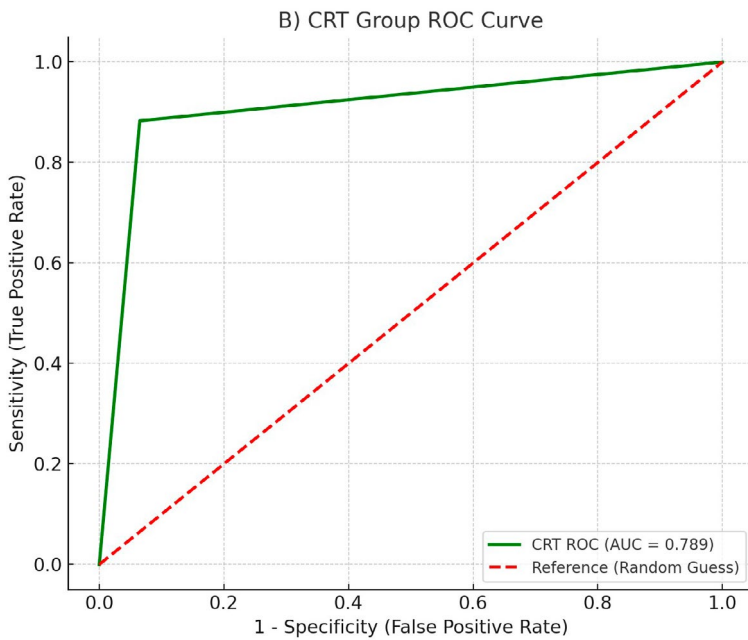
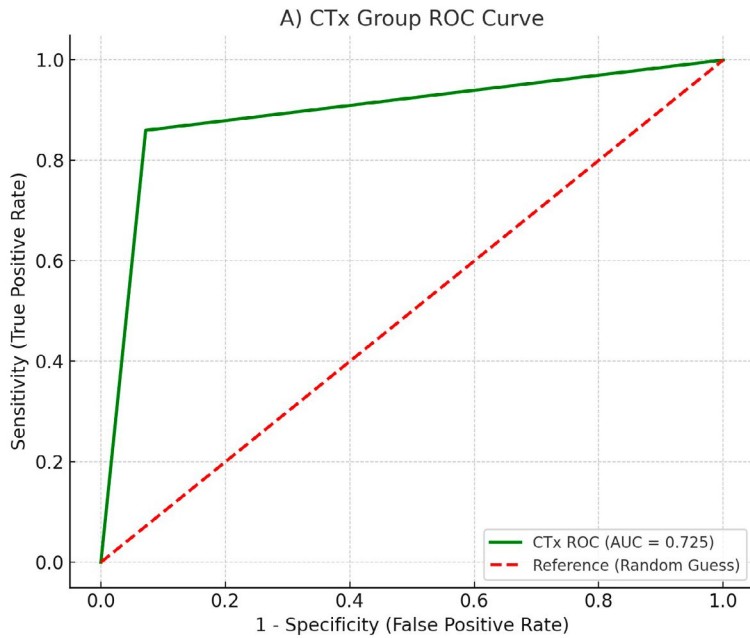


Fig. 3.7.1. Receiver operating characteristic (ROC) curves for tumor volume reduction rate (TVRR)

(A) CTx cut-off value for TVRR was lower than 25.3 %, with AUC = 0.725; (B) CRT cut-off value for TVRR was higher than 48.7 %, with AUC = 0.789.

3.8. Magnetic resonance imaging-assessed tumor regression grade

Table 3.8.1 shows the distribution of patients by mrTRG and pTRG in both CTx and CRT treatment groups. There were no patients who did not respond to treatment as assessed by mrTRG5 (mrTRG5 category) or pTRG (pTRG0 category), i.e. all the patients had a response to treatment. A statistically significant association was found between mrTRG and pTRG assessment in the CTx and CRT groups (respectively $p < 0.001$ and $p = 0.003$).

Table 3.8.1. Distribution of patients by MRI-assessed and pathological tumor regression grade in the chemotherapy and chemoradiotherapy groups

Grade	CTx group (n = 40)		p	CRT group (n = 49)		p
	mrTRG	pTRG		mrTRG	pTRG	
TRG0	NA	0	< 0.001	NA	0	0.003
TRG1	3 (7.5)	7 (17.5)		7 (14.2)	1 (2.3)	
TRG2	7 (17.5)	22 (55)		17 (34.7)	28 (57.14)	
TRG3	20 (50)	7 (17.5)		24 (48.8)	14 (28.57)	
TRG4	10 (25)	4 (10)		1 (2.3)	6 (12)	
TRG5	0	NA		0	NA	

NA, not applicable as there are no mrTRG0 and pTRG5 in the scales. CTx, chemotherapy; CRT, chemoradiotherapy; mrTRG, MRI-based tumor regression grade; pTRG, pathological tumor regression grade.

In terms of mrTRG status evaluated by MRI preoperatively in comparison to pTRG by histopathological results, sensitivity was recorded at 95 %, while specificity was 87 %, and coincidence rate was 92.5 %.

3.9. Magnetic resonance imaging volumetry and tumor volume reduction rate between good and bad responders

Table 3.9.1 shows comparison of tumor volume and TVRR between good and bad responders classified by MRI-assessed tumor regression grade. There were no significant differences in tumor volumes between good and poor responders of both groups before treatment. In the CTx group, the median tumor volumes before treatment for good and poor responders were 52.25 cm³ (IQR 34.94–57.81) and 43.39 cm³ (IQR 22.58–50.25), respectively ($p = 0.542$). In the CRT group, the corresponding median tumor volumes were 50.79 cm³ (36.60–57.73) and 41.40 cm³ (29.90–56.44) ($p = 0.430$).

Meanwhile, a significant difference in the median tumor volume after treatment between good and poor responders was observed only in the CRT group. Good responders had a median tumor volume of 18.00 cm³ (IQR 7.07–22.72) as compared to 20.20 cm³ (IQR 17.00–30.20) of poor responders

($p = 0.038$). In the CTx group, the corresponding median tumor volume values were 28.53 cm³ (IQR 22.32–36.53) and 28.03 cm³ (IQR 18.68–38.96) ($p = 0.962$). TVRR results further highlighted CRT effectiveness, with good responders achieving a greater median TVRR than poor responders (64.85 %, IQR 52.47 %–83.13 % vs. 44.10 %, IQR 36.90 %–53.50 %, $p < 0.001$). In the CTx group, there was no significant difference in the median TVRR between good and poor responders ($p = 0.217$).

Table 3.9.1. Comparison of tumor volumetry parameters between good and poor responders classified by MRI-assessed tumor regression grade in the chemotherapy and chemoradiation groups

Parameter	CTx group (n = 40)		p	CRT group (n = 49)		p
	Good responders mrTRG1-2	Poor responders mrTRG3-4-5		Good responders mrTRG1-2	Poor responders mrTRG3-4-5	
Volume before treatment, cm ³	52.25 (34.94–57.81)	43.39 (22.58–50.25)	0.542	50.79 (36.60–57.73)	41.40 (29.90–56.44)	0.430
Volume after treatment, cm ³	28.53 (22.32–36.53)	28.03 (18.68–38.96)	0.962	18.00 (7.07–22.72)	20.20 (17.00–30.20)	0.038
TVRR, %	33.45 (21.94–37.91)	29.85 (20.44–41.83)	0.217	64.85 (52.47–83.13)	44.10 (36.90–53.50)	< 0.001

Values are median (interquartile range). CTx, chemotherapy; CRT, chemoradiotherapy; mrTRG, MRI-based tumor regression grade; TVRR, tumor volume reduction rate.

A similar situation was observed while evaluating based on the pTRG (Table 3.9.2). There were no significant differences in tumor volumes between good and poor responders in both the groups, before treatment. After treatment, a significant difference in the tumor volume was observed only in the CRT group. The median tumor volume after treatment was 17.50 cm³ (5.68–22.50) for good responders and 20.10 cm³ (16.98–30.45) for poor responders ($p = 0.042$). Moreover, in the CRT group, good responders achieved a significantly greater median TVRR than poor responders (61.30 %, IQR 46.17 %–85.00 % and 48.70 %, IQR 38.43 %–58.00 %, respectively, $p = 0.030$).

Table 3.9.2. Comparison of tumor volumetry between good and poor responders classified by pathological tumor regression grade in the chemotherapy and chemoradiation groups

Parameter	CTx group (n = 40)		p	CRT group (n = 49)		p
	Good responders pTRG3-4	Poor responders pTRG0-1-2		Good responders pTRG3-4	Poor responders pTRG0-1-2	
Volume before treatment, cm ³	45.98 (35.89–64.43)	48.77 (29.63–57.84)	0.712	44.58 (34.00–54.70)	48.19 (32.98–58.74)	0.578
Volume after treatment, cm ³	24.63 (15.13–44.30)	31.30 (22.76–39.02)	0.488	17.50 (5.68–22.50)	20.10 (16.98–30.45)	0.042
TVRR, %	36.35 (26.33–65.75)	30.05 (24.48–36.55)	0.121	61.30 (46.17–85.00)	48.70 (38.43–58.00)	0.030

Values are median (interquartile range). CTx, chemotherapy; CRT, chemoradiotherapy; pTRG, pathological tumor regression grade; TVRR, tumor volume reduction rate.

The analysis determined TVRR cut-off values to differentiate between good and poor responders in both groups based on mrTRG and pTRG classifications. For mrTRG, the cut-off TVRR value in the CTx group was 19.0 %, classifying patients with a higher TVRR as good responders, while those below this threshold were poor responders. In the CRT group, the cut-off value was 34.3 %, reflecting greater tumor reduction with CRT. For pTRG, the cut-off TVRR value was 22.5 % for CTx and 45.7 % for CRT, similarly distinguishing good from poor responders.

4. DISCUSSION

4.1. T and N staging and restaging in rectal cancer

MRI is an invaluable tool in the fight against CRC. It provides precise locoregional staging and a thorough evaluation of tumor traits, which are essential for shaping treatment plans and boosting patient outcomes [4].

In this study, two-thirds (nearly 67 %) of the patients were males. The mean age was 64.26 (SD 9.17), ranging from 37 to 83 years. Age distribution and male predominance are consistent with global statistics showing that rectal cancer incidence increases with age and has a slight male predominance [3, 36, 44, 166].

MRI analysis before treatment showed that most patients in the CTx group had stage T3b and T3c tumors. There was a significant decrease in the proportions of patients with cancers of higher stages after treatment, with stage T3b cancer being the most common (47.5 %), indicating effective tumor downstaging. In the CRT group, pre-treatment staging was more diverse, with shifts post-treatment majorly toward T3b (75.5 %), showing a significant impact of CRT. Many studies have shown that after neoadjuvant therapy, the number of lymph nodes typically reduces, and the short-axis diameter either diminishes or vanishes entirely – this shows nodal downstaging [102, 167, 168]. The majority of patients in the CTx group had stage N2 cancer before treatment; the percentage of patients with stage N0 cancer increased to 37.5 % after treatment, indicating nodal downstaging. In the CRT group, the percentage of patients with stage N2 cancer decreased to 6.1 % after treatment, with N0 at 38.8 %. Both treatments effectively reduced nodal stages ($p = 0.001$), with CRT slightly better achieving N0. MRI utility is noted, though its specificity in lymph node assessment is limited [127, 167, 169, 170]. Overall, CTx and CRT demonstrate significant tumor and nodal downstaging, with CRT having a slight advantage in nodal outcomes. Borgheresi et al. concluded that MRI is the primary imaging technique advocated for lymph node assessment in rectal cancer [104]. CTx showed a more varied tumor stage distribution after treatment than CRT. However, CRT was slightly more successful in achieving N0 nodal staging in more patients, as reflected in both MRI and pathological results.

The results of this study in predicting tumor response to CTx and CRT treatment using yMRI (according to T0/1/2/3/4), showed a sensitivity of 79.49 % and a specificity of 80.00 %. In predicting nodal status (N0/1/2), yMRI demonstrated a sensitivity of 67.53 % and a specificity of 71.65 %. Various studies [31, 89] show variable sensitivity and specificity in rectal cancer T and N staging, ranging up to 87 % and 75 %, respectively, for T

staging, and up to 78 % and 67 %, respectively, for N staging. According to our data, yMRI achieved similar levels of accuracy, with sensitivity for T staging at 79.49 % and specificity at 80.00 %, and for N staging at 67.53 % and 71.65 %, respectively. These results align with evidence suggesting yMRI higher reliability in T staging than N staging, particularly in assessing tumor downstaging post-neoadjuvant therapy. These findings emphasize the utility of yMRI in assessing tumor responses to neoadjuvant therapies; however, its evaluation of lymph nodes remains limited.

4.2. Diffusion-weighted magnetic resonance imaging for evaluating rectal cancer and locoregional lymph nodes

Radiologists need to recognize the limitations of MRI in accurately detecting lymph node metastases, even when incorporating advanced techniques such as DWI and ADC mapping [4, 170–172]. In this study, tumor ADC values increased in both CTx and CRT groups following treatment, reflecting reduced cellular density and increased water diffusivity. These findings align with the notion that treatment leads to structural changes within the tumor microenvironment, with CRT showing a more pronounced response.

Tumor ADC values before treatment were slightly higher in the CRT group compared to the CTx group. A combined optimal cut-off ADC value to discriminate between the healthy and invaded rectal wall was $705 \times 10^{-3} \text{ mm}^2/\text{s}$, yielding a sensitivity of 75 % and a specificity of 73 %. After treatment, both groups showed a significant increase in the ADC values, with the CRT group having higher values. An optimal cut-off ADC value to distinguish the healthy from invaded rectal wall after treatment was $991 \times 10^{-3} \text{ mm}^2/\text{s}$, achieving a sensitivity of 75 % and a specificity of 73 %. This observation supports a greater tumor response often associated with CRT, due to its combined effects of radiation and chemotherapy.

Nodal ADC values before treatment were comparable between the two groups, with an optimal cut-off ADC value of $655 \times 10^{-3} \text{ mm}^2/\text{s}$ yielding a sensitivity of 58 % and a specificity of 60 % for detecting metastatic nodes. After treatment, CRT resulted in greater nodal ADC values, with a post-treatment cut-off value of $770 \times 10^{-3} \text{ mm}^2/\text{s}$, achieving a sensitivity of 62 % and a specificity of 67 %. These results suggest a more effective reduction in nodal cellularity following CRT.

Our findings highlight the potential of ADC as a biomarker for monitoring treatment response in rectal cancer. While the results suggest that CRT may elicit a more robust response, they also emphasize the challenges of accurately staging lymph nodes using MRI alone. Emerging evidence underscores the value of DWI, which has shown stronger associations with pathological staging

compared to conventional MRI techniques [4, 33, 173]. These observations reinforce the need for integrated imaging approaches to improve diagnostic accuracy and guide treatment planning effectively.

4.3. Mesorectal fascia as a prognostic indicator

Positive MRF involvement indicates more advanced disease and is associated with poorer survival outcomes [175]. This highlights the critical role of accurately assessing MRF and CRM status in rectal cancer to guide surgical strategies. Accurate evaluation has an impact on decisions between radical resections requiring extensive intervention or more conservative approaches that preserve tissue but carry a higher risk of incomplete tumor removal [176, 177].

In this study, MRI staging before treatment identified similar proportions of MRF-negative (MRF-) patients in the CTx and CRT groups. After treatment, there was a statistically significant increase in the percentage of MRF- patients in the CRT group ($p = 0.001$), while in the CTx group no significant change was documented ($p = 0.110$). These findings suggest that CRT is more effective in reducing MRF involvement, supporting its role in better tumor regression.

Pathological analysis revealed a higher proportion of CRM-negative (CRM-) patients after treatment in both groups. This difference was significant in the CRT group ($p = 0.043$) but not in the CTx group ($p = 0.101$). MRI findings suggested some overestimation of MRF involvement, often mistaking post-treatment fibrosis for residual disease, particularly in the CTx group.

The overall coincidence rate between ymrMRF and CRM status across both groups was 70.8 %, with significant differences noted ($p = 0.005$). Sensitivity and specificity for ymrMRF in predicting CRM status were higher in the CRT group (60.00 % sensitivity, 88.37 % specificity) compared to the CTx group (41.67 % sensitivity, 83.33 % specificity). However, these values suggested that ymrMRF was a poor prognostic factor for CRM status as its moderate sensitivity limited its reliability, particularly in the CTx group.

Post-treatment evaluation of MRF and CRM remains critical for surgical planning and minimizing recurrence risk. Standardized imaging protocols are necessary to address variability in interpretations, particularly when distinguishing fibrosis from viable tumor tissue. Multicentric trials are needed to establish validated thresholds for ymrMRF and CRM assessments, enabling improved surgical decisions and better outcomes for high-risk patients [9, 178, 179].

4.4. Extramural vascular invasion as a prognostic indicator

EMVI was identified as a substantial independent risk factor for both local and distant rectal cancer recurrence [26, 94]. The presence of EMVI on MRI was associated with cancer invasion into blood vessels outside the rectal wall, indicating a higher likelihood of metastasis and poorer prognosis [94, 180]. Patients classified as high-risk based on positive EMVI results were often recommended aggressive treatment modalities, such as neoadjuvant CRT [181]. Notably, the strong correlation between MRI-assessed EMVI and pathological outcomes established its role as an excellent prognostic factor for both disease progression and treatment response.

In this study, an increase in the number of patients with negative EMVI status after treatment was observed in both groups. However, in the CTx group, this change was statistically significant ($p = 0.024$), while in the CRT group, no significant difference was noted ($p = 0.838$). These findings suggested that chemotherapy had a more substantial impact on reducing EMVI compared to CRT, although further studies are required to confirm this. Pathological analysis revealed no significant differences in the EMVI status after treatment in both groups ($p = 0.482$ for the CTx group and $p = 1.00$ for the CRT group).

Both groups demonstrated a significant reduction in EMVI scores after treatment, with p -values of 0.001 for the CTx group and 0.001 for the CRT group. Before treatment, the most severe EMVI scores (score 3 or 4) were observed in 57.5 % of the CTx group and 38.8 % of the CRT group, but these decreased to 15.0 % and 26.6 %, respectively, after treatment. Despite these improvements, no significant differences were observed between the groups in terms of pathological pLVI, indicating similar post-treatment outcomes.

The overall coincidence rate between ymrEMVI and pLVI in the combined group was 91.25 %, with high sensitivity (88.57 %), specificity (93.55 %), PPV (88.57 %), and NPV (93.55 %). However, when analyzed individually, the CRT group demonstrated superior accuracy, with a coincidence rate of 100 %, compared to 82.5 % in the CTx group. These findings suggest that CRT provides more reliable radiological-pathological associations, potentially due to its more profound impact on the tumor microenvironment.

These results underscored the utility of MRI in monitoring EMVI status and its correlation with pathological outcomes. As an excellent prognostic factor, EMVI status was shown to guide treatment planning and predict long-term outcomes in rectal cancer patients. While both treatment strategies effectively reduced the proportions of patients with high EMVI scores, the discrepancy in ymrEMVI and pLVI coincidence rates between groups highlighted the need for standardized imaging protocols. Multicentric studies are deemed essential to validate these findings and optimize imaging-based

evaluations of EMVI for better treatment stratification and prognostic assessment.

4.5. Interplay between magnetic resonance imaging volumetry, tumor volume reduction rate, and tumor regression grade

Significant tumor volume reduction was observed in both treatment groups in our study. MRI scans and pathological evaluations demonstrated the efficacy of the therapeutic strategies used. The data also showed that, in comparison to the CTx group, the CRT group had a greater decrease in tumor volume. In particular, significant differences were identified in post-therapy volumes, with the CRT group exhibiting a lower median tumor volume ($p < 0.001$). The CRT group also demonstrated a higher median TVRR of 53.3 % (IQR 41.9 %–67.5 %) compared to 31.1 % (IQR 25.6 %–40.9 %) in the CTx group ($p < 0.001$). This suggests that CRT is more effective in reducing tumor volume and achieving greater TVRR than CTx. Moreover, it shows that individuals undergoing CRT may have better clinical outcomes due to increased tumor shrinking, and the combination therapy was more successful overall [131–133].

Furthermore, ROC curve analysis demonstrated a capability for detecting treatment responses based on TVRR. The cut-off value for TVRR in the CTx group was determined to be 25.3 %, with an area under the curve (AUC) of 0.725. In contrast, the CRT group had a higher cut-off value of 48.7 %, with an AUC of 0.789. Based on these data, the TVRR seems to be a reliable predictor for identifying differences in the effectiveness of treatment. This information can be useful for physicians in assessing the effectiveness of therapies they are administering [131–133]. The fact that CRT appears to be more effective in reducing tumor volumes, it is possible that combining chemotherapy and radiation therapy will result in pTRG that are more favorable [182]. By decreasing the size of the tumor and maybe reducing the progression of the disease, the combined strategy can help surgeons achieve better surgical results while reducing the amount of surgery required and protecting surrounding good tissue.

Further analysis of mrTRG revealed notable differences between the CTx and CRT groups, with a statistically significant association observed for both mrTRG and pTRG assessments ($p < 0.001$ and $p = 0.003$, respectively). Additionally, the high sensitivity (95 %), specificity (87 %), and coincidence rate (92.5 %) highlight the accuracy of mrTRG as a tool for evaluating treatment response, particularly when combined with volumetric measures such as tumor volume and TVRR [137, 184].

The post-therapy analyses further emphasized the superior efficacy of CRT. Good responders in the CRT group achieved significantly lower post-therapy tumor volumes (17.50 cm³, IQR 5.68–22.50) compared to poor responders (20.10 cm³, IQR 16.98–30.45, $p = 0.042$) and demonstrated significantly higher TVRR values (61.30 %, IQR 46.17 %–85.00 % vs. 48.70 %, IQR 38.43 %–58.00 %, $p = 0.030$). In contrast, the CTx group showed no statistically significant differences in post-therapy tumor volumes ($p = 0.962$) or TVRR ($p = 0.217$) between good and poor responders. These findings suggest that CRT achieves more consistent and pronounced tumor shrinkage, likely reflecting its ability to enhance local tumor control.

The ROC curve analysis underscored the utility of TVRR as a predictor of treatment response, with higher cut-off values observed in the CRT group (34.3 %) compared to the CTx group (19.0 %). The area under the curve (AUC) was also greater for CRT (AUC = 0.789) than for CTx (AUC = 0.725), indicating superior predictive accuracy for CRT. Similarly, when analyzed using pTRG classifications, TVRR showed cut-off values of 45.7 % for CRT and 22.5 % for CTx. The AUC for pTRG-based prediction was 0.796 for CRT and 0.732 for CTx, again highlighting higher predictive reliability in the CRT group. These findings suggest that TVRR, particularly in the CRT context, serves as a robust marker to differentiate good responders from poor responders and can guide clinical decisions. Moreover, integrating pTRG classification further enhances the utility of TVRR in accurately assessing treatment outcomes.

These findings align with growing evidence supporting the role of MRI in forecasting post-treatment pathological responses [185]. The integration of mrTRG and volumetric measures, such as TVRR and post-therapy tumor volumes, enhances the accuracy of response assessments. In clinical practice, the high correlation between these parameters highlights their combined value in evaluating therapeutic effectiveness and guiding personalized treatment strategies.

The importance of mrTRG is further supported by its association with key prognostic outcomes. Studies have consistently shown that tumor regression grades are significant predictors of disease-free survival, local failure, metastasis-free survival, and overall survival in patients undergoing preoperative CRT for rectal cancer [164, 187]. This reinforces the need to integrate imaging-based tools such as mrTRG and volumetric measures to refine treatment strategies and improve patient counseling regarding long-term outcomes, recovery expectations, and treatment pathways.

Understanding the interplay between tumor characteristics and treatment responses remains crucial for optimizing rectal cancer management. The lack of significant differences in pre-therapy tumor volumes between treatment

groups, alongside the variability in post-therapy responses, underscores the need for tailored approaches. These findings advocate for personalized treatment plans that account for individual patient and tumor characteristics, ultimately enhancing therapeutic outcomes and long-term survival rates for rectal cancer patients

CONCLUSIONS

1. Magnetic resonance imaging is valuable in downstaging T stages in both groups, with a sensitivity of 79.49 % and a specificity of 80 %. It also shows significant but limited capability in downstaging N stages, with a sensitivity of 67.53 % and a specificity of 71.65 %. While magnetic resonance imaging demonstrates significant downstaging in both groups, differences in T and N stage responses show that chemoradiotherapy ensures greater tumor and nodal regression as compared to chemotherapy.
2. Changes in apparent diffusion coefficient values before and after treatment appeared to be significant in evaluating downstaging of T stage in both groups and N stage in the chemoradiotherapy group. However, they were not significant in evaluating the effect of neoadjuvant treatment on the N stage in the chemotherapy group.
3. Magnetic resonance imaging-assessed extramural vascular invasion status after neoadjuvant treatment as compared to pathologically confirmed lymphovascular invasion demonstrated significant agreement and may be used as a noninvasive prognostic factor. Magnetic resonance imaging-assessed mesorectal fascia status after neoadjuvant treatment as compared to the pathologically confirmed circumferential resection margin showed associations, but not strong, and may serve as a prognostic factor. No significant differences in extramural vascular invasion and mesorectal fascia status in both treatment groups were detected.
4. Changes in the tumor volume reduction rate and magnetic resonance imaging-assessed tumor regression grade were significantly greater in the chemoradiotherapy than chemotherapy group. These parameters may serve as noninvasive tools in identifying good and poor responders in both neoadjuvant treatment groups.

LIMITATIONS OF THE STUDY

This study had several limitations that need to be considered. First, the sample size of 89 patients, while substantial, is relatively modest for clinical research, potentially limiting the statistical power and generalizability of the findings, particularly given the skewed gender distribution favoring male patients. Second, the tumor boundaries on each image slice were manually traced to define an irregular ROI. Finally, it is a single-center patient cohort, and the results may not directly apply to different patient populations or healthcare settings.

PRACTICAL RECOMMENDATIONS

1. In local staging of rectal cancer, MRI provides diagnostic (T and N staging) and prognostic (MRF and EMVI involvement) information useful to categorize patient risk and personalize patient treatment.
2. As MRI assessment of tumor response in rectal cancer remains challenging, standardized MRI techniques and structured reporting are recommended to enable consistent accuracy.
3. TVRR combined with mrTRG metrics and pathological assessments (pTRG) adds additional information to evaluate treatment effectiveness, especially with the administration of combination therapies.

SANTRAUKA

SUTRUMPINIMAI

- ADC** – tariamas difuzijos koeficientas (angl. *apparent diffusion coefficient*)
- AJCC** – Amerikos jungtinis vėžio komitetas (angl. *American Joint Committee on Cancer*)
- AUC** – plotas po kreive (angl. *area under the curve*)
- CRM** – cirkuliarioji rezekcijos riba (angl. *circumferential resection margin*)
- CRT** – chemospindulinis gydymas
- CTx** – chemoterapinis gydymas
- DCE** – dinaminė kontrastavimo seka
- EMVI** – ekstramuralinė veninė invazija
- ESGAR** – Europos gastrointestinalinės ir abdominalinės radiologijos draugija (angl. *European Society of Gastrointestinal and Abdominal Radiology*)
- LVI** – limfovaskulinė invazija
- FOLFOX** – fluorouracilas, leukovorinas, and oksaliplatina
- M** – atokiosios metastazės
- MRT** – magnetinio rezonanso tomografija
- MRF** – mezorektinė fascija
- mrT** – MRT vertinta T stadija
- mrN** – MRT vertinta N stadija
- mrTRG** – MRT vertintas naviko regresijos laipsnis
- N** – limfmazgių stadija
- NPV** – neigiama prognostinė vertė
- pLVI** – patologinė limfovaskulinė invazija
- pTRG** – patologinis naviko regresijos laipsnis
- pCRM** – patologinė cirkuliarioji rezekcijos riba (angl. *pathological circumferential resection margin*)
- RT** – radioterapinis gydymas
- RSNA** – Šiaurės Amerikos radiologų asociacija (angl. *Radiological Society of North America*)
- SAR** – Abdominalinės radiologijos asociacija (angl. *Society of Abdominal Radiology*)
- y** – po gydymo

ymrT	– MRT vertinta T stadija po gydymo
ymrN	– MRT vertinta N stadija po gydymo
yCRM	– cirkuliarioji rezekcijos riba po gydymo (angl. <i>circumferential resection margin after treatment</i>)
ypT	– patloginė T stadija po gydymo
ypN	– patloginė N stadija po gydymo
T	– naviko/naviko T stadija
TNM	– naviko, limfmazgių ir atokiųjų metastazių klasifikavimo sistema
TPV	– teigiama prognostinė vertė
TVRR	– naviko tūrio sumažėjimo rodiklis (angl. <i>tumor volume reduction rate</i>)
UICC	– Tarptautinė vėžio kontrolės sąjunga (angl. <i>Union for International Cancer Control</i>)

IVADAS

Storosios žarnos vėžys yra reikšminga pasaulinė sveikatos problema, pasižyminti dideliu sergamumu ir mirtingumu. Pagal sergamumo rodiklius, storosios žarnos vėžys užima trečiąją vietą pasaulyje, o pagal mirtingumo rodiklius – antrąją vietą [1]. 2022 metais visame pasaulyje buvo užregistruota daugiau nei 1,9 mln. naujų storosios žarnos vėžio atvejų [2], tuo tarpu Europoje – daugiau nei 538 tūkst. naujų atvejų [3].

Pastaraisiais metais magnetinio rezonanso tomografija (MRT) tapo pagrindiniu diagnostikos metodu pradiniam tiesiosios žarnos vėžio stadijos nustatymui, kuris yra esminis gydymo taktikos pasirinkimui [4]. Daugybė tyrimų pabrėžė MRT svarbą tiksliai nustatant ligos stadiją ir išryškino pagrindinius prognostinius veiksnius, vertinant bei pristatant tyrimo rezultatus [5–7].

Pirminio MRT tyrimo metu nustatomos naviko (T) ir limfmazgių (N) stadijos, pagal kurias pacientai skirstomi į gydymo grupes – neoadjuvantinės terapijos ir (ar) chirurginio planavimo [6, 8]. Pagrindiniai MRT tikslai tiesiosios žarnos vėžio diagnostikoje apima naviko lokalizacijos nustatymą, jo invazijos į žarnyno sienelę įvertinimą, taip pat plitimo į gretimas anatomines struktūras, tokias kaip mezorektinė fascija (MRF), pilvaplėvė ir dubens organai, analizę [8]. Be to, MRT yra svarbus vertinant kitus reikšmingus prognostinius veiksnius, tokius kaip metastaziniai limfmazgiai ar ekstramuralinė veninė invazija (EMVI) [9].

Šis išsamus vertinimas leidžia sukurti bendrą prognostinį naviko profilio aprašymą ir padeda kliniciams suskirstyti pacientus į mažos, vidutinės ir didelės rizikos grupes. Tokia klasifikacija suteikia galimybę parinkti tinkamiausias gydymo strategijas – nuo chirurgijos mažos rizikos navikams iki

neoadjuvantinės radioterapijos ar chemoradioterapijos agresyviems, didelės rizikos navikams [5, 7, 10].

Gerėjant vaizdinių tyrimų galimybėms, radiologo vaidmuo tapo itin svarbus. Siekiant organų tausojimo, radiologams tenka didesnė atsakomybė ne tik vertinant naviką ir limfmazgius, bet ir analizuojant kitas struktūras, laikomas svarbiais prognostiniais veiksniais. MRT papildydamas endoskopinį tyrimą sudaro esminę kompleksinio vietinio naviko atsako į neoadjuvantinį gydymą vertinimo dalį. Šis procesas leidžia įvertinti, ar pacientams vis dar būtina standartinė chirurginė rezekcija, ar galima taikyti konservatyvius stebėjimo metodus, pavyzdžiui, stebėjimo ir laukimo (angl. *watch and wait*) strategiją [11, 12]. Toks požiūris padeda pritaikyti individualizuotą gydymo planą, maksimaliai atitinkantį paciento būklę, bei siekti išsaugoti organus ir pagerinti gyvenimo kokybę.

Norint palengvinti radiologų darbą, buvo sukurti įvairūs vaizdinimo protokolai, stadijavimo ir aprašymo šablonai, skirti tiesiosios žarnos vėžio ir jo išplitimo vertinimui [13]. Be to, įvesti nauji diagnostiniai klasifikavimo kriterijai, kurie leidžia tiksliau įvertinti vietinį naviko atsaką po neoadjuvantinės terapijos [13, 14].

Svarbu pažymėti, jog remiantis tyrimais radiologo patirties lygis tiesiogiai veikia daugiadisciplininių komisijų sprendimus ir pacientų gydymo rezultatus [17]. Daugelis naujų diagnostinių metodų, įskaitant atsako klasifikavimo sistemas, prieš jų įtraukimą į klininkines gaires dažnai buvo išbandyti tik mažose ekspertų radiologų grupėse [13, 18, 19]. Europos gastrointestalinės ir abdominalinės radiologijos draugijos (angl. *European Society of Gastrointestinal and Abdominal Radiology*, ESGAR) išleistas stadijavimo gairės vis dažniau integruojamos į kasdienę klinikinę praktiką, prisidedant prie radiologų darbo standartizavimo ir užtikrinant vieningą požiūrį į tiesiosios žarnos vėžio diagnostiką bei gydymo planavimą [20, 21].

Tiksli naviko stadija yra būtina ne tik neoadjuvantinio gydymo planavimui, bet ir chirurginės taktikos bei rezekcinių ribų nustatymui. MRT suteikia chirurgams itin svarbią informaciją apie naviko charakteristikas, o radioterapeutams – galimybę tiksliai apibrėžti radioterapijos ribas, kas reikšmingai gali paveikti gydymo rezultatus [22]. Tačiau, nepaisant reikšmingos pažangos vaizdinimo technologijose, nuoseklumo ir tikslumo užtikrinimas radiologiniuose aprašymuose išlieka vienu didžiausių iššūkių. Šie aspektai yra esminiai siekiant optimizuoti diagnostiką ir užtikrinti, kad gydymo planai būtų grindžiami patikimais ir vienodais duomenimis [23].

Siekiant įveikti šiuos iššūkius, kelios žymios radiologijos organizacijos, tokios kaip ESGAR, Abdominalinės radiologijos asociacija (angl. *Society of Abdominal Radiology*, SAR) ir Šiaurės Amerikos radiologų asociacija (angl. *Radiological Society of North America*, RSNA), parengė struktūrizuotus ap-

rašymų šablonus [24, 25]. Šie šablonai užtikrina tikslų ir sistemingą esminių tiesiosios žarnos vėžio bei jo plitimo aspektų įvertinimą. Be to, šablonai yra suderinti su naviko, limfmazgių ir atokiųjų metastazių klasifikavimo sistema (TNM), kurią sukūrė Amerikos jungtinis vėžio komitetas (angl. *American Joint Committee on Cancer*, AJCC) ir Tarptautinė vėžio kontrolės sąjunga (angl. *Union for International Cancer Control*, UICC) [24, 25]. Standartizuotas požiūris padeda užtikrinti vieningą duomenų interpretavimą, leidžia tiksliau planuoti gydymą ir gerina tarpdisciplininį bendradarbiavimą klinikinėje praktikoje.

1. TIKSLAS IR UŽDAVINIAI

1.1. Tikslas

Nustatyti magnetinio rezonanso tomografijos parametrų pokyčius ir jų diagnostinę reikšmę pacientams, sergantiems II ir III stadijos tiesiosios žarnos vėžiu, gydomiems skirtingais neoadjuvantinio gydymo metodais – FOLFOX be spindulinio gydymo ir kombinuotu chemospinduliniu gydymu.

1.2. Uždaviniai

1. Įvertinti magnetinio rezonanso tomografijos vaidmenį nustatant naviko (T) ir limfmazgių (N) stadijų pokyčius po neoadjuvantinio gydymo chemoterapinio ir chemospindulinio gydymo grupėse.
2. Įvertinti magnetinio rezonanso tomografijos tariamo difuzijos koeficiento vertę tiesiosios žarnos navike ir patologiniuose limfmazgiuose prieš ir po neoadjuvantinio gydymo, siekiant įvertinti jų vaidmenį gydymo atsakui.
3. Įvertinti mezorektinės fascijos invazijos ir ekstramuralinės veninės invazijos pokyčius po gydymo chemoterapinio ir chemospindulinio gydymo grupėse bei įvertinti šių parametrų, kaip neinvazinių prognostinių veiksnių, reikšmę.
4. Įvertinti naviko tūrio sumažėjimo rodiklio ir magnetinio rezonanso tomografija vertinto naviko regresijos laipsnio pokyčius prieš ir po gydymo chemoterapinio ir chemospindulinio gydymo grupėse bei įvertinti šių parametrų, kaip neinvazinių prognostinių veiksnių, reikšmę.

1.3. Darbo naujumas

MRT tyrimas yra efektyvus vaizdinis metodas, skirtas tiesiosios žarnos vėžiu sergančių pacientų vertinimui. Aukštos skiriamosios gebos MRT leidžia itin tiksliai įvertinti minkštuosius audinius ir jų pakitimus, tiksliai vizualizuo-

ti navikus bei nustatyti jų santykį su gretimomis anatomicinėmis struktūromis. Dėl šių savybių MRT šiuo metu laikomas „auksiniu standartu“ vertinant vietinį tiesiosios žarnos vėžio išplitimą.

Pacientai skirstomi į mažos, vidutinės arba didelės rizikos grupes, remiantis naviko stadija (T), limfmazgių stadija (N) bei įvertinant prognostinius veiksnius: mezorektinės fascijos (MRF) / chirurginės rezekcijos ribos (angl. *circumferential resection margin*, CRM) invaziją ir EMVI. Ši klasifikacija padeda nuspręsti, ar pacientą galima operuoti nedelsiant, ar būtinas neoadjuvantinis spindulinis gydymas ir chemoterapija, siekiant sumažinti naviko dydį ar tūrį.

Metaanalizių duomenimis, MRT jautrumas ir specifiskumas tiesiosios žarnos vėžio T stadijai nustatyti yra atitinkamai 94 proc. ir 85 proc. Tačiau N stadijos nustatymo tikslumas yra labiau ribotas – jautrumas ir specifiskumas svyruoja atitinkamai nuo 58 proc. iki 77 proc. ir nuo 62 proc. iki 74 proc. Naujais tyrimais rodo, kad difuzijos sekų (DWI) įvertinimas gali būti veiksmingesnis nei įprastinės MRT sekos nustatant navikus prieš ir po neoadjuvantinio gydymo.

Šiame perspektyviniame tyrime dalyvavo pacientai, kuriems, remiantis radiologiniais tyrimais, buvo diagnozuotas II arba III stadijos tiesiosios žarnos vėžys. Tyrimo tikslas buvo įvertinti naviko ir limfmazgių stadijos mažėjimą dviejose gydymo grupėse: pacientų, gydytų FOLFOX chemoterapija, ir pacientų, gydytų standartine chemospinduline terapija. Be T ir N stadijų pradinio bei pakartotinio įvertinimo po gydymo, buvo analizuotos ADC reikšmės funkcinėse MRT DWI sekose ir palyginti gydymo grupių rezultatai. Vienas iš tyrimo tikslų buvo nustatyti DWI sekų gebėjimą atspindėti specifinius histopatologinius skirtumus tarp limfmazgių su ir be metastazių.

Siekiant įvertinti chemoterapinio ir chemospindulinio gydymo efektyvumą bei jų skirtumus, buvo matuojamas naviko tūris, skaičiuojamas TVRR ir nagrinėjamos sąsajos tarp magnetinio rezonanso naviko regresijos laipsnio (mrTRG) ir patologinio naviko regresijos laipsnio (pTRG). Taip pat buvo vertinami EMVI požymiai ir EMVI balų pokyčiai abiejose gydymo grupėse.

Norint užtikrinti veiksmingą tiesiosios žarnos vėžio gydymą, būtina suprasti ne tik T ir N stadijų, MRF bei EMVI pokyčių reikšmę, bet ir įvertinti naviko tūrio, naviko tūrio sumažėjimo rodiklio bei MRT naviko regresijos laipsnio pokyčių svarbą. Šie rodikliai leidžia taikyti daugiadisciplininį požiūrį, skatinantį glaudų radiologų, chirurgų, onkologų – hematologų, radioterapeutų ir patologų bendradarbiavimą. Išsamus naviko savybių ir jo atsako į gydymą vertinimas suteikia galimybę kiekvienam specialistui priimti labiau pagrįstus ir individualizuotus sprendimus, gerinančius pacientų gydymo rezultatus.

2. METODIKA

2.1. Tyrimo eiga

Tyrimas buvo atliktas Lietuvos sveikatos mokslų universiteto ligoninės Kauno klinikų Radiologijos, Chirurgijos bei Onkologijos ir hematologijos klinikose 2015–2023 metais, gavus Kauno regioninio biomedicinos tyrimų etikos komiteto leidimą Nr. BE-2-32 (2015 m. liepos 17 d.). Visi pacientai prieš įtraukimą į studiją pasirašė informuoto asmens sutikimo formą.

Tai buvo perspektyvinis tyrimas. Buvo įtraukti pacientai, kuriems diagnozuotas II ir III stadijos tiesiosios žarnos vėžys, remiantis radiologiniais tyrimais (krūtinės ir pilvo KT, dubens MRT). Iš pradžių visi pacientai buvo suskirstyti pagal naviko rezektabilumą. Dalyviai buvo suskirstyti į dvi gydymo grupes santykiu 1:1 (6 priedas). Pirmoji pacientų grupė (40 pacientų) gavo naują standartinę priešoperacinę chemoterapijos gydymą, FOLFOX4, iš viso 8 ciklus. Gydymo efektyvumas buvo vertinamas naudojant radiologinius metodus (dubens MRT), vertinant vėžio žymenų dinamiką ir galimybę atlikti radikalią operaciją (siekiant R0 rezekcijos). Jei išliko T4 dydžio navikas arba N(+), kaip įvertino TNM, priešoperaciniu laikotarpiu navikui buvo skiriama papildoma frakcionuota radioterapija (50 Gy/25fr) kartu su 2 chemoterapijos ciklais su 5-Fu/Lv (MAYO režimas). Pacientams buvo atlikta operacija, jei sumažėjo naviko dydis (T1–3, N0). Pooperaciniu laikotarpiu chemoterapija pagal FOLFOX4 schemą buvo tęsiama 4 ciklus (iki 6 mėnesių viso sisteminio gydymo), jei buvo pasiekta R0 rezekcija. Antroji, kontrolinė chemospindulinio tyrimo grupė (49 pacientai), priešoperaciniu laikotarpiu gavo standartinę chemoradiacinę gydymą. Po operacijos buvo įvertintas naviko regresijos laipsnis. Jei navikas žymiai sumažėjo po chemoterapijos (pT0N0 arba pT1–2N0), buvo tęsiamas standartinis gydymas – 4 chemoterapijos ciklai su 5 Fu/Lv. Likusiems pII ar pIII stadijos navikams buvo suplanuota adjuvantinė chemoterapija FOLFOX režimu, iš viso 8 ciklai. Po gydymo pacientai bus stebimi 10 metų.

Dubens MRT tyrimas buvo atliekamas nevalgiusiems pacientams, kurių žarnynas buvo išvalytas mikrokлизma. Literatūros duomenimis, mikrokлизma pagerina vaizdų kokybę, sumažinant tiesiosios žarnos turinio ir dujų artefaktus [6]. Atvykęs į tyrimą pacientas užpildė standartinę MRT sutikimo formą (10 priedas, paciento apklausos forma magnetinio rezonanso tomografijai). Asmuo buvo informuotas apie tyrimo eigą. Visi tiriamieji persirengė specialiais drabužiais. MRT skenavimas buvo atliktas naudojant Siemens 1.5-T Magnetom Avanto aparatą su paviršine rite. MRT tyrimas atliekamas gulimoje padėtyje ant nugaros, pradinei MRT stadijai nustatyti ir pakartotinai praėjus 6–8 savaitėmis po pravesto gydymo. Prieš pradėdant tyrimą, kad būtų nuslo-

pinta žarnų peristaltika pacientams buvo sušvirksčiama 20 mg/ml N-butyl scopolamine (Buscopan, Boehringer, Ingelheim, Vokietija). Restadijavimo metu, į veną buvo suleidžiama vienkartinė (0,2 mg/kg) kontrastinės medžiagos dozė (Magnevist Bayer Schering Pharma, Berlynas, Vokietija) 2 ml/s greičiu. Tyrimą atliko vienas radiologijos technologas, procedūrą prižiūrėjo radiologas. Į MRT protokolą buvo įtrauktos T2 sagitalinės, ašinės ir koronarinės sekos, mažo lauko/FOV T2 ašinės sekos, DWI/ADC ašinės sekos. Restadijavimo metu, papildomai atliktos T1 ašinės sekos.

Statistinė duomenų analizė atlikta vartojant SPSS 20.0 bei Excel programą. Shapiro–Wilk testas naudotas patikrinti, ar duomenys atitinka normalųjį skirstinį. Kai duomenys buvo pasiskirstę pagal normalųjį skirstinį, jie buvo išreikšti vidurkiu su standartiniu nuokrypiu (SN) ir lyginti su Student t kriterijumi. Kai duomenys nebuvo pasiskirstę pagal normalųjį skirstinį, jie buvo išreikšti mediana su tarpkvartiliniu pločiu (TKP) ir lyginti su neparametriiniu Mann–Whitney U testu. Dispersijos ANOVA parametrinė analizė naudota daugiau nei dviejų grupių kiekybinių parametrų lyginime. ROC kreivės panaudotos ADC prognostinėms vertėms apskaičiuoti. ROC kreivių analizės pagalba taip pat apskaičiuoti plotas po kreive (angl. *area under the curve*, AUC), jautrumas, specifiškumas, teigiama prognostinė vertė (TPV) ir neigiama prognostinė vertė (NPV). Skirtumai buvo statistiškai reikšmingi kai $p < 0,05$.

3. REZULTATAI

3.1. Tyrimo populiacijos charakteristikos

Į tyrimą įtraukti 89 pacientai: 40 pacientų, kuriems buvo taikytas chemoterapinis gydymas pagal FOLFOX schemą (CTx) ir 49 pacientai, kuriems buvo taikytas standartinis chemospindulinis gydymas (CRT). Pacientų demografiniai duomenys pateikti 3.1.1 lentelėje.

3.1.1 lentelė. Chemoterapinės ir chemospindulinės grupių pacientų charakteristikos

Charakteristika	CTx grupė (n = 40)	CRT grupė (n = 49)	p
Amžius, vidurkis (SN), metai	61,58 (8,81)	66,45 (8,95)	0,36
Moterys, n (proc.)	13 (32,5)	16 (32,7)	0,63
Vyrai, n (proc.)	27 (67,5)	33 (67,3)	

CTx – chemoterapinė grupė; CRT – chemospindulinė grupė.

3.2. Naviko lokalizacija

40 CTx grupės pacientų pasiskirstymas pagal tiesiosios žarnos vėžio lokalizaciją buvo: 12 (30 proc.) apatinio trečdaliao tiesiosios žarnos vėžio atvejų, 13 (32,5 proc.) vidurinio trečdaliao tiesiosios žarnos vėžio atvejų ir 15 (37,5 proc.) viršutinio trečdaliao tiesiosios žarnos vėžio atvejų. Tuo tarpu 49 CRT grupės pacientai pasiskirstė taip: 18 (36,73 proc.) tiesiosios žarnos apatinio trečdaliao vėžio atvejų, 21 (42,86 proc.) vidurinio trečdaliao vėžio atvejų ir 10 (20,41 proc.) viršutinio trečdaliao vėžio atvejų.

3.3. Naviko stadijos charakteristikos

3.3.1. T ir N stadija

CTx ir CRT grupių pacientų pasiskirstymas pagal MRT vertintas T ir N stadijas prieš ir po gydymo pateiktas 3.3.1.1 lentelėje. Statistiškai reikšmingi procentinio pasiskirstymo pokyčiai buvo stebėti CTx grupėje, vertinant T stadiją, bei CTx ir CRT grupėse, vertinant N stadiją ($p = 0,001$).

3.3.1.1 lentelė. Pacientų pasiskirstymas pagal MRT vertintas naviko ir limfmazgių stadijas prieš ir po gydymo chemoterapijos ir chemospindulinio gydymo grupėse

Stadija	CTx grupė (n = 40)		p	CRT grupė (n = 49)		P
	T stadija	mrT		ymrT	mrT	
T0	0	2 (5)	0,001	0	4 (8,2)	0,060
T1	0	0		0	0	
T2	0	6 (15)		3 (6,1)	0	
T3a	0	10 (25)		19 (38,8)	8 (16,3)	
T3b	16 (40)	19 (47,5)		14 (28,5)	37 (75,5)	
T3c	13 (32,5)	2 (5)		7 (14,3)	0	
T3d	5 (12,5)	1 (2,5)		6 (12,2)	0	
T4a	6 (15,0)	0		0	0	
N stadija	mrN	ymrN	0,001	mrN	ymrN	0,001
N0	0	15 (37,5)		1 (2)	19 (38,8)	
N1	13 (32,5)	11 (27,5)		17 (34,7)	27 (55,1)	
N2	27 (67,5)	14 (35,0)		31 (63,3)	3 (6,1)	

Reikšmės yra skaičius (proc.). CTx – chemoterapinė grupė; CRT – chemospindulinė grupė; mrT – radiologinė T stadija prieš gydymą; ymrT – radiologinė T stadija po gydymo; mrN – radiologinė N stadija prieš gydymą; ymrN – radiologinė N stadija po gydymo.

Pacientų pasiskirstymas pagal T ir N stadijas po gydymo ir patologines T ir N stadijas CTx ir CRT grupėse pateiktas 3.3.1.2. lentelėje.

3.3.1.2 lentelė. Pacientų pasiskirstymas pagal MRT vertintą ir patologinę naviko ir limfmazgių stadiją chemoterapijos ir chemospindulinio gydymo grupėse

Stadija	CTx grupė (n = 40)		p	CRT grupė (n = 49)		p
	T stadija	ymrT		pT	ymrT	
T0	2 (5)	4 (10)	0,008	4 (8,2)	9 (18,4)	0,001
T1	0	1 (2,5)		0	2 (4,1)	
T2	6 (15)	8 (20)		0	9 (18,4)	
T3a	10 (25)	27 (67,5)		8 (16,3)	29 (59,2)	
T3b	19 (47,5)			37 (75,5)		
T3c	2 (5)			0		
T3d	1 (2,5)			0		
T4a	0	0		0	0	
N stadija	ymrN	pN	ymrN	pN		
N0	15 (37,5)	21 (52,5)	0,001	19 (38,8)	33 (67,3)	0,001
N1	11 (27,5)	15 (37,5)		27 (55,1)	12 (24,5)	
N2	14 (35,0)	4 (10,0)		3 (6,1)	4 (8,2)	

Reikšmės yra skaičius (proc.). CTx – chemoterapinė grupė; CRT – chemospindulinė grupė; ymrT – radiologinė T stadija po gydymo; pT – patologinė T stadija; ymrN – radiologinė N stadija po gydymo; pN – patologinė N stadija.

Tiesiosios žarnos vėžio gydymo rezultatų vertinimas parodė reikšmingą T ir N stadijų sumažėjimą po gydymo, tačiau N stadijos sumažėjimo rezultatai buvo prastesni lyginant su T stadijos sumažėjimo rezultatais. CTx grupėje ymrT ir pT sutapimo dažnis siekė 77,5 proc. ($p = 0,008$), o ymrN ir pN sutapimo dažnis buvo 51,4 proc. ($p = 0,001$). CRT grupėje ymrT ir pT sutapimo dažnis siekė 79,4 proc. ($p = 0,001$), o ymrN ir pN sutapimo dažnis – 56,4 proc. ($p = 0,001$).

Buvo apskaičiuotas jautrumas, specifiskumas, teigiama prognostinė vertė (TPV) ir neigiama prognostinė vertė (NPV), lyginant ymrT su pT ir ymrN su pN (3.3.1.3. lentelė).

3.3.1.3 lentelė. Jautrumo, specifiskumo, TPV, NPV analizė tarp ymrT ir pT bei ymrN ir pN stadijų

Rodiklis	CTx grupė (n = 40)		CRT grupė (n = 49)		Bendra CTx + CRT grupė (n = 89)	
	ymrT vs. pT	ymrN vs. pN	ymrT vs. pT	ymrN vs. pN	ymrT vs. pT	ymrN vs. pN
Jautrumas, proc.	83,33	75,00	84,56	69,39	79,49	67,53
Specifiškumas, proc.	83,00	68,80	87,20	76,00	80,00	71,65

3.3.1.3 lentelės tęsinys

Rodiklis	CTx grupė (n = 40)		CRT grupė (n = 49)		Bendra CTx + CRT grupė (n = 89)	
	ymrT vs. pT	ymrN vs. pN	ymrT vs. pT	ymrN vs. pN	ymrT vs. pT	ymrN vs. pN
TPV, proc.	80,00	75,00	83,20	69,39	80,00	72,00
NPV, proc.	85,71	73,00	77,00	70,56	80,00	73,65

CTx – chemoterapinė grupė; CRT – chemospindulinė grupė; TPV – teigiama prognostinė vertė; NPV – neigiama prognostinė vertė.

3.4. Mezőrektinės fascijos invazija ir cirkuliuojanti rezekcijos riba

Pacientų pasiskirstymas pagal mezőrektinės fascijos invazijos prieš gydymą ir po gydymo bei cirkuliuojančios rezekcijos ribos būklę pateiktas 3.4.1 lentelėje. Abiejose CTx ir CRT gydymo grupėse po gydymo padidėjo pacientų, klasifikuotų kaip MRF–, procentinė dalis. Tačiau reikšmingas pagerėjimas statistiškai buvo pastebėtas tik CRT grupėje ($p = 0,001$). CTx grupėje reikšmingo skirtumo tarp pradinio mrMRF ir po gydymo ymrMRF būklės tarp neigiamų ir teigiamų atvejų nenustatyta ($p = 0,110$). Patologinė analizė parodė statistiškai reikšmingai didesnę CRM– pacientų dalį taip pat tik CRT grupėje ($p = 0,043$).

3.4.1 lentelė. Pacientų pasiskirstymas pagal mezőrektinės fascijos bei cirkuliuojančios rezekcijos ribos būklę chemoterapinėje ir chemospindulinio gydymo grupėse

Rodiklis	CTx grupė (n = 40)		p	CRT grupė (n = 49)		p
	mrMRF	ymrMRF		mrMRF	ymrMRF	
Neigiama (–)	20 (50)	28 (70)	0,110	20 (40,8)	38 (77,6)	0,001
Teigiama (+)	20 (50)	12 (30)		29 (59,2)	11 (22,4)	
	ymrMRF	pCRM	0,101	ymrMRF	pCRM	0,043
Neigiama (–)	28 (70)	35 (87,5)		38 (77,6)	46 (93,9)	
Teigiama (+)	12 (30)	5 (12,5)		11 (22,4)	3 (6,1)	

Reikšmės yra skaičius (proc.). CTx – chemoterapinė grupė; CRT – chemospindulinė grupė; mrMRF – mezőrektinė fascija prieš gydymą; ymrMRF – mezőrektinė fascija po gydymo; pCRM – patologinė cirkuliuojanti rezekcijos riba.

ymrMRF ir CRM būklės sutapimo rodiklis bendroje (CTx ir CRT) grupėje buvo 70,8 proc. Taip pat buvo apskaičiuotas šių parametrų jautrumas, specifiskumas, TPV ir NPV (3.4.2 lentelė).

3.4.2 lentelė. Sutapimo rodiklis ir diagnostinis tikslumas tarp MRT vertintos mezorektinės fascijos ir patologiškai patvirtintos cirkuliariosios rezekcijos ribos po gydymo chemoterapinėje, chemospindulinėje ir kombinuotoje grupėse

Rodiklis	CTx grupė (n = 40)	CRT grupė (n = 49)	Bendra CTx + CRT grupė (n = 89)
Sutapimo rodiklis, proc.	80,0	63,3	70,8
Jautrumas, proc.	41,67	60,00	50,00
Specifiškumas, proc.	83,33	88,37	85,56
TPV, proc.	41,67	54,55	47,83
NPV, proc.	83,33	90,48	86,96

Sutapimo rodiklis – tarp ymrMRF ir CRM. CTx – chemoterapinė grupė; CRT – chemospindulinė grupė; TPV – teigiama prognostinė vertė; NPV – neigiama prognostinė vertė.

3.5. Ekstramuralinė veninė invazija ir jos balo pasiskirstymas

Pacientų pasiskirstymas pagal EMVI būklę prieš gydymą ir po gydymo, limfovaskulinę invaziją bei EMVI balus pateiktas 3.5.1. lentelėje. Po neoadjuvantinio gydymo tik CTx grupėje statistiškai reikšmingai padaugėjo pacientų, kuriems buvo nustatyta neigiama EMVI ($p = 0,024$). Po gydymo atlikta patloginė analizė neatskleidė reikšmingų skirtumų tarp EMVI būklės šiose grupėse ($p = 0,482$ CTx grupėje ir $p = 1,00$ CRT grupėje).

3.5.1 lentelė. Pacientų pasiskirstymas pagal ekstramuralinę veninę invaziją ir jos balą chemoterapijos ir chemospindulinio gydymo grupėse

Rodiklis	CTx grupė (n = 40)		p	CRT grupė (n = 49)		p
	mrEMVI	yMrEMVI		mrEMVI	yMrEMVI	
EMVI–	17 (42,5)	28 (70)	0,024	27 (55,1)	29 (59,2)	0,838
EMVI+	23 (57,5)	12 (30)		22 (44,9)	20 (40,8)	
	yMrEMVI	pLVI	0,482	yMrEMVI	pLVI	1,0
EMVI–	28 (70)	24 (60)		34 (69,4)	34 (69,4)	
EMVI+	12 (30)	16 (40)		15 (30,6)	15 (30,6)	
EMVI balas	Prieš gydymą	Po gydymo		Prieš gydymą	Po gydymo	
0	17 (42,5)	28 (70,0)	0,001	26 (53,1)	34 (69,4)	0,001
1	0	0		2 (4,1)	0	
2	0	6 (15,0)		2 (4,1)	2 (4,1)	
3	13 (32,5)	5 (12,5)		10 (20,4)	9 (18,4)	
4	10 (25,0)	1 (2,5)		9 (18,4)	4 (8,2)	

Reikšmės yra skaičius (proc.). CTx – chemoterapinė grupė; CRT – chemospindulinė grupė; mrEMVI – ekstramuralinė veninė invazija prieš gydymą; yMrEMVI – ekstramuralinė veninė invazija po gydymo; pLVI – patologo patvirtinta limfovaskulinė invazija.

ymrEMVI ir pLVI būklės sutapimo rodiklis bendroje CTx ir CRT grupėje buvo 91,25 proc. Taip pat buvo pastebėtas didelis jautrumas (88,57 proc.), specifiškumas (93,55 proc.), TPV (88,57 proc.) ir NPV (93,55 proc.) (3.5.2 lentelė). Atskirų grupių sutapimo rodikliai buvo 82,5 proc. CTx grupėje ir 100,0 proc. CRT grupėje.

3.5.2 lentelė. *Sutapimo rodiklis, jautrumo, specifiškumo, TPV, NPV analizė tarp ymrEMVI ir pLVI grupių*

Rodiklis	CTx grupė (n = 40)	CRT grupė (n = 49)	Bendra CTx + CRT grupė (n = 89)
Sutapimo rodiklis, proc.	82,5	100,00	91,25
Jautrumas, proc.	80,00	100,00	88,57
Specifiškumas, proc.	85,71	100,00	93,55
TPV, proc.	80,00	100,00	88,57
NPV, proc.	85,71	100,00	93,55

Sutapimo rodiklis – tarp ymrEMVI ir pLVI; TPV – teigiama prognostinė vertė; NPV – neigiama prognostinė vertė; ymrEMVI – ekstramuralinė veninė invazija po gydymo; pLVI – patologo patvirtinta limfovaskulinė invazija.

3.6. Funkcinė difuzijos seka ir tariamas difuzijos koeficientas

3.6.1. Tariamo difuzijos koeficiento vertinimas. T ir N stadijos prieš gydymą

Šiame tyrime vidutinė naviko DWI tariamo difuzijos koeficiento (ADC) reikšmė prieš gydymą CTx grupėje buvo $699,75 (SN 95,35) \times 10^{-3} \text{ mm}^2/\text{s}$, o CRT grupėje – $708,88 (SN 114,57) \times 10^{-3} \text{ mm}^2/\text{s}$ (3.6.1.1 lentelė). Sujungus abi grupes, vidutinė naviko ADC reikšmė prieš gydymą buvo $704,32 (SN 104,96) \times 10^{-3} \text{ mm}^2/\text{s}$.

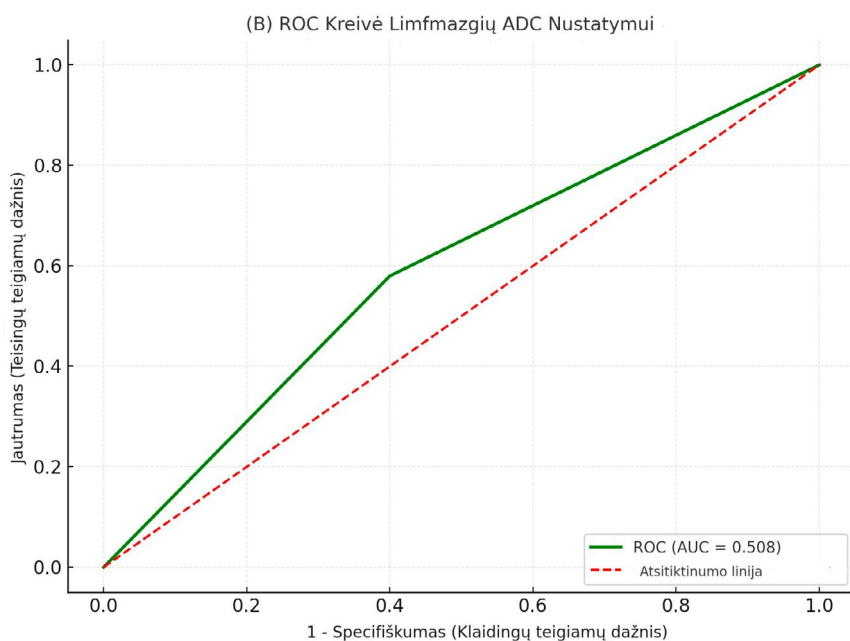
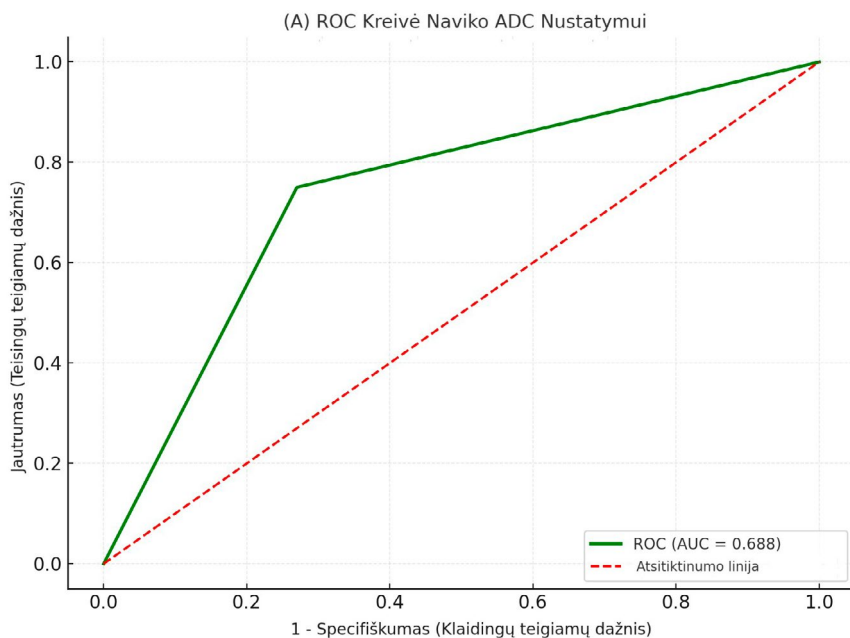
Prieš gydymą tiek CTx, tiek CRT grupių limfmazgių ADC reikšmės buvo panašios: CTx grupėje vidutinė reikšmė siekė $639,33 (SN 71,83) \times 10^{-3} \text{ mm}^2/\text{s}$, o CRT grupėje – šiek tiek didesnė, $654,39 (SN 71,83) \times 10^{-3} \text{ mm}^2/\text{s}$ (3.6.1.1 lentelė).

3.6.1.1 lentelė. Tiesiosios žarnos naviko ir sritinių limfmazgių ADC vertės prieš gydymą

Stadija	CTx grupė (n = 40)			CRT grupė (n = 49)		
	T ADC _{min}	T ADC _{vid}	T ADC _{maks}	T ADC _{min}	T ADC _{vid}	T ADC _{maks}
T0	–	–	–	–	–	–
T1	–	–	–	–	–	–
T2	–	–	–	709,64 (69,92)	775,16 (51,60)	940,67 (80,60)
T3a	–	–	–	691,21 (118,03)	847,18 (82,84)	1003,16 (111,91)
T3b	605,38 (29,44)	811,12 (84,36)	1016,88 (127,06)	665,14 (114,89)	843,53 (98,75)	1021,93 (155,42)
T3c	663,39 (17,95)	783,69 (40,00)	1004,00 (83,37)	656,43 (148,31)	835,35 (90,07)	1014,29 (92,40)
T3d	623,00 (35,38)	789,30 (93,94)	955,60 (121,52)	651,00 (92,45)	818,25 (55,13)	985,50 (116,09)
T4a	644,17 (36,01)	837,33 (61,17)	1030,50 (147,47)	–	–	–
p	0,324	0,438	0,724	0,793	0,696	0,865
RV	1228,28 (124,82)			1219,80 (128,44)		
Stadija	N ADC _{min}	N ADC _{vid}	N ADC _{maks}	N ADC _{min}	N ADC _{vid}	N ADC _{maks}
N0	–	–	–	779,00 (00,00)	950,50 (00,00)	922,00 (00,00)
N1	688,00 (106,51)	788,42 (67,51)	988,85 (107,59)	638,59 (132,30)	911,59 (86,77)	984,53 (122,17)
N2	605,41 (91,09)	810,63 (72,02)	1015,85 (118,69)	581,94 (102,80)	846,50 (79,29)	911,06 (119,51)
p	0,595	0,358	0,492	0,290	0,149	0,476
ILN	844,05 (102,80)			858,05 (102,08)		

Reikšmės yra vidurkiai (standartinis nuokrypis). T ADC – naviko ADC reikšmės prieš gydymą; RV – „sveikos“ sienos ADC; N ADC – limfmazgio ADC reikšmės prieš gydymą; ILN – „sveiko“ limfmazgio ADC.

ROC kreivės analizė (3.6.1.1 pav. A) ADC reikšmėms, skirtoms tiesiosios žarnos vėžio aptikimui, parodė AUC reikšmę 0,688 ($p < 0,001$); optimalus ribinis ADC reikšmės dydis buvo $705 \times 10^{-3} \text{ mm}^2/\text{s}$ su 75 proc. jautrumu ir 73 proc. specifiškumu. Limfmazgių ADC reikšmių ROC kreivė (3.6.1.1 pav. B) parodė AUC reikšmę 0,508 ($p < 0,001$), o ribinė reikšmė buvo $655 \times 10^{-3} \text{ mm}^2/\text{s}$, su 58 proc. jautrumu ir 60 proc. specifiškumu.



3.6.1.1 pav. ROC kreivių analizė optimalioms tariamo difuzijos koeficiento reikšmėms nustatyti

(A) Tiesiosios žarnos vėžio optimali ribinė ADC reikšmė buvo $705 \times 10^{-3} \text{ mm}^2/\text{s}$, o AUC – 0,688; (B) limfmazgių optimali ribinė ADC reikšmė buvo $655 \times 10^{-3} \text{ mm}^2/\text{s}$, o AUC – 0,508.

3.6.2. ADC parametų vertinimas. T ir N stadijos po gydymo

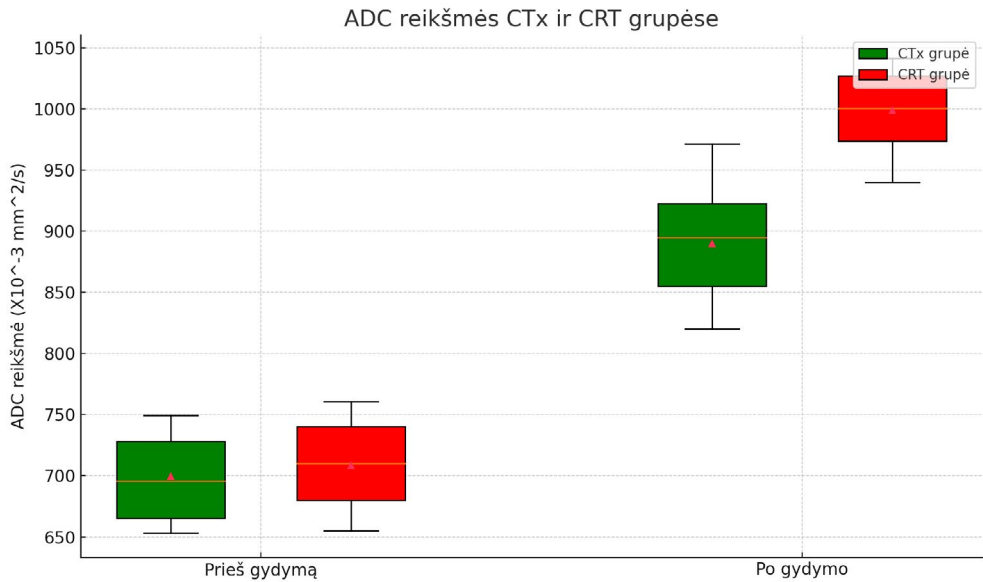
Po gydymo vidutinės naviko (T) ADC reikšmės padidėjo abiejose grupėse: 890,35 (SN 105,81) $\times 10^{-3}$ mm²/s CTx grupėje ir 999,41 (SN 115,97) $\times 10^{-3}$ mm²/s CRT grupėje (3.6.2.1 lentelė).

3.6.2.1 lentelė. Tiesiosios žarnos naviko ir sritinių limfmazgių ADC vertės po gydymo

yT	CTx grupė (n = 40)			CRT grupė (n = 49)		
	yT ADC _{min}	yT ADC _{vid}	yT ADC _{maks}	yT ADC _{min}	yT ADC _{vid}	yT ADC _{maks}
T0	822,00 (32,52)	926,00 (0,70)	1030,00 (31,11)	874,25 (85,63)	969,62 (77,46)	1065,00 (102,12)
T1	–	–	–	–	–	–
T2	761,33 (137,00)	928,33 (124,59)	1095,33 (125,54)	–	–	–
T3a	7837,10 (75,44)	907,00 (85,65)	1076,90 (161,81)	840,38 (138,46)	940,25 (90,34)	1040,13 (114,45)
T3b	725,95 (108,41)	911,57 (87,47)	1097,21 (138,64)	804,08 (110,32)	948,40 (85,78)	1092,73 (149,59)
T3c	751,00 (72,12)	903,50 (1,00)	955,50 (74,24)	–	–	–
T3d	636,00 (00,00)	909,50 (00,00)	983,00 (00,00)	–	–	–
T4a	–	–	–	–	–	–
p	0,256	0,217	0,559	0,150	0,855	0,619
RV	1227,67 (169,29)			1219,80 (148,13)		
yN	yN ADC _{min}	yN ADC _{vid}	yN ADC _{maks}	yN ADC _{min}	yN ADC _{vid}	yN ADC _{maks}
N0	849,80 (112,71)	923,96 (98,39)	1098,13 (134,06)	811,21 (125,37)	969,86 (68,60)	1128,53 (102,49)
N1	828,36 (117,74)	916,68 (96,49)	1105,00 (112,79)	888,96 (108,88)	933,96 (89,31)	1078,96 (158,80)
N2	811,07 (91,66)	891,78 (90,56)	1172,50 (166,09)	918,67 (154,37)	949,00 (133,92)	1079,33 (193,45)
p	0,626	0,645	0,825	0,787	0,373	0,495
yILN	876,20 (70,19)			899,80 (71,92)		

Reikšmės yra vidurkis (standartinis nuokrypis). CTx – chemoterapija; CRT – chemospindulinė terapija; yT ADC – naviko ADC reikšmės po gydymo; RV – „sveikos“ sienos ADC; yN ADC – limfmazgio ADC reikšmės po gydymo; ILN – „sveiko“ limfmazgio ADC.

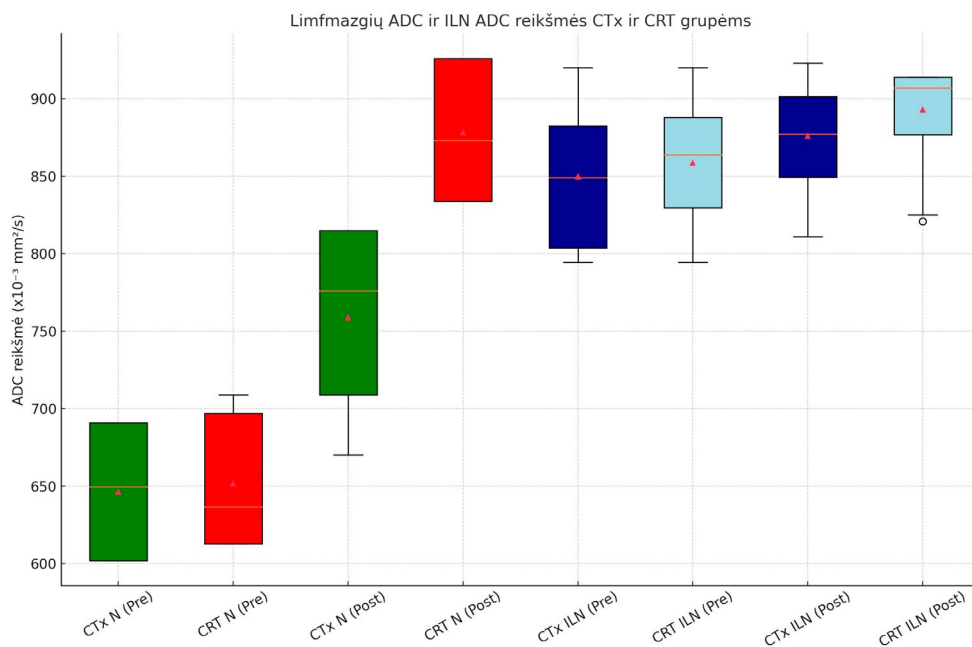
Po gydymo ADC reikšmės buvo didesnės CRT grupėje (3.6.2.1 pav.).



3.6.2.1 pav. Diagramos, vaizduojančios vidutines navikų ADC reikšmes prieš ir po gydymo abiejose gydymo grupėse

ADC reikšmės pateikiamos $\times 10^{-3} \text{ mm}^2/\text{s}$. CTx – chemoterapijos grupė; CRT – chemospindulinio gydymo grupė; ADC – tariamas difuzijos koeficientas.

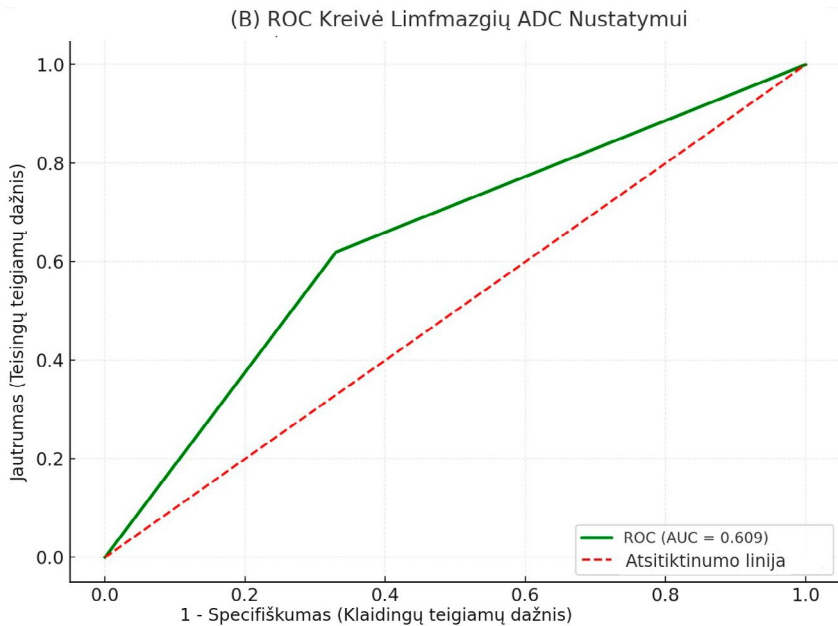
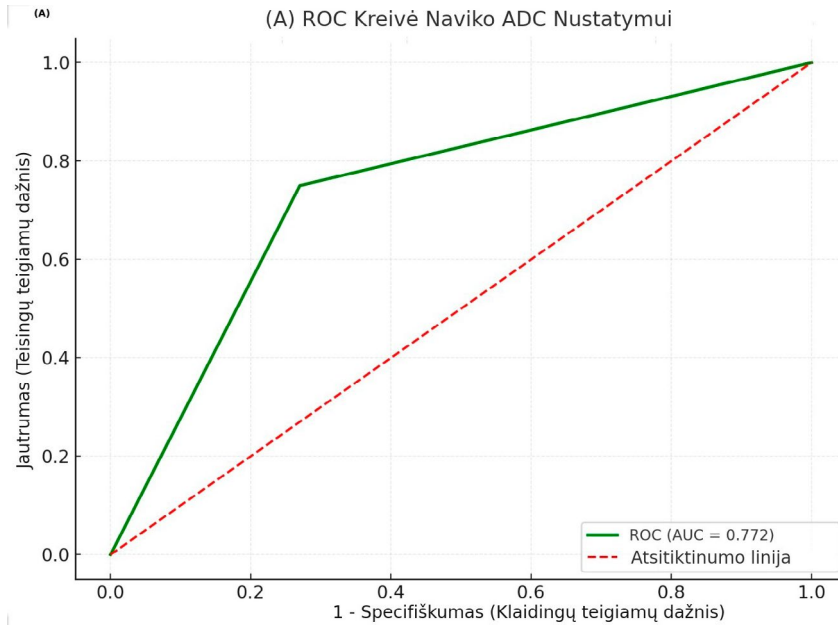
Po gydymo reikšmingai padidėjo ir limfmazgių (N) ADC reikšmės. CTx grupėje limfmazgių vidutinė ADC reikšmė buvo 755,38 (SN 105,81) $\times 10^{-3} \text{ mm}^2/\text{s}$, o CRT grupėje buvo šiek tiek didesnė – 884,78 (SN 73,22) $\times 10^{-3} \text{ mm}^2/\text{s}$ (3.6.2.2 pav.).



3.6.2.2 pav. Diagramos, vaizduojančios vidutines limfmazgių ADC reikšmes prieš ir po gydymo abiejose gydymo grupėse

ADC reikšmės pateikiamos $\times 10^{-3} \text{ mm}^2/\text{s}$. CTx ir CRT N_ADC Pre – limfmazgių vidutinės ADC reikšmės prieš gydymą CTx ar CRT grupėse; CTx ir CRT N_ADC Post – limfmazgių vidutinės ADC reikšmės po gydymo CTx ar CRT grupėse; CTx ir CRT ILN Pre/Post – „sveikų“ limfmazgių vidutinės ADC reikšmės prieš ir po gydymo.

Po gydymo ADC reikšmių ROC kreivės analizė, skirta tiesiosios žarnos vėžiui nustatyti (3.6.2.3 pav. A), parodė AUC reikšmę 0,772 ($p < 0,001$). Optimalus ribinis dydis buvo $991 \times 10^{-3} \text{ mm}^2/\text{s}$ su 75 proc. jautrumu ir 73 proc. specifiškumu. Limfmazgių ADC reikšmių ROC kreivė (3.6.2.3 pav. B) parodė AUC reikšmę 0,609 ($p < 0,001$), o ribinė reikšmė buvo $770 \times 10^{-3} \text{ mm}^2/\text{s}$, su 62 proc. jautrumu ir 67 proc. specifiškumu.



3.6.2.3 pav. Tariamą difuzijos koeficiento (ADC) ROC kreivių analizė

(A) Tiesiosios žarnos vėžio ADC ROC kreivės analizė. Optimali ribinė ADC reikšmė buvo $991 \times 10^{-3} \text{ mm}^2/\text{s}$. AUC 0,772; (B) limfmazgių ADC ROC kreivės analizė. Optimali ribinė ADC reikšmė buvo $772 \times 10^{-3} \text{ mm}^2/\text{s}$. AUC 0,508.

3.7. Naviko tūris ir naviko tūrio sumažėjimo rodiklis

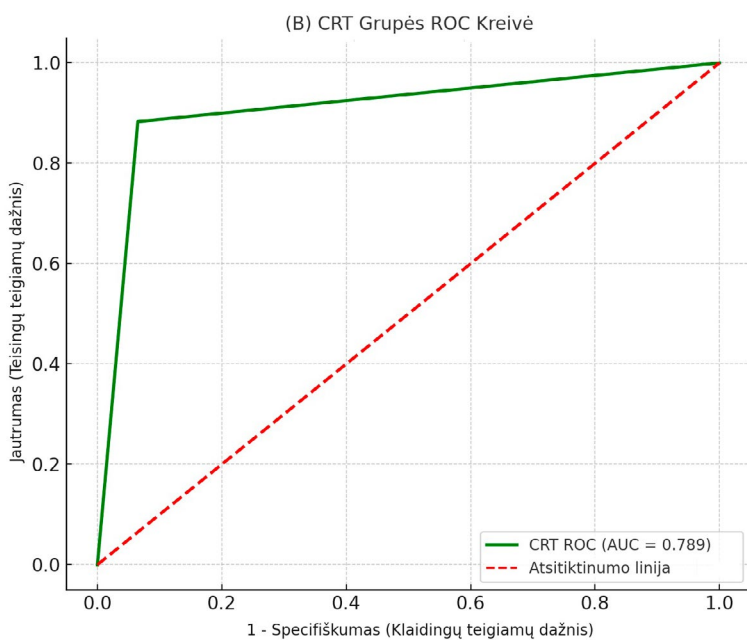
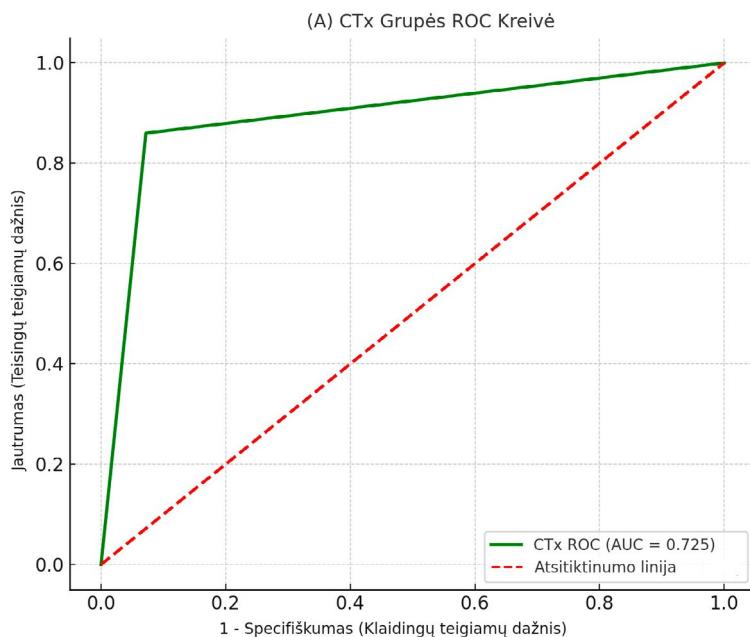
Prieš gydymą naviko tūriai buvo panašūs CTx ir CRT grupėse ($p = 0,73$). Tačiau po gydymo CRT grupėje buvo nustatytas reikšmingai mažesnis vidutinis tūris, palyginti su CTx grupe ($p < 0,001$). Be to, TVRR buvo reikšmingai didesnis CRT grupėje, rodantis didesnę naviko tūrio sumažėjimą, palyginti su CTx grupe ($p < 0,001$) (3.7.1 lentelė).

3.7.1 lentelė. Tūrio pasiskirstymas chemoterapijos ir chemospindulinės terapijos grupėse

Rodiklis	CTx grupė (n = 40)	CRT grupė (n = 49)	p
Tūris prieš gydymą, cm ³	46.75 (34.74–59.81)	46.5 (34.0–57.1)	0.73
Tūris po gydymo, cm ³	28.4 (22.04–39.56)	19.85 (15.5–25.52)	< 0.001
TVRR, proc.	31.1 (25.6–40.9)	53.3 (41.9–67.5)	< 0.001

Reikšmės yra mediana (tarpkvartilinis plotis). CTx – chemoterapijos grupė, CRT – chemospindulinės terapijos grupė, TVRR – naviko tūrio sumažėjimo rodiklis.

TVRR ribinės reikšmės CTx ir CRT grupėms buvo apskaičiuotos naudojant ROC analizę, siekiant atskirti abi gydymo grupes. ROC analizės pagalba buvo nustatytas TVRR AUC (3.7.1 pav.).



3.7.1 pav. Naviko tūrio sumažėjimo rodiklio (TVRR) ROC kreivių analizė

(A) CTx grupės TVRR ribinė reikšmė buvo 25,3 proc., AUC = 0,725; (B) CRT grupės TVRR ribinė reikšmė buvo 48,7 proc., AUC = 0,789.

3.8. Magnetinio rezonanso tomografijos naviko regresijos laipsnis

3.8.1 lentelėje pateikiami apibendrinti duomenys apie CTx ir CRT gydymo grupes, remiantis mrTRG ir pTRG duomenis. Nebuvo nei vieno mrTRG5 (atsakė į gydymą) ar pTRG0 (atsakė į gydymą) atvejo, nes visi pacientai daugiau ar mažiau atsakė į gydymą. Nustatytos statistiškai reikšmingos sąsajos pagal mrTRG ir pTRG vertinimus abiejose grupėse ($p < 0,001$ ir $p = 0,003$, atitinkamai).

3.8.1 lentelė. Pacientų pasiskirstymas pagal naviko regresijos laipsnį chemoterapijos ir chemospindulinės terapijos grupėse

Laipsnis	CTx grupė (n = 40)		p	CRT grupė (n = 49)		p
	mrTRG	pTRG		mrTRG	pTRG	
TRG0	–	0	< 0,001	–	0	0,003
TRG1	3 (7,5)	7 (17,5)		7 (14,2)	1 (2,3)	
TRG2	7 (17,5)	22 (55)		17 (34,7)	28 (57,14)	
TRG3	20 (50)	7 (17,5)		24 (48,8)	14 (28,57)	
TRG4	10 (25)	4 (10)		1 (2,3)	6 (12)	
TRG5	0	–		0	–	

Reikšmės yra skaičius (proc.). mrTRG0 ir pTRG5 reikšmių skalėse nėra, todėl lentelėje pažymėta kaip „–“. CTx – chemoterapijos grupė, CRT – chemospindulinės terapijos grupė, mrTRG – naviko regresijos laipsnis, nustatytas remiantis MRT; pTRG – patologinis naviko regresijos laipsnis.

Vertinant mrTRG būklę pagal priešoperacinius MRT duomenis ir lyginant su pTRG pagal histopatologinius rezultatus, jautrumas siekė 95 proc., specifškumas – 87 proc., o sutapimo rodiklis buvo 92,5 proc.

3.9. Sąsajos tarp naviko tūrio, naviko tūrio sumažėjimo rodiklio, magnetinio rezonanso tomografija ir patologo vertinto naviko regresijos laipsnio

Analizė parodė, kad prieš gydymą naviko tūriai tarp gero ir blogo atsako į gydymą pacientų abiejose grupėse reikšmingai nesiskyrė (3.9.1 lentelė). Po gydymo naviko tūris reikšmingai skyrėsi gero ir blogo atsako pacientų tik CRT grupėje: gero atsako pacientų naviko tūrio mediana buvo 18,00 cm³ (TKP 7,07–22,72), o blogo atsako pacientų – 20,20 cm³ (TKP 17,00–30,20) ($p = 0,038$). TVRR rezultatai dar labiau pabrėžė CRT veiksmingumą: gero atsako pacientų TVRR mediana siekė 64,85 proc. (TKP 52,47–83,13) palyginti su 44,10 proc. (TKP 36,90–53,50) blogo atsako pacientų tarpe ($p < 0,001$), o CTx grupė neparodė reikšmingo skirtumo ($p = 0,217$).

3.9.1 lentelė. Naviko tūrio ir naviko tūrio sumažėjimo rodiklio rezultatai pagal magnetinio rezonanso tomografiją vertintą naviko regresijos laipsnį

Rodiklis	CTx grupė (n = 40)		p	CRT grupė (n = 49)		p
	Gero atsako mrTRG1-2	Blogo atsako mrTRG3-4-5		Gero atsako mrTRG1-2	Blogo atsako mrTRG3-4-5	
Naviko tūris prieš gydymą, cm ³	52,25 (34,94–57,81)	43,39 (22,58–50,25)	0,542	50,79 (36,60–57,73)	41,40 (29,90–56,44)	0,430
Naviko tūris po gydymo, cm ³	28,525 (22,32–36,53)	28,025 (18,68–38,96)	0,962	18,00 (7,07–22,72)	20,20 (17,00–30,20)	0,038
TVRR, %	33,45 (21,94–37,91)	29,85 (20,44–41,83)	0,217	64,85 (52,47–83,13)	44,10 (36,90–53,50)	< 0,001

Reikšmės yra medianos (tarpkvartiliniai pločiai). CTx – chemoterapijos grupė, CRT – chemospindulinės terapijos grupė, mrTRG – magnetinio rezonanso tomografija vertintas naviko regresijos laipsnis, TVRR – naviko tūrio sumažėjimo rodiklis.

Panašūs duomenys buvo nustatyti ir remiantis pTRG (3.9.2 lentelė). CRT ir CTx grupėse gero atsako pacientų naviko tūrio mediana prieš gydymą statistiškai reikšmingai nesiskyrė nuo blogo atsako pacientų naviko tūrio medianos. Tačiau po gydymo, tik CRT grupė parodė reikšmingą skirtumą: naviko tūrio mediana po gydymo buvo 17,50 cm³ (TKP 5,68–22,50) gero atsako pacientams ir 20,10 cm³ (TKP 16,98–30,45) blogo atsako pacientams (p = 0,042). Taip pat šioje grupėje gero atsako pacientai pasiekė reikšmingai didesnę TVRR nei blogo atsako pacientai: 61,30 proc. (TKP 46,17–85,00) palyginti su 48,70 proc. (TKP 38,43–58,00) (p = 0,030).

3.9.2 lentelė. Naviko tūrio ir naviko tūrio sumažėjimo rodiklio rezultatai pagal patologo vertintą naviko regresijos laipsnį

Rodiklis	CTx grupė (n = 40)		p	CRT grupė (n = 49)		p
	Gero atsako pTRG3-4	Blogo atsako pTRG0-1-2		Gero atsako pTRG3-4	Blogo atsako pTRG0-1-2	
V prieš gydymą, cm ³	45,98 (35,89–64,43)	48,77 (29,63–57,84)	0,712	44,58 (34,00–54,70)	48,19 (32,98–58,74)	0,578
V po gydymo, cm ³	24,63 (15,13–44,30)	31,30 (22,76–39,02)	0,488	17,50 (5,68–22,50)	20,10 (16,98–30,45)	0,042
TVRR, %	36,35 (26,33–65,75)	30,05 (24,48–36,55)	0,121	61,30 (46,17–85,00)	48,70 (38,43–58,00)	0,030

Reikšmės yra medianos (tarpkvartiliniai pločiai). pTRG – patologinis naviko regresijos laipsnis, V prieš gydymą – naviko tūris prieš gydymą, V po gydymo – naviko tūris po gydymo, TVRR – naviko tūrio sumažėjimo rodiklis.

Buvo nustatytos ribinės TVRR reikšmės, leidžiančios atskirti gero ir blogo atsako pacientus abiejose grupėse pagal mrTRG ir pTRG klasifikacijas. CTx grupėje TVRR ribinė reikšmė buvo 19,0 proc., nurodanti, kad pacientai, kurių TVRR buvo didesnis nei ribinė reikšmė, buvo laikomi gero atsako pacientais, o tie, kurių TVRR buvo mažesnis – blogo atsako pacientais. CRT grupėje TVRR ribinė reikšmė buvo 34,3 proc., taip pat skirianti gero nuo blogo atsako pacientus.

IŠVADOS

1. Magnetinio rezonanso tomografija yra vertinga T stadijos mažėjimo vertinime abiejose grupėse, pasižyminti 79,49 proc. jautrumu ir 80 proc. specifiškumu. Magnetinio rezonanso tomografija taip pat rodo reikšmingą, bet ribotą gebėjimą įvertinti N stadijos mažėjimą: jautrumas siekia 67,53 proc., o specifiškumas – 71,65 proc. Nors magnetinio rezonanso tomografija T reikšmingai įvertina stadijas abiejose grupėse, T ir N stadijų atsako skirtumai rodo, kad chemospindulinis gydymas užtikrina geresnius naviko ir limfmazgių regresijos rodiklius, palyginti su chemoterapija.
2. Tariamo difuzijos koeficiento pokyčiai prieš ir po gydymo buvo reikšmingi vertinant T stadijos sumažėjimą abiejose gydymo grupėse ir N stadijos sumažėjimą chemospindulinio gydymo grupėje, tačiau N stadijos neoadjuvantinio gydymo poveikio vertinime pokyčiai nebuvo reikšmingi chemoterapinio gydymo grupėje.
3. Ekstramuralinės veninės invazijos būseną, vertinta magnetinio rezonanso tomografija, palyginus su patologiškai nustatyta limfovaskuline invazija parodė reikšmingą atitikmenį ir gali būti naudojamas kaip neinvazinis prognostinis veiksnys. Mezorektinės fascijos būseną, vertinta magnetinio rezonanso tomografija, palyginus su patologiškai nustatyta cirkuliariąja rezekcijos riba parodė silpnas sąsajas, todėl jos laikymas neinvaziniu prognostiniu veiksniu yra diskutuotinas. Esminių ekstramuralinės veninės invazijos ir mezorektinės fascijos būsenos pokyčių tarp gydymo grupių nenustatyta.
4. Naviko tūrio sumažėjimo rodiklio ir magnetinio rezonanso tomografija vertinto naviko regresijos laipsnio pokyčiai chemospindulinio gydymo grupėje buvo reikšmingai didesni nei chemoterapinio gydymo grupėje. Šie rodikliai gali būti naudojami kaip neinvaziniai įrankiai, skirti atpažinti gero ir blogo atsako pacientus abiejose neoadjuvantinio gydymo grupėse.

PRAKTINĖS REKOMENDACIJOS

Bendras šio darbo tikslas buvo išsamiai ištirti diagnostinius MRT metodus ir pritaikyti juos kasdieniniame tiesiosios žarnos vėžio ištyrimo kontekste.

1. MRT tyrimas yra pagrindinis diagnostinis metodas ne tik pradiniam tiesiosios žarnos vėžio stadijavimui ir restadijavimui (T ir N), tačiau ir akcentuojant pagrindinius prognostinius veiksnius (MRF ir EMVI), kas yra itin svarbu ir naudingą norint suskirstyti paciento rizikas ir individualizuoti paciento gydymą.
2. Kadangi tiesiosios žarnos vėžio atsako į gydymą/restadijavimo MRT vertinime vis dar kyla iššūkių, rekomenduojama vadovautis standartizuotais MRT ištyrimo ir aprašymo kriterijais.
3. Prie šiuo metu jau esančių standartinių TN ir MRF vertinimų, paskutiniiais metais pridėtų EMVI vertinimų, galima būtų pridėti TVRR kartu su mrTRG metrika, kas galėtų suteikti papildomos informacijos, vertinant gydymo efektyvumą, ypač taikant kombinuotą gydymą.

REFERENCES

1. Chen X, Leng W, Zhou Y, et al.: Pathological response and safety of FOLFOXIRI for neoadjuvant treatment of high-risk relapsed locally advanced colon cancer: study protocol for a single-arm, open-label phase II trial. *BMJ Open*. 2023, 13:062659. doi: 10.1136/bmjopen-2022-062659
2. Marcellinaro R, Spoletini D, Grieco M, Avella P, Cappuccio M, Troiano R, Lisi G, Garbarino GM, Carlini M. Colorectal Cancer: Current Updates and Future Perspectives. *J Clin Med*. 2023 Dec 21;13(1):40. doi: 10.3390/jcm13010040. PMID: 38202047; PMCID: PMC10780254.
3. Ferlay J, Ervik M, Lam F, Laversanne M, Colombet M, Mery L, Piñeros M, Znaor A, Soerjomataram I, Bray F (2024). Global Cancer Observatory: Cancer Today. Lyon, France: International Agency for Research on Cancer. Available from: <https://gco.iarc.who.int/today>, accessed [DD Month YYYY].
4. Fernandes MC, Gollub MJ, Brown G. The importance of MRI for rectal cancer evaluation. *Surg Oncol*. 2022 Aug;43:101739. doi: 10.1016/j.suronc.2022.101739. Epub 2022 Mar 18. PMID: 35339339; PMCID: PMC9464708.
5. Brown G, Daniels IR. Preoperative staging of rectal cancer: the MERCURY research project. In: Buchler MW, Weitz J, Ulrich B, et al., editors. *Rectal Cancer Treatment*. Berlin, Heidelberg: Springer, 2005:58–74.
6. Beets-Tan R.G.H., Lambregts D.M.J., Maas M., Bipat S., Barbaro B., Curvo-Semedo L., Fenlon H.M., Gollub M.J., Gourtsoyianni S., Halligan S., et al. Magnetic resonance imaging for clinical management of rectal cancer: Updated recommendations from the 2016 European Society of Gastrointestinal and Abdominal Radiology (ESGAR) consensus meeting. *Eur. Radiol*. 2018;28:1465–1475. doi: 10.1007/s00330-017-5026-2.
7. MERCURY Study Group. Extramural depth of tumor invasion at thin-section MR in patients with rectal cancer: results of the MERCURY study. *Radiology* 2007;243:132–139.
8. Seo N, Kim H, Cho MS, Lim JS. Response Assessment with MRI after Chemoradiotherapy in Rectal Cancer: Current Evidences. *Korean J Radiol*. 2019 Jul;20(7):1003-1018. <https://doi.org/10.3348/kjr.2018.0611>
9. Bates DDB, Homs ME, Chang KJ, Lalwani N, Horvat N, Sheedy SP. MRI for Rectal Cancer: Staging, mrCRM, EMVI, Lymph Node Staging and Post-Treatment Response. *Clin Colorectal Cancer*. 2022 Mar;21(1):10-18. doi: 10.1016/j.clcc.2021.10.007. Epub 2021 Nov 14. PMID: 34895835; PMCID: PMC8966586.
10. Smith HG, Nilsson PJ, Shogan BD, Harji D, Gambacorta MA, Romano A, Brandl A, Qvortrup C. Neoadjuvant treatment of colorectal cancer: comprehensive review. *BJS Open*. 2024 May 8;8(3):zrae038. doi: 10.1093/bjsopen/zrae038. PMID: 38747103; PMCID: PMC11094476.
11. Haak HE, Maas M, Lahaye MJ, et al (2020) Selection of Patients for Organ Preservation After Chemoradiotherapy: MRI Identifies Poor Responders Who Can Go Straight to Surgery. *Ann Surg Oncol* 27:2732–2739.
12. Jayaprakasam VS, Alvarez J, Omer DM, Gollub MJ, Smith JJ, Petkovska I. Watch-and-Wait Approach to Rectal Cancer: The Role of Imaging. *Radiology*. 2023 Apr;307(1):e221529. doi: 10.1148/radiol.221529. Epub 2023 Mar 7. PMID: 36880951; PMCID: PMC10068893.
13. Caruso, D., Polici, M., Bellini, D. et al. ESR Essentials: Imaging in colorectal cancer—practice recommendations by ESGAR. *Eur Radiol* (2024). <https://doi.org/10.1007/s00330-024-10645-3>.

14. Alvfeldt G, Aspelin P, Blomqvist L, Sellberg N. Radiology reporting in rectal cancer using magnetic resonance imaging: Comparison of reporting completeness between different reporting styles and structure. *Acta Radiol Open*. 2024 Jul 1;13(7):20584601241258675. doi: 10.1177/20584601241258675. PMID: 39044838; PMCID: PMC11265246.
15. Lambregts DMJ, Boellaard TN, Beets-Tan RGH. Response evaluation after neoadjuvant treatment for rectal cancer using modern MR imaging: a pictorial review. *Insights Imaging*. 2019 Feb 13;10(1):15. doi: 10.1186/s13244-019-0706-x. PMID: 30758688; PMCID: PMC6375095.
16. Nobel, J.M., van Geel, K. & Robben, S.G.F. Structured reporting in radiology: a systematic review to explore its potential. *Eur Radiol* 32, 2837–2854 (2022). <https://doi.org/10.1007/s00330-021-08327-5>.
17. Nasir S, Anwar S, Ahmed M. Multidisciplinary team (MDT) meeting and Radiologist workload, a prospective review in a tertiary care hospital. *Pak J Med Sci*. 2017 Nov-Dec;33(6):1501-1506. doi: 10.12669/pjms.336.12905. PMID: 29492086; PMCID: PMC5768852.
18. Stephen Waite, Jinel Scott, Brian Gale, Travis Fuchs, Srinivas Kolla, and Deborah Reede. Interpretive Error in Radiology. *American Journal of Roentgenology* 2017 208:4, 739-749. DOI:10.2214/AJR.16.16963
19. Plumb AAO, Lambregts D, Bellini D, Stoker J, Taylor S; ESGAR Research Committee. Making useful clinical guidelines: the ESGAR perspective. *Eur Radiol*. 2019 Jul;29(7):3757-3760. doi: 10.1007/s00330-019-6002-9. Epub 2019 Feb 7. PMID: 30729331; PMCID: PMC6554243.
20. Miranda, J.; Causa Andrieu, P.; Nincevic, J.; Gomes de Farias, L.d.P.; Khasawneh, H.; Arita, Y.; Stanietzky, N.; Fernandes, M.C.; De Castria, T.B.; Horvat, N. Advances in MRI-Based Assessment of Rectal Cancer Post-Neoadjuvant Therapy: A Comprehensive Review. *J. Clin. Med*. 2024, 13, 172. <https://doi.org/10.3390/jcm13010172>.
21. Horvat N, Carlos Tavares Rocha C, Clemente Oliveira B, Petkovska I, Gollub MJ. MRI of Rectal Cancer: Tumor Staging, Imaging Techniques, and Management. *Radiographics*. 2019 Mar-Apr;39(2):367-387. doi: 10.1148/rg.2019180114. Epub 2019 Feb 15. PMID: 30768361; PMCID: PMC6438362.
22. Saklani AP, Bae SU, Clayton A, Kim NK. Magnetic resonance imaging in rectal cancer: a surgeon's perspective. *World J Gastroenterol*. 2014 Feb 28;20(8):2030-41. doi: 10.3748/wjg.v20.i8.2030. PMID: 24616572; PMCID: PMC3934473.
23. Beaton, L., Bandula, S., Gaze, M.N. et al. How rapid advances in imaging are defining the future of precision radiation oncology. *Br J Cancer* 120, 779–790 (2019). <https://doi.org/10.1038/s41416-019-0412-y>
24. European Society of Radiology (ESR). ESR paper on structured reporting in radiology—update 2023. *Insights Imaging* 14, 199 (2023). <https://doi.org/10.1186/s13244-023-01560-0>.
25. Granata V, Caruso D, Grassi R, Cappabianca S, Reginelli A, Rizzati R, Masselli G, Golfieri R, Rengo M, Regge D, Lo Re G, Pradella S, Fusco R, Faggioni L, Laghi A, Miele V, Neri E, Coppola F. Structured Reporting of Rectal Cancer Staging and Restaging: A Consensus Proposal. *Cancers (Basel)*. 2021 Apr 28;13(9):2135. doi: 10.3390/cancers13092135. PMID: 33925250; PMCID: PMC8125446.
26. Di Fabio F, Allievi N, Lord A, Bhagwanani A, Venkatasubramaniam A, Arnold S, Moran B. MRI-predicted extramural vascular invasion and tumour deposit are main predictors of disease-free survival in patients undergoing surgical resection for rectal cancer. *BJS Open*. 2024 Jan 3;8(1):zrad139. doi: 10.1093/bjsopen/zrad139. PMID: 38170894; PMCID: PMC10763995.

27. Pesapane F, Tantrige P, De Marco P, Carriero S, Zugni F, Nicosia L, Bozzini AC, Rotili A, Latronico A, Abbate F, Origgi D, Santicchia S, Petralia G, Carrafiello G, Cassano E. Advancements in Standardizing Radiological Reports: A Comprehensive Review. *Medicina* (Kaunas). 2023 Sep 17;59(9):1679. doi: 10.3390/medicina59091679. PMID: 37763797; PMCID: PMC10535385.
28. Parres, D.; Albiol, A.; Paredes, R. Improving Radiology Report Generation Quality and Diversity through Reinforcement Learning and Text Augmentation. *Bioengineering* 2024, 11, 351. <https://doi.org/10.3390/bioengineering11040351>.
29. Han J, Tao M, Wu X, Li D, Ma Y, Dawood S, Steele CW, Tan KK, Wang Q. Reporting quality of practice guidelines on colorectal cancer: evaluation using the RIGHT reporting checklist. *Ann Transl Med*. 2021 Jul;9(14):1175. doi: 10.21037/atm-21-2798. PMID: 34430616; PMCID: PMC8350680.
30. Nobel, J.M., Kok, E.M. & Robben, S.G.F. Redefining the structure of structured reporting in radiology. *Insights Imaging* 11, 10 (2020). <https://doi.org/10.1186/s13244-019-0831-6>.
31. Borgheresi A, De Muzio F, Agostini A, Ottaviani L, Bruno A, Granata V, Fusco R, Danti G, Flammia F, Grassi R, Grassi F, Bruno F, Palumbo P, Barile A, Miele V, Giovagnoni A. Lymph Nodes Evaluation in Rectal Cancer: Where Do We Stand and Future Perspective. *J Clin Med*. 2022 May 5;11(9):2599. doi: 10.3390/jcm11092599. PMID: 35566723; PMCID: PMC9104021.
32. Curvo-Semedo L, Lambregts DM, Maas M, Beets GL, Caseiro-Alves F, Beets-Tan RG: Diffusion-weighted MRI in rectal cancer: apparent diffusion coefficient as a potential non-invasive marker of tumor aggressiveness. *J Magn Reson Imaging*. 2012, 35:1365-71. 10.1002/jmri.23589.
33. Schurink, Niels & Lambregts, Doenja & Beets-Tan, Regina. (2018: Diffusion-weighted imaging in rectal cancer: current applications and future perspectives. *The British Journal of Radiology*. 92. 20180655, 10.1259/bjr.20180655
34. Bishehsari F, Mahdavinia M, Vacca M, Malekzadeh R, Mariani-Costantini R. Epidemiological transition of colorectal cancer in developing countries: environmental factors, molecular pathways, and opportunities for prevention. *World J Gastroenterol*. 2014 May 28;20(20):6055-72. doi: 10.3748/wjg.v20.i20.6055. PMID: 24876728; PMCID: PMC4033445.
35. World Health Organization. (2013). International classification of diseases for oncology (ICD-O), 3rd ed., 1st revision. World Health Organization. <https://iris.who.int/handle/10665/96612>.
36. Rawla P, Sunkara T, Barsouk A. Epidemiology of colorectal cancer: incidence, mortality, survival, and risk factors. *Prz Gastroenterol*. 2019;14(2):89-103. doi: 10.5114/pg.2018.81072. Epub 2019 Jan 6. PMID: 31616522; PMCID: PMC6791134.
37. GBD 2017 Colorectal Cancer Collaborators. The global, regional, and national burden of colorectal cancer and its attributable risk factors in 195 countries and territories, 1990-2017: a systematic analysis for the Global Burden of Disease Study 2017. *Lancet Gastroenterol Hepatol*. 2019 Dec;4(12):913-933. doi: 10.1016/S2468-1253(19)30345-0. Epub 2019 Oct 21. Erratum in: *Lancet Gastroenterol Hepatol*. 2020 Mar;5(3):e2. doi: 10.1016/S2468-1253(20)30017-0. PMID: 31648977; PMCID: PMC7026697.
38. Shirvani Shiri M, Emamgholipour S, Heydari H, Fekri N, Karami H. The Effect of Human Development Index on Obesity Prevalence at the Global Level: A Spatial Analysis. *Iran J Public Health*. 2023 Apr;52(4):829-839. doi: 10.18502/ijph.v52i4.12456. PMID: 37551189; PMCID: PMC10404321.
39. Lotfollahzadeh S, Kashyap S, Tsoaris A, et al. Rectal Cancer. [Updated 2023 Jul 4]. In: *StatPearls* [Internet]. Treasure Island (FL): StatPearls Publishing; 2024Jan. Available from: <https://www.ncbi.nlm.nih.gov/books/NBK493202>.

40. Bachir Benarba, Atanasio Pandiella, Colorectal cancer and medicinal plants: Principle findings from recent studies, *Biomedicine & Pharmacotherapy*, Volume 107, 2018, Pages 408-423, ISSN 0753-3322, <https://doi.org/10.1016/j.biopha.2018.08.006>.
41. Johns LE, Houlston RS: A systematic review and meta-analysis of familial colorectal cancer risk. *Am J Gastroenterol* 96 (10): 2992-3003, 2001.
42. Imperiale TF, Juluri R, Sherer EA, et al.: A risk index for advanced neoplasia on the second surveillance colonoscopy in patients with previous adenomatous polyps. *Gastrointest Endosc* 80 (3): 471-8, 2014.
43. Klepp P, Brackmann S, Cvancarova M, Hoivik ML, Hovde Ø, Henriksen M, Huppertz-Hauss G, Bernklev T, Hoie O, Kempster-Monstad I, Solberg IC, Stray N, Jahnsen J, Vatn MH, Moum B. Risk of colorectal cancer in a population-based study 20 years after diagnosis of ulcerative colitis: results from the IBSEN study. *BMJ Open Gastroenterol*. 2020 Mar 26;7(1):e000361. doi: 10.1136/bmjgast-2019-000361. PMID: 32337058; PMCID: PMC7170403.
44. Sawicki T, Ruszkowska M, Danielewicz A, Niedźwiedzka E, Arłukowicz T, Przybyłowicz KE. A Review of Colorectal Cancer in Terms of Epidemiology, Risk Factors, Development, Symptoms and Diagnosis. *Cancers (Basel)*. 2021 Apr 22;13(9):2025. doi: 10.3390/cancers13092025. PMID: 33922197; PMCID: PMC8122718.
45. Masdor NA, Mohammed Nawi A, Hod R, Wong Z, Makpol S, Chin SF. The Link between Food Environment and Colorectal Cancer: A Systematic Review. *Nutrients*. 2022 Sep 23;14(19):3954. doi: 10.3390/nu14193954. PMID: 36235610; PMCID: PMC9573320.
46. Choi Y, Kim N. Sex Difference of Colon Adenoma Pathway and Colorectal Carcinogenesis. *World J Mens Health*. 2024 Apr;42(2):256-282. <https://doi.org/10.5534/wjmh.230085>.
47. Yu J, Feng Q, Kim JH, Zhu Y. Combined Effect of Healthy Lifestyle Factors and Risks of Colorectal Adenoma, Colorectal Cancer, and Colorectal Cancer Mortality: Systematic Review and Meta-Analysis. *Front Oncol*. 2022 Jul 22;12:827019. doi: 10.3389/fonc.2022.827019. PMID: 35936678; PMCID: PMC9353059.
48. Beniwal SS, Lamo P, Kaushik A, Lorenzo-Villegas DL, Liu Y, MohanaSundaram A. Current Status and Emerging Trends in Colorectal Cancer Screening and Diagnostics. *Biosensors (Basel)*. 2023 Oct 13;13(10):926. doi: 10.3390/bios13100926. PMID: 37887119; PMCID: PMC10605407.
49. Hossain MS, Karuniawati H, Jairoun AA, Urbi Z, Ooi J, John A, Lim YC, Kibria KMK, Mohiuddin AKM, Ming LC, Goh KW, Hadi MA. Colorectal Cancer: A Review of Carcinogenesis, Global Epidemiology, Current Challenges, Risk Factors, Preventive and Treatment Strategies. *Cancers (Basel)*. 2022 Mar 29;14(7):1732. doi: 10.3390/cancers14071732. PMID: 35406504; PMCID: PMC8996939.
50. Gürses B, Böge M, Altınmakas E, Balık E. Multiparametric MRI in rectal cancer. *Diagn Interv Radiol*. 2019 May;25(3):175-182. doi: 10.5152/dir.2019.18189. PMID: 31063142; PMCID: PMC6521905.
51. Lisanne J.H. Smits, Annabel S. van Lieshout, Alexander A.J. Grüter, Karin Horsthuis, Jurriaan B. Tuynman, Multidisciplinary management of early rectal cancer – The role of surgical local excision in current and future clinical practice, *Surgical Oncology*, Volume 40, 2022, 101687, ISSN 0960-7404, <https://doi.org/10.1016/j.suronc.2021.101687>.

52. Moreno CC, Mittal PK, Sullivan PS, Rutherford R, Staley CA, Cardona K, Hawk NN, Dixon WT, Kitajima HD, Kang J, Small WC, Oshinski J, Votaw JR. Colorectal Cancer Initial Diagnosis: Screening Colonoscopy, Diagnostic Colonoscopy, or Emergent Surgery, and Tumor Stage and Size at Initial Presentation. *Clin Colorectal Cancer*. 2016 Mar;15(1):67-73. doi: 10.1016/j.clcc.2015.07.004. Epub 2015 Jul 29. PMID: 26602596.
53. Eng, Cathy et al., Colorectal cancer, *The Lancet*, Volume 404, Issue 10449, 294 – 310. Published: June 20, 2024 DOI: [https://doi.org/10.1016/S0140-6736\(24\)00360-X](https://doi.org/10.1016/S0140-6736(24)00360-X).
54. R. Glynne-Jones , L. Wyrwicz , E. Tiret, G. Brown , C. Rodin del , A. Cervantes & D. Arnold , on behalf of the ESMO Guidelines Committee. Rectal cancer: ESMO Clinical Practice Guidelines for diagnosis, treatment and follow-up. *Annals of Oncology* 28 (Supplement 4): iv22–iv40, 2017 doi:10.1093/annonc/mdx224.
55. De Muzio F, Fusco R, Cutolo C, Giacobbe G, Bruno F, Palumbo P, Danti G, Grazzini G, Flammia F, Borgheresi A, Agostini A, Grassi F, Giovagnoni A, Miele V, Barile A, Granata V. Post-Surgical Imaging Assessment in Rectal Cancer: Normal Findings and Complications. *J Clin Med*. 2023 Feb 13;12(4):1489. doi: 10.3390/jcm12041489. PMID: 36836024; PMCID: PMC9966470.
56. Marino MA, Avendano D, Zapata P, Riedl CC, Pinker K. Lymph Node Imaging in Patients with Primary Breast Cancer: Concurrent Diagnostic Tools. *Oncologist*. 2020 Feb;25(2):e231-e242. doi: 10.1634/theoncologist.2019-0427. Epub 2019 Oct 14. PMID: 32043792; PMCID: PMC7011661.
57. Bogveradze N, Snaebjornsson P, Grotenhuis BA, van Triest B, Lahaye MJ, Maas M, Beets GL, Beets-Tan RGH, Lambregts DMJ. MRI anatomy of the rectum: key concepts important for rectal cancer staging and treatment planning. *Insights Imaging*. 2023 Jan 18;14(1):13. doi: 10.1186/s13244-022-01348-8. PMID: 36652149; PMCID: PMC9849549.
58. Nataly Horvat, Camila Carlos Tavares Rocha, Brunna Clemente Oliveira, Iva Petkovska, and Marc J. Gollub. MRI of Rectal Cancer: Tumor Staging, Imaging Techniques, and Management. *RadioGraphics* 2019 39:2, 367-387. <https://doi.org/10.1148/rg.2019180114>.
59. Adigun AO, Adebile TM, Okoye C, Ogundipe TI, Ajekigbe OR, Mbaezue RN, Okobi OE. Causes and Prevention of Early-Onset Colorectal Cancer. *Cureus*. 2023 Sep 12;15(9):e45095. doi: 10.7759/cureus.45095. PMID: 37842356; PMCID: PMC10569084.
60. William Hamilton, Sarah E.R. Bailey. Colorectal cancer in symptomatic patients: How to improve the diagnostic pathway. *Best Practice & Research Clinical Gastroenterology*. Volume 66, 2023, 101842, ISSN 1521-6918. <https://doi.org/10.1016/j.bpg.2023.101842>.
61. Li Y, Xin J, Sun Y, Han T, Zhang H, An F. Magnetic resonance imaging-guided and targeted theranostics of colorectal cancer. *Cancer Biol Med*. 2020 May 15;17(2):307-327. doi: 10.20892/j.issn.2095-3941.2020.0072. PMID: 32587771; PMCID: PMC7309460.
62. Wouter H. Zwart et al., The Multimodal Management of Locally Advanced Rectal Cancer: Making Sense of the New Data. *Am Soc Clin Oncol Educ Book* 42, 264-277(2022). DOI:10.1200/EDBK_351411
63. Santiago, I., Figueiredo, N., Parés, O. et al. MRI of rectal cancer—relevant anatomy and staging key points. *Insights Imaging* 11, 100 (2020). <https://doi.org/10.1186/s13244-020-00890-7>.
64. Binda, C.; Secco, M.; Tuccillo, L.; Coluccio, C.; Liverani, E.; Jung, C.F.M.; Fabbri, C.; Gibiino, G. Early Rectal Cancer and Local Excision: A Narrative Review. *J. Clin. Med*. 2024, 13, 2292. <https://doi.org/10.3390/jcm13082292>.

65. Berardi R, Morgese F, Rinaldi S, Torniai M, Mentrasti G, Scortichini L, Giampieri R. Benefits and Limitations of a Multidisciplinary Approach in Cancer Patient Management. *Cancer Manag Res.* 2020 Sep 30;12:9363-9374. doi: 10.2147/CMAR.S220976. PMID: 33061625; PMCID: PMC7533227.
66. Pham TT, Liney GP, Wong K, Barton MB. Functional MRI for quantitative treatment response prediction in locally advanced rectal cancer. *Br J Radiol.* 2017 Apr;90(1072):20151078. doi: 10.1259/bjr.20151078. Epub 2017 Mar 7. PMID: 28055248; PMCID: PMC5605058.
67. Gao, Y., Pham, J., Yoon, S. et al. Recent Advances in Functional MRI to Predict Treatment Response for Locally Advanced Rectal Cancer. *Curr Colorectal Cancer Rep* 17, 77–87 (2021). <https://doi.org/10.1007/s11888-021-00470-x>.
68. Xu Q, Xu Y, Sun H, Jiang T, Xie S, Ooi BY, Ding Y. MRI Evaluation of Complete Response of Locally Advanced Rectal Cancer After Neoadjuvant Therapy: Current Status and Future Trends. *Cancer Manag Res.* 2021 Jun 1;13:4317-4328. doi: 10.2147/CMAR.S309252. PMID: 34103987; PMCID: PMC8179813.
69. Messina C, Bignone R, Bruno A, Bruno A, Bruno F, Calandri M, Caruso D, Coppolino P, Robertis R, Gentili F, Grazzini I, Natella R, Scalise P, Barile A, Grassi R, Albano D. Diffusion-Weighted Imaging in Oncology: An Update. *Cancers (Basel).* 2020 Jun 8;12(6):1493. doi: 10.3390/cancers12061493. PMID: 32521645; PMCID: PMC7352852.
70. Lee, S.; Lim, J.; Shin, J.; Kim, S.; Hwang, H. Pathologic Complete Response Prediction after Neoadjuvant Chemoradiation Therapy for Rectal Cancer Using Radiomics and Deep Embedding Network of MRI. *Appl. Sci.* 2021, 11, 9494. <https://doi.org/10.3390/app11209494>.
71. Lambregts, D.M.J., van Heeswijk, M.M., Delli Pizzi, A. et al. Diffusion-weighted MRI to assess response to chemoradiotherapy in rectal cancer: main interpretation pitfalls and their use for teaching. *Eur Radiol* 27, 4445–4454 (2017). <https://doi.org/10.1007/s00330-017-4830-z>.
72. Nerad E, Delli Pizzi A, Lambregts DMJ, Maas M, Wadhvani S, Bakers FCH, van den Bosch HCM, Beets-Tan RGH, Lahaye MJ. The Apparent Diffusion Coefficient (ADC) is a useful biomarker in predicting metastatic colon cancer using the ADC-value of the primary tumor. *PLoS One.* 2019 Feb 5;14(2):e0211830. doi: 10.1371/journal.pone.0211830. PMID: 30721268; PMCID: PMC6363286.
73. van Heeswijk MM, Lambregts DMJ, Maas M, Lahaye MJ, Ayas Z, Slenter JMGM, Beets GL, Bakers FCH, Beets-Tan RGH. Measuring the apparent diffusion coefficient in primary rectal tumors: is there a benefit in performing histogram analyses? *Abdom Radiol (NY).* 2017 Jun;42(6):1627-1636. doi: 10.1007/s00261-017-1062-2. PMID: 28160039; PMCID: PMC5486825.
74. Çelik H, Barlık F, Sökmen S, Terzi C, Canda AE, Sağol Ö, Sarıoğlu S, Ünlü M, Bilkay Görken İ, Arıcan Alıcıkuş Z, Öztop İ. Diagnostic performance of magnetic resonance imaging in preoperative local staging of rectal cancer after neoadjuvant chemoradiotherapy. *Diagn Interv Radiol.* 2023 Mar 29;29(2):219-227. doi: 10.4274/dir.2022.221333. Epub 2023 Jan 2. PMID: 36971272; PMCID: PMC10679710.
75. Azamat S, Karaman Ş, Azamat IF, Ertaş G, Kulle CB, Keskin M, Sakin RND, Bakır B, Oral EN, Kartal MG. Complete Response Evaluation of Locally Advanced Rectal Cancer to Neoadjuvant Chemoradiotherapy Using Textural Features Obtained from T2 Weighted Imaging and ADC Maps. *Curr Med Imaging.* 2022;18(10):1061-1069. doi: 10.2174/1573405618666220303111026. PMID: 35240976; PMCID: PMC9720879.
76. Baliyan V, Das CJ, Sharma R, Gupta AK. Diffusion weighted imaging: Technique and applications. *World J Radiol.* 2016 Sep 28;8(9):785-798. doi: 10.4329/wjr.v8.i9.785. PMID: 27721941; PMCID: PMC5039674.

77. Yacheva, A.; Dardanov, D.; Zlatareva, D. The Multipurpose Usage of Diffusion-Weighted MRI in Rectal Cancer. *Medicina* 2023, 59, 2162. <https://doi.org/10.3390/medicina59122162>.
78. Choi, S.J.; Kim, K.W.; Ko, Y.; Cho, Y.C.; Jang, J.S.; Ahn, H.; Kim, D.W.; Kim, M.Y. Whole Process of Standardization of Diffusion-Weighted Imaging: Phantom Validation and Clinical Application According to the QIBA Profile. *Diagnostics* 2024, 14, 583. <https://doi.org/10.3390/diagnostics14060583>.
79. Shen FU, Lu J, Chen L, Wang Z, Chen Y. Diagnostic value of dynamic contrast-enhanced magnetic resonance imaging in rectal cancer and its correlation with tumor differentiation. *Mol Clin Oncol*. 2016 Apr;4(4):500-506. doi: 10.3892/mco.2016.762. Epub 2016 Feb 3. PMID: 27073650; PMCID: PMC4812157.
80. Rebecca A.P. Dijkhoff, Regina G.H. Beets-Tan, Doenja M.J. Lambregts, Geerard L. Beets, Monique Maas. Value of DCE-MRI for staging and response evaluation in rectal cancer: A systematic review,
81. *European Journal of Radiology*, Volume 95, 2017, Pages 155-168, ISSN 0720-048X,
82. <https://doi.org/10.1016/j.ejrad.2017.08.009>.
83. Wang C, Padgett KR, Su MY, Mellon EA, Maziero D, Chang Z. Multi-parametric MRI (mpMRI) for treatment response assessment of radiation therapy. *Med Phys*. 2022 Apr;49(4):2794-2819. doi: 10.1002/mp.15130. Epub 2021 Aug 10. PMID: 34374098; PMCID: PMC9769892.
84. Ciolina, M., Caruso, D., De Santis, D. et al. Dynamic contrast-enhanced magnetic resonance imaging in locally advanced rectal cancer: role of perfusion parameters in the assessment of response to treatment. *Radiol med* 124, 331–338 (2019). <https://doi.org/10.1007/s11547-018-0978-0>.
85. Taberna M, Gil Moncayo F, Jané-Salas E, Antonio M, Arribas L, Vilajosana E, Peralvez Torres E, Mesía R. The Multidisciplinary Team (MDT) Approach and Quality of Care. *Front Oncol*. 2020 Mar 20;10:85. doi: 10.3389/fonc.2020.00085. PMID: 32266126; PMCID: PMC7100151.
86. Bednarski, B.K., Taggart, M. & Chang, G.J. MDT—How it is important in rectal cancer. *Abdom Radiol* 48, 2807–2813 (2023). <https://doi.org/10.1007/s00261-023-03977-z>.
87. Fokas, E., Appelt, A., Glynn-Jones, R. et al. International consensus recommendations on key outcome measures for organ preservation after (chemo)radiotherapy in patients with rectal cancer. *Nat Rev Clin Oncol* 18, 805–816 (2021). <https://doi.org/10.1038/s41571-021-00538-5>.
88. Hagen F Kennecke, Rebecca Auer, May Cho, N Arvind Dasari, Cynthia Davies-Venn, Cathy Eng, Jennifer Dorth, Julio Garcia-Aguilar, Manju George, Karyn A Goodman, Lillian Kreppel, Joshua E Meyer, Jose Monzon, Leonard Saltz, Deborah Schrag, J Joshua Smith, Jason A Zell, Prajnan Das, the National Cancer Institute Rectal-Anal Task Force , NCI Rectal-Anal Task Force consensus recommendations for design of clinical trials in rectal cancer, *JNCI: Journal of the National Cancer Institute*, Volume 115, Issue 12, December 2023, Pages 1457–1464, <https://doi.org/10.1093/jnci/djad143>.
89. Chang S, Goldstein NE, Dharmarajan KV. Managing an Older Adult with Cancer: Considerations for Radiation Oncologists. *Biomed Res Int*. 2017;2017:1695101. doi: 10.1155/2017/1695101. Epub 2017 Dec 13. PMID: 29387715; PMCID: PMC5745659.
90. Roeder F, Jensen AD, Lindel K, Mattke M, Wolf F, Gerum S. Geriatric Radiation Oncology: What We Know and What Can We Do Better? *Clin Interv Aging*. 2023 May 4;18:689-711. doi: 10.2147/CIA.S365495. PMID: 37168037; PMCID: PMC10166100.
91. Elnaggar M, Pratheepan P, Paramagurunathan B, et al. (March 27, 2023) The Accuracy of Different Modalities Used for Preoperative Primary Tumour Localisation in Operated Colorectal Cancer Patients. *Cureus* 15(3): e36737. doi:10.7759/cureus.36737.

92. Hope TA, Gollub MJ, Arya S, Bates DDB, Ganeshan D, Harisinghani M, Jhaveri KS, Kassam Z, Kim DH, Korngold E, Lalwani N, Moreno CC, Nougaret S, Paroder V, Paspulati RM, Golia Pernicka JS, Petkovska I, Pickhardt PJ, Rauch GM, Rosenthal MH, Sheedy SP, Horvat N. Rectal cancer lexicon: consensus statement from the society of abdominal radiology rectal & anal cancer disease-focused panel. *Abdom Radiol (NY)*. 2019 Nov;44(11):3508-3517. doi: 10.1007/s00261-019-02170-5. PMID: 31388697; PMCID: PMC6824987.
93. Lambregts, D.M.J., Bogveradze, N., Blomqvist, L.K. et al. Current controversies in TNM for the radiological staging of rectal cancer and how to deal with them: results of a global online survey and multidisciplinary expert consensus. *Eur Radiol* 32, 4991–5003 (2022). <https://doi.org/10.1007/s00330-022-08591-z>.
94. Brown P.J., on behalf of the YCR BCIP Study Group. Rossington H., Taylor J., Lambregts D.M.J., Morris E., West N.P., Quirke P., Tolan D. Standardised reports with a template format are superior to free text reports: The case for rectal cancer reporting in clinical practice. *Eur. Radiol*. 2019;29:5121–5128. doi: 10.1007/s00330-019-06028-8.
95. Sofic A, Husic-Selimovic A, Efendic A, Sehic A, Julardzija F, Cizmich M, Beslagic E, Aladjuz-Granov L. MRI Evaluation of Extramural Venous Invasion (EMVI) with Rectal Carcinoma Using High Resolution T2 and Combination of High Resolution T2 and Contrast Enhanced T1 Weighted Imaging. *Acta Inform Med*. 2021 Jun;29(2):113-117. doi: 10.5455/aim.2021.29.113-117. PMID: 34584334; PMCID: PMC8443141.
96. Inoue, A., Sheedy, S.P., Heiken, J.P. et al. MRI-detected extramural venous invasion of rectal cancer: Multimodality performance and implications at baseline imaging and after neoadjuvant therapy. *Insights Imaging* 12, 110 (2021). <https://doi.org/10.1186/s13244-021-01023-4>.
97. Ludwig KA. Sphincter-sparing resection for rectal cancer. *Clin Colon Rectal Surg*. 2007 Aug;20(3):203-12. doi: 10.1055/s-2007-984864. PMID: 20011201; PMCID: PMC2789515.
98. Yu G, Chi H, Zhao G, Wang Y. Tumor regression and safe distance of distal margin after neoadjuvant therapy for rectal cancer. *Front Oncol*. 2024 Apr 4;14:1375334. doi: 10.3389/fonc.2024.1375334. PMID: 38638858; PMCID: PMC11024319.
99. Sorrentino, L.; Sileo, A.; Daveri, E.; Battaglia, L.; Guaglio, M.; Centonze, G.; Sabella, G.; Patti, F.; Villa, S.; Milione, M.; et al. Impact of Microscopically Positive (≤ 1 mm) Distal Margins on Disease Recurrence in Rectal Cancer Treated by Neoadjuvant Chemoradiotherapy. *Cancers* 2023, 15, 1828. <https://doi.org/10.3390/cancers15061828>,
100. Xu L, Zhang C, Zhang Z, Qin Q, Sun X. Value of 3Tesla MRI in the preoperative staging of mid-low rectal cancer and its impact on clinical strategies. *Asia Pac J Clin Oncol*. 2020 Oct;16(5):e216-e222. doi: 10.1111/ajco.13368. Epub 2020 Aug 6. PMID: 32762144; PMCID: PMC7590102.
101. Daprà V, Airoidi M, Bartolini M, Fazio R, Mondello G, Tronconi MC, Prete MG, D'Agostino G, Foppa C, Spinelli A, Puccini A, Santoro A. Total Neoadjuvant Treatment for Locally Advanced Rectal Cancer Patients: Where Do We Stand? *Int J Mol Sci*. 2023 Jul 29;24(15):12159. doi: 10.3390/ijms241512159. PMID: 37569532; PMCID: PMC10418822.
102. Yuval JB, Thompson HM, Firat C, Verheij FS, Widmar M, Wei IH, Pappou E, Smith JJ, Weiser MR, Paty PB, Nash GM, Shia J, Gollub MJ, Garcia-Aguilar J. MRI at Restaging After Neoadjuvant Therapy for Rectal Cancer Overestimates Circumferential Resection Margin Proximity as Determined by Comparison With Whole-Mount Pathology. *Dis Colon Rectum*. 2022 Apr 1;65(4):489-496. doi: 10.1097/DCR.0000000000002145. PMID: 34803147; PMCID: PMC8916980.

103. Kaur H, Choi H, You YN, Rauch GM, Jensen CT, Hou P, Chang GJ, Skibber JM, Ernst RD. MR imaging for preoperative evaluation of primary rectal cancer: practical considerations. *Radiographics*. 2012 Mar-Apr;32(2):389-409. doi: 10.1148/rg.322115122. PMID: 22411939.
104. Pikūnienė I, Saladžinskas Ž, Basevičius A, Strakšytė V, Žilinskas J, Ambrazienė R. MRI Evaluation of Rectal Cancer Lymph Node Staging Using Apparent Diffusion Coefficient. *Cureus*. 2023 Sep 10;15(9):e45002. doi: 10.7759/cureus.45002. PMID: 37701166; PMCID: PMC10493462.
105. Kim BC, Kim YE, Chang HJ, Lee SH, Youk EG, Lee DS, Lee JB, Lee EJ, Kim MJ, Sohn DK, Oh JH. Lymph node size is not a reliable criterion for predicting nodal metastasis in rectal neuroendocrine tumours. *Colorectal Dis*. 2016 Jul;18(7):O243-51. doi: 10.1111/codi.13377. PMID: 27166857.
106. Zhuang Z, Zhang Y, Wei M, Yang X, Wang Z: Magnetic Resonance Imaging Evaluation of the Accuracy of Various Lymph Node Staging Criteria in Rectal Cancer: A Systematic Review and Meta-Analysis. *Front. Oncol*. 2021, 11:709070. 10.3389/fonc.2021.709070.
107. Chen JN, Liu Z, Wang ZJ, Mei SW, Shen HY, Li J, Pei W, Wang Z, Wang XS, Yu J, Liu Q. Selective lateral lymph node dissection after neoadjuvant chemoradiotherapy in rectal cancer. *World J Gastroenterol*. 2020 Jun 7;26(21):2877-2888. doi: 10.3748/wjg.v26.i21.2877. PMID: 32550762; PMCID: PMC7284184.
108. Sluckin TC, van Geffen EGM, Hazen SJA, Horsthuis K, Beets-Tan RGH, Marijnen CAM, Tanis PJ, Kusters M; Dutch Snapshot Research Group. Prognostic Implications of Lateral Lymph Nodes in Rectal Cancer: A Population-Based Cross-sectional Study With Standardized Radiological Evaluation After Dedicated Training. *Dis Colon Rectum*. 2024 Jan 1;67(1):42-53. doi: 10.1097/DCR.0000000000002752. Epub 2023 Jun 1. PMID: 37260270; PMCID: PMC10715698.
109. Tan J, Yang B, Xu Z, Zhou S, Chen Z, Huang J, Gao H, Zheng S, Wen L, Han F. Tumor deposit indicates worse prognosis than metastatic lymph node in gastric cancer: a propensity score matching study. *Ann Transl Med*. 2019 Nov;7(22):671. doi: 10.21037/atm.2019.10.33. PMID: 31930072; PMCID: PMC6944619.
110. Pu H, Pang X, Fu J, Zheng R, Chen Y, Zhang D, Fang X. Significance of tumor deposits combined with lymph node metastasis in stage III colorectal cancer patients: a retrospective multi-center cohort study from China. *Int J Colorectal Dis*. 2022 Jun;37(6):1411-1420. doi: 10.1007/s00384-022-04149-z. Epub 2022 May 20. PMID: 35595975; PMCID: PMC9167180.
111. Jin, Y., Yin, H., Zhang, H. et al. Predicting tumor deposits in rectal cancer: a combined deep learning model using T2-MR imaging and clinical features. *Insights Imaging* 14, 221 (2023). <https://doi.org/10.1186/s13244-023-01564-w>.
112. Wang S, Guan X, Ma M, Zhuang M, Ma T, Liu Z, Chen H, Jiang Z, Chen Y, Wang G, Wang X. Reconsidering the prognostic significance of tumour deposit count in the TNM staging system for colorectal cancer. *Sci Rep*. 2020 Jan 9;10(1):89. doi: 10.1038/s41598-019-57041-2. PMID: 31919408; PMCID: PMC6952424.
113. Ueno H, Nagtegaal ID, Quirke P, Sugihara K, Ajioka Y. Tumor deposits in colorectal cancer: Refining their definition in the TNM system. *Ann Gastroenterol Surg*. 2023 Jan 12;7(2):225-235. doi: 10.1002/ags3.12652. PMID: 36998291; PMCID: PMC10043773.
114. Delibegovic S. Introduction to Total Mesorectal Excision. *Med Arch*. 2017 Dec;71(6):434-438. doi: 10.5455/medarh.2017.71.434-438. PMID: 29416206; PMCID: PMC5788513.

115. Marieke L Rutgers, Thijs A Burghgraef, Jeroen C Hol, Rogier M Crolla, Nanette A van Geloven, Jeroen W Leijtens, Fatih Polat, Apollo Pronk, Anke B Smits, Jurriaan B Tuyman, Emiel G Verdaasdonk, Colin Sietses, Esther C Consten, Roel Hompes, Total mesorectal excision in MRI-defined low rectal cancer: multicentre study comparing oncological outcomes of robotic, laparoscopic and transanal total mesorectal excision in high-volume centres, *BJS Open*, Volume 8, Issue 3, June 2024, zrae029, <https://doi.org/10.1093/bjsopen/zrae029>.
116. Santiago I, Rodrigues B, Barata M, Figueiredo N, Fernandez L, Galzerano A, Parés O, Matos C. Re-staging and follow-up of rectal cancer patients with MR imaging when “Watch-and-Wait” is an option: a practical guide. *Insights Imaging*. 2021 Aug 9;12(1):114. doi: 10.1186/s13244-021-01055-w. PMID: 34373961; PMCID: PMC8353037.
117. Shihab OC, Quirke P, Heald RJ, Moran BJ, Brown G. Magnetic resonance imaging-detected lymph nodes close to the mesorectal fascia are rarely a cause of margin involvement after total mesorectal excision. *Br J Surg*. 2010 Sep;97(9):1431-6. doi: 10.1002/bjs.7116. PMID: 20603854.
118. Varela C, Kim NK. Surgical Treatment of Low-Lying Rectal Cancer: Updates. *Ann Coloproctol*. 2021 Dec;37(6):395-424. doi: 10.3393/ac.2021.00927.0132. Epub 2021 Dec 22. PMID: 34961303; PMCID: PMC8717072.
119. Chand M, Siddiqui MR, Swift I, Brown G. Systematic review of prognostic importance of extramural venous invasion in rectal cancer. *World J Gastroenterol*. 2016 Jan 28;22(4):1721-6. doi: 10.3748/wjg.v22.i4.1721. PMID: 26819536; PMCID: PMC4722002.
120. Smith NJ, Barbachano Y, Norman AR, Swift RI, Abulafi AM, Brown G. Prognostic significance of magnetic resonance imaging-detected extramural vascular invasion in rectal cancer. *Br J Surg*. 2008 Feb;95(2):229-36. doi: 10.1002/bjs.5917. PMID: 17932879.
121. Cuicchi D, Castagna G, Cardelli S, Larotonda C, Petrello B, Poggioli G. Restaging rectal cancer following neoadjuvant chemoradiotherapy. *World J Gastrointest Oncol*. 2023 May 15;15(5):700-712. doi: 10.4251/wjgo.v15.i5.700. PMID: 37275455; PMCID: PMC10237020.
122. Awiwi MO, Kaur H, Ernst R, Rauch GM, Morani AC, Stanietzky N, Palmquist SM, Salem UI. Restaging MRI of Rectal Adenocarcinoma after Neoadjuvant Chemoradiotherapy: Imaging Findings and Potential Pitfalls. *Radiographics*. 2023 Apr;43(4):e220135. doi: 10.1148/rg.220135. PMID: 36927125.
123. López-Campos F, Martín-Martín M, Fornell-Pérez R, García-Pérez JC, Die-Trill J, Fuentes-Mateos R, López-Durán S, Domínguez-Rullán J, Ferreiro R, Riquelme-Oliveira A, Hervás-Morón A, Couñago F. Watch and wait approach in rectal cancer: Current controversies and future directions. *World J Gastroenterol*. 2020 Aug 7;26(29):4218-4239. doi: 10.3748/wjg.v26.i29.4218. PMID: 32848330; PMCID: PMC7422545.
124. Cambray, M., González-Viguera, J., Losa, F. et al. Determining the optimal interval between neoadjuvant radiochemotherapy and surgery in rectal cancer: a retrospective cohort study. *Int J Colorectal Dis* 38, 154 (2023). <https://doi.org/10.1007/s00384-023-04457-y>.
125. Delli Pizzi A, Basilico R, Cianci R, Seccia B, Timpani M, Tavoletta A, Caposiena D, Faricelli B, Gabrielli D, Caulo M. Rectal cancer MRI: protocols, signs and future perspectives radiologists should consider in everyday clinical practice. *Insights Imaging*. 2018 Aug;9(4):405-412. doi: 10.1007/s13244-018-0606-5. Epub 2018 Apr 19. PMID: 29675627; PMCID: PMC6108973.

126. Yu Z, Xu C, Song B, Zhang S, Chen C, Li C, Zhang S. Tissue fibrosis induced by radiotherapy: current understanding of the molecular mechanisms, diagnosis and therapeutic advances. *J Transl Med.* 2023 Oct 9;21(1):708. doi: 10.1186/s12967-023-04554-0. PMID: 37814303; PMCID: PMC10563272.
127. Horvat N, El Homsy M, Miranda J, Mazaheri Y, Gollub MJ, Paroder V. Rectal MRI Interpretation After Neoadjuvant Therapy. *J Magn Reson Imaging.* 2023 Feb;57(2):353-369. doi: 10.1002/jmri.28426. Epub 2022 Sep 8. PMID: 36073323; PMCID: PMC9851947.
128. Horvat N, Hope TA, Pickhardt PJ, Petkovska I. Mucinous rectal cancer: concepts and imaging challenges. *Abdom Radiol (NY).* 2019 Nov;44(11):3569-3580. doi: 10.1007/s00261-019-02019-x. PMID: 30993392; PMCID: PMC7357860.
129. Heijnen LA, Maas M, Beets-Tan RG, Berkhof M, Lambregts DM, Nelemans PJ, Riedl R, Beets GL. Nodal staging in rectal cancer: why is restaging after chemoradiation more accurate than primary nodal staging? *Int J Colorectal Dis.* 2016 Jun;31(6):1157-62. doi: 10.1007/s00384-016-2576-8. Epub 2016 Apr 7. PMID: 27055660; PMCID: PMC4867151.
130. Stefanou, A.J.; Dessureault, S.; Sanchez, J.; Felder, S. Clinical Tools for Rectal Cancer Response Assessment following Neoadjuvant Treatment in the Era of Organ Preservation. *Cancers* 2023, 15, 5535. <https://doi.org/10.3390/cancers15235535>.
131. Roberto García-Figueiras, Sandra Baleato-González, Anwar R. Padhani, Antonio Luna-Alcalá, Ana Marhuenda, Joan C. Vilanova, Iria Osorio-Vázquez, Anxo Martínez-de-Alegría, and Antonio Gómez-Caamaño. Advanced Imaging Techniques in Evaluation of Colorectal Cancer. *RadioGraphics* 2018 38:3, 740-765. doi.org/10.1148/rg.2018170044.
132. Maheshwari, Ekta; Bajaj, Gitanjali; Jambhekar, Kedar; Pandey, Tarun; Ram, Roopa. Magnetic Resonance Imaging of Rectal Cancer. *Journal of Gastrointestinal and Abdominal Radiology* 2019; 02(01): 018 – 032. DOI: 10.1055/s-0039-1683772.
133. Han YB, Oh SN, Choi MH, Lee SH, Jang HS, Lee MA, Kim JG. Clinical impact of tumor volume reduction in rectal cancer following preoperative chemoradiation. *Diagn Interv Imaging.* 2016 Sep;97(9):843-50. doi: 10.1016/j.diii.2016.05.004. Epub 2016 Jun 14. PMID: 27316573.
134. Bilge Birlik, Funda Obuz, Funda D. Elibol, Ahmet O. Celik, Selman Sokmen, Cem Terzi, Ozgul Sagol, Sulen Sarioglu, Ilknur Gorken, Ilhan Oztop, Diffusion-weighted MRI and MR-volumetry - in the evaluation of tumor response after preoperative chemoradiotherapy in patients with locally advanced rectal cancer, *Magnetic Resonance Imaging, Volume 33, Issue 2, 2015, Pages 201-212, ISSN 0730-725X*, <https://doi.org/10.1016/j.mri.2014.08.041>.
135. Castorina P, Ferini G, Martorana E, Forte S. Tumor Volume Regression during and after Radiochemotherapy: A Macroscopic Description. *J Pers Med.* 2022 Mar 26;12(4):530. doi: 10.3390/jpm12040530. PMID: 35455646; PMCID: PMC9025192.
136. Pikūnienė I, Strakšytė V, Basevičius A, Žilinskas J, Ambrazienė R, Jančiauskienė R, Saladžinskas Ž. Prognostic Value of Tumor Volume, Tumor Volume Reduction Rate and Magnetic Resonance Tumor Regression Grade in Rectal Cancer. *Medicina (Kaunas).* 2023 Dec 18;59(12):2194. doi: 10.3390/medicina59122194. PMID: 38138297; PMCID: PMC10744935.
137. van der Stel SD, van den Berg JG, Snaebjornsson P, Seignette IM, Witteveen M, Grotenhuis BA, Beets GL, Post AL, Ruers TJM. Size and depth of residual tumor after neoadjuvant chemoradiotherapy in rectal cancer - implications for the development of new imaging modalities for response assessment. *Front Oncol.* 2023 Sep 5;13:1209732. doi: 10.3389/fonc.2023.1209732. PMID: 37736547; PMCID: PMC10509550.

138. Isaic A, Motofelea AC, Costachescu D, et al. What Is the Comparative Efficacy of Surgical, Endoscopic, Transanal Resection, and Radiotherapy Modalities in the Treatment of Rectal Cancer?. *Healthcare (Basel)*. 2023;11(16):2347. Published 2023 Aug 20. doi:10.3390/healthcare11162347
139. Jankovic A, Kovac JD, Dakovic M, et al. MRI Tumor Regression Grade Combined with T2-Weighted Volumetry May Predict Histopathological Response in Locally Advanced Rectal Cancer following Neoadjuvant Chemoradiotherapy-A New Scoring System Proposal. *Diagnostics (Basel)*. 2023;13(20):3226. Published 2023 Oct 17. doi:10.3390/diagnostics13203226
140. Weber MC, Berlet M, Stoess C, et al. A nationwide population-based study on the clinical and economic burden of anastomotic leakage in colorectal surgery. *Langenbecks Arch Surg*. 2023;408(1):55. Published 2023 Jan 23. doi:10.1007/s00423-023-02809-4
141. Kokaine L, Gardovskis A, Gardovskis J. Evaluation and Predictive Factors of Complete Response in Rectal Cancer after Neoadjuvant Chemoradiation Therapy. *Medicina (Kaunas)*. 2021 Sep 30;57(10):1044. doi: 10.3390/medicina57101044. PMID: 34684080; PMCID: PMC8537499.
142. Patel UB, Taylor F, Blomqvist L, George C, Evans H, Tekkis P, Quirke P, Sebag-Montefiore D, Moran B, Heald R, Guthrie A, Bees N, Swift I, Pennert K, Brown G. Magnetic resonance imaging-detected tumor response for locally advanced rectal cancer predicts survival outcomes: MERCURY experience. *J Clin Oncol*. 2011 Oct 1;29(28):3753-60. doi: 10.1200/JCO.2011.34.9068. Epub 2011 Aug 29. PMID: 21876084.
143. The AJCC Cancer Staging System, 8th Edition.
144. Weiser, M.R. AJCC 8th Edition: Colorectal Cancer. *Ann Surg Oncol* 25, 1454–1455 (2018). <https://doi.org/10.1245/s10434-018-6462-1>.
145. Glimelius B. Recent advances in rectal cancer treatment - are we on the right track? *Ups J Med Sci*. 2024 Feb 21;129. doi: 10.48101/ujms.v129.10537. PMID: 38449909; PMCID: PMC10916366.
146. Troester AM, Gaertner WB. Contemporary management of rectal cancer. *Surg Open Sci*. 2024 Jan 19;18:17-22. doi: 10.1016/j.sopen.2024.01.009. PMID: 38312301; PMCID: PMC10832461.
147. Son GM. Organ preservation for early rectal cancer using preoperative chemoradiotherapy. *Ann Coloproctol*. 2023 Jun;39(3):191-192. doi: 10.3393/ac.2023.00409.0058. Epub 2023 Jun 29. PMID: 37415474; PMCID: PMC10338160.
148. Gani C, Gani N, Zschaeck S, Eberle F, Schaeffeler N, Hehr T, Berger B, Fischer SG, Claßen J, Zipfel S, Rödel C, Teufel M, Zips D. Organ Preservation in Rectal Cancer: The Patients' Perspective. *Front Oncol*. 2019 May 10;9:318. doi: 10.3389/onc.2019.00318. PMID: 31134146; PMCID: PMC6524150.
149. Guida AM, Sensi B, Formica V, D'Angelillo RM, Roselli M, Del Vecchio Blanco G, Rossi P, Capolupo GT, Caricato M, Sica GS. Total neoadjuvant therapy for the treatment of locally advanced rectal cancer: a systematic minireview. *Biol Direct*. 2022 Jun 13;17(1):16. doi: 10.1186/s13062-022-00329-7. PMID: 35698084; PMCID: PMC9195214.
150. Beppu N, Ikeda M, Kataoka K, Kimura K, Ikeuchi H, Uchino M, Nakamoto Y, Okamoto R, Yanagi H. Total Neoadjuvant Chemotherapy in Rectal Cancer: Current Facts and Future Strategies. *J Anus Rectum Colon*. 2023 Jan 25;7(1):1-7. doi: 10.23922/jarc.2022-060. Erratum in: *J Anus Rectum Colon*. 2023 Apr 25;7(2):139. doi: 10.23922/jarc.E003. PMID: 36743465; PMCID: PMC9876605.

151. Sclafani F, Brown G, Cunningham D, Wotherspoon A, Tait D, Peckitt C, Evans J, Yu S, Sena Teixeira Mendes L, Tabernero J, Glimelius B, Cervantes A, Thomas J, Begum R, Oates J, Chau I. PAN-EX: a pooled analysis of two trials of neoadjuvant chemotherapy followed by chemoradiotherapy in MRI-defined, locally advanced rectal cancer. *Ann Oncol.* 2016 Aug;27(8):1557-65. doi: 10.1093/annonc/mdw215. Epub 2016 May 23. PMID: 27217542.
152. Boublikova L, Novakova A, Simsa J, Lohynska R. Total neoadjuvant therapy in rectal cancer: the evidence and expectations. *Crit Rev Oncol Hematol.* 2023 Dec;192:104196. doi: 10.1016/j.critrevonc.2023.104196. Epub 2023 Nov 4. PMID: 37926376.
153. Viktil E, Hanekamp BA, Nesbakken A, Løberg EM, Sjo OH, Negård A, Dormagen JB, Schulz A. Early rectal cancer: The diagnostic performance of MRI supplemented with a rectal micro-enema and a modified staging system to identify tumors eligible for local excision. *Acta Radiol Open.* 2024 Apr 18;13(5):20584601241241523. doi: 10.1177/20584601241241523. PMID: 38645439; PMCID: PMC11027598.
154. Alberda WJ, Dassen HP, Dwarkasing RS, Willemsen FE, van der Pool AE, de Wilt JH, Burger JW, Verhoef C. Prediction of tumor stage and lymph node involvement with dynamic contrast-enhanced MRI after chemoradiotherapy for locally advanced rectal cancer. *Int J Colorectal Dis.* 2013 Apr;28(4):573-80. doi: 10.1007/s00384-012-1576-6. Epub 2012 Sep 22. PMID: 23001160.
155. Kok END, Eppenga R, Kuhlmann KFD, Groen HC, van Veen R, van Dieren JM, de Wijkerslooth TR, van Leerdam M, Lambregts DMJ, Heerink WJ, Hoetjes NJ, Ivashchenko O, Beets GL, Aalbers AGJ, Nijkamp J, Ruers TJM. Accurate surgical navigation with real-time tumor tracking in cancer surgery. *NPJ Precis Oncol.* 2020 Apr 8;4:8. doi: 10.1038/s41698-020-0115-0. PMID: 32285009; PMCID: PMC7142120.
156. Golia Pernicka JS, Bates DDB, Fuqua JL 3rd, Knezevic A, Yoon J, Nardo L, Petkovska I, Paroder V, Nash GM, Markowitz AJ, Gollub MJ. Meaningful words in rectal MRI synoptic reports: How “polypoid” may be prognostic. *Clin Imaging.* 2021 Dec;80:371-376. doi: 10.1016/j.clinimag.2021.08.010. Epub 2021 Aug 26. PMID: 34517303; PMCID: PMC8585689.
157. Yu L, Xu TL, Zhang L, Shen SH, Zhu YL, Fang H, Zhang HZ. Impact of neoadjuvant chemoradiotherapy on the local recurrence and distant metastasis pattern of locally advanced rectal cancer: a propensity score-matched analysis. *Chin Med J (Engl).* 2021 Sep 15;134(18):2196-2204. doi: 10.1097/CM9.0000000000001641. PMID: 34553701; PMCID: PMC8478402.
158. Taylor FG, Quirke P, Heald RJ, Moran BJ, Blomqvist L, Swift IR, Sebag-Montefiore D, Tekkis P, Brown G; Magnetic Resonance Imaging in Rectal Cancer European Equivalence Study Study Group. Preoperative magnetic resonance imaging assessment of circumferential resection margin predicts disease-free survival and local recurrence: 5-year follow-up results of the MERCURY study. *J Clin Oncol.* 2014 Jan 1;32(1):34-43. doi: 10.1200/JCO.2012.45.3258. Epub 2013 Nov 25. PMID: 24276776.
159. Yiqun S, Tong T, Fangqi L, Sanjun C, Chao X, Yajia G, Ye X. Recognition of Anterior Peritoneal Reflections and Their Relationship With Rectal Tumors Using Rectal Magnetic Resonance Imaging. *Medicine (Baltimore).* 2016 Mar;95(9):e2889. doi: 10.1097/MD.0000000000002889. PMID: 26945377; PMCID: PMC4782861.
160. Klaver CEL, van Huijgevoort NCM, de Buck van Overstraeten A, Wolthuis AM, Tanis PJ, van der Bilt JDW, Sagaert X, D’Hoore A. Locally Advanced Colorectal Cancer: True Peritoneal Tumor Penetration is Associated with Peritoneal Metastases. *Ann Surg Oncol.* 2018 Jan;25(1):212-220. doi: 10.1245/s10434-017-6037-6. Epub 2017 Oct 26. PMID: 29076043; PMCID: PMC5740196.

161. Tong T, Sun Y, Cai S, Zhang Z, Gu Y. Extramural depth of rectal cancer tumor invasion at thin-section MRI: predicting treatment response to neoadjuvant chemoradiation. *Oncotarget*. 2015 Oct 6;6(30):30277-86. doi: 10.18632/oncotarget.4623. PMID: 26309163; PMCID: PMC4745797.
162. Kim TH, Firat C, Thompson HM, Gangai N, Zheng J, Capanu M, Bates DDB, Paroder V, García-Aguilar J, Shia J, Gollub MJ, Horvat N. Extramural Venous Invasion and Tumor Deposit at Diffusion-weighted MRI in Patients after Neoadjuvant Treatment for Rectal Cancer. *Radiology*. 2023 Aug;308(2):e230079. doi: 10.1148/radiol.230079. PMID: 37581503; PMCID: PMC10478788.
163. Gursoy Coruh A, Peker E, Elhan A, Erden I, Erden A. Evaluation of Extramural Venous Invasion by Diffusion-Weighted Magnetic Resonance Imaging and Computed Tomography in Rectal Adenocarcinoma. *Can Assoc Radiol J*. 2019 Nov;70(4):457-465. doi: 10.1016/j.carj.2019.06.006. Epub 2019 Sep 30. PMID: 31582328.
164. Ale Ali H, Kirsch R, Razaz S, Jhaveri A, Thippavong S, Kennedy ED, Jhaveri KS. Extramural venous invasion in rectal cancer: overview of imaging, histopathology, and clinical implications. *Abdom Radiol (NY)*. 2019 Jan;44(1):1-10. doi: 10.1007/s00261-018-1673-2. PMID: 29967984.
165. Seierstad T, Hole KH, Grøholt KK, Dueland S, Ree AH, Flatmark K, Redalen KR. MRI volumetry for prediction of tumour response to neoadjuvant chemotherapy followed by chemoradiotherapy in locally advanced rectal cancer. *Br J Radiol*. 2015 Jul;88(1051):20150097. doi: 10.1259/bjr.20150097. Epub 2015 Apr 22. PMID: 25899892; PMCID: PMC4628535.
166. Song C, Chung JH, Kang SB, Kim DW, Oh HK, Lee HS, Kim JW, Lee KW, Kim JH, Kim JS. Impact of Tumor Regression Grade as a Major Prognostic Factor in Locally Advanced Rectal Cancer after Neoadjuvant Chemoradiotherapy: A Proposal for a Modified Staging System. *Cancers (Basel)*. 2018 Sep 7;10(9):319. doi: 10.3390/cancers10090319. PMID: 30205529; PMCID: PMC6162780.
167. Siddiqui MR, Bhoday J, Battersby NJ, Chand M, West NP, Abulafi AM, Tekkis PP, Brown G. Defining response to radiotherapy in rectal cancer using magnetic resonance imaging and histopathological scales. *World J Gastroenterol*. 2016 Oct 7;22(37):8414-8434. doi: 10.3748/wjg.v22.i37.8414. PMID: 27729748; PMCID: PMC5055872.
168. Stoffel EM, Murphy CC. Epidemiology and Mechanisms of the Increasing Incidence of Colon and Rectal Cancers in Young Adults. *Gastroenterology*. 2020 Jan;158(2):341-353. doi: 10.1053/j.gastro.2019.07.055. Epub 2019 Aug 5. PMID: 31394082; PMCID: PMC6957715.
169. Zhang Z, Chen Y, Wen Z, Wu X, Que Y, Ma Y, Wu Y, Liu Q, Fan W, Yu S. MRI for nodal restaging after neoadjuvant therapy in rectal cancer with histopathologic comparison. *Cancer Imaging*. 2023 Jul 13;23(1):67. doi: 10.1186/s40644-023-00589-0. PMID: 37443085; PMCID: PMC10339540.
170. Chan DKH, Tan KK. Lower lymph node yield following neoadjuvant therapy for rectal cancer has no clinical significance. *J Gastrointest Oncol*. 2019 Feb;10(1):42-47. doi: 10.21037/jgo.2018.10.02. PMID: 30788158; PMCID: PMC6351311.
171. Elsholtz FHJ, Asbach P, Haas M, Becker M, Beets-Tan RGH, Thoeny HC, Padhani AR, Hamm B. Introducing the Node Reporting and Data System 1.0 (Node-RADS): a concept for standardized assessment of lymph nodes in cancer. *Eur Radiol*. 2021 Aug;31(8):6116-6124. doi: 10.1007/s00330-020-07572-4. Epub 2021 Feb 14. Erratum in: *Eur Radiol*. 2021 Sep;31(9):7217. doi: 10.1007/s00330-021-07795-z. PMID: 33585994; PMCID: PMC8270876.

172. Cho P, Park CS, Park GE, Kim SH, Kim HS, Oh SJ. Diagnostic Usefulness of Diffusion-Weighted MRI for Axillary Lymph Node Evaluation in Patients with Breast Cancer. *Diagnostics (Basel)*. 2023 Jan 31;13(3):513. doi: 10.3390/diagnostics13030513. PMID: 36766617; PMCID: PMC9914452.
173. Belfiore, M.P.; Gallo, L.; Reginelli, A.; Parrella, P.M.; Russo, G.M.; Caliendo, V.; Fasano, M.; Ciani, G.; Zeccolini, R.; Liguori, C.; et al. Quantitative Evaluation of the Lymph Node Metastases in the Head and Neck Malignancies Using Diffusion-Weighted Imaging and Apparent Diffusion Coefficient Mapping: A Bicentric Study. *Magnetochemistry* 2023, 9, 124. <https://doi.org/10.3390/magnetochemistry9050124>
174. Donners, R., Yiin, R.S.Z., Blackledge, M. et al. Whole-body diffusion-weighted MRI of normal lymph nodes: prospective apparent diffusion coefficient histogram and nodal distribution analysis in a healthy cohort. *Cancer Imaging* 21, 64 (2021). <https://doi.org/10.1186/s40644-021-00432-4>.
175. Hui C. L. et al. Role of imaging and synoptic MRI reporting in determining optimal management paradigm for rectal cancer: a narrative review // *Digestive Medicine Research*. 2020. Vol. 3. p. 47. DOI:10.21037/dmr-20-147.
176. Osman, M.F., Ibrahim, S.H., Ghoneim, S.M.M. et al. Role of apparent diffusion coefficient in assessment of loco-regional nodal spread in cancer rectum: correlative study with histopathological findings. *Egypt J Radiol Nucl Med* 54, 48 (2023). <https://doi.org/10.1186/s43055-023-00995-1>.
177. Simunovic M, Grubac V, Zbuk K, Wong R, Coates A. Role of the status of the mesorectal fascia in the selection of patients with rectal cancer for preoperative radiation therapy: a retrospective cohort study. *Can J Surg*. 2018 Oct 1;61(5):332-338. doi: 10.1503/cjs.009417. PMID: 30247008; PMCID: PMC6153109.
178. Liu Q, Luo D, Cai S, Li Q, Li X. Circumferential resection margin as a prognostic factor after rectal cancer surgery: A large population-based retrospective study. *Cancer Med*. 2018 Aug;7(8):3673-3681. doi: 10.1002/cam4.1662. Epub 2018 Jul 10. PMID: 29992773; PMCID: PMC6089167.
179. Luo D, Li J, He W, Yang Y, Cai S, Li Q, Li X. Incidence, predictors and prognostic implications of positive circumferential resection margin in colon cancer: A retrospective study in a Chinese high-volume cancer center. *Front Oncol*. 2022 Sep 20;12:871570. doi: 10.3389/fonc.2022.871570. PMID: 36203420; PMCID: PMC9530821.
180. Dieguez A. Rectal cancer staging: focus on the prognostic significance of the findings described by high-resolution magnetic resonance imaging. *Cancer Imaging*. 2013 Jul 22;13(2):277-97. doi: 10.1102/1470-7330.2013.0028. PMID: 23876415; PMCID: PMC3719056.
181. Salmerón-Ruiz A, Luengo Gómez D, Medina Benítez A, Láinez Ramos-Bossini AJ. Primary staging of rectal cancer on MRI: an updated pictorial review with focus on common pitfalls and current controversies. *Eur J Radiol*. 2024 Jun;175:111417. doi: 10.1016/j.ejrad.2024.111417. Epub 2024 Mar 11. PMID: 38484688.
182. Chen Y, Yang X, Wen Z, Liu Y, Lu B, Yu S, Xiao X. Association between high-resolution MRI-detected extramural vascular invasion and tumour microcirculation estimated by dynamic contrast-enhanced MRI in rectal cancer: preliminary results. *BMC Cancer*. 2019 May 27;19(1):498. doi: 10.1186/s12885-019-5732-z. PMID: 31133005; PMCID: PMC6537147.

183. Geffen EGMV, Nederend J, Sluckin TC, Hazen SJA, Horsthuis K, Beets-Tan RGH, Marijnen CAM, Tanis PJ, Kusters M; Dutch Snapshot Research Group. Prognostic significance of MRI-detected extramural venous invasion according to grade and response to neo-adjuvant treatment in locally advanced rectal cancer A national cohort study after radiologic training and reassessment. *Eur J Surg Oncol*. 2024 Jun;50(6):108307. doi: 10.1016/j.ejso.2024.108307. Epub 2024 Mar 29. PMID: 38581757.
184. Chen L, Liu X, Zhang W, Qin S, Wang Y, Lin J, Chen Q, Liu G. The predictive value of tumor volume reduction ratio on three-dimensional endorectal ultrasound for tumor response to chemoradiotherapy for locally advanced rectal cancer. *Ann Transl Med*. 2022 Jun;10(12):666. doi: 10.21037/atm-22-2418. PMID: 35845508; PMCID: PMC9279805.
185. Niu S, Chen Y, Peng F, Wen J, Xiong J, Yang Z, Peng J, Bao Y, Ding L. The role of MRI after neoadjuvant chemotherapy in predicting pathological tumor regression grade and clinical outcome in patients with locally advanced rectal adenocarcinoma. *Front Oncol*. 2023 Jun 12;13:1118518. doi: 10.3389/fonc.2023.1118518. PMID: 37377906; PMCID: PMC10292078.
186. Chen HLR, Seow-En I, Chok AY, Ngo NT, Cheng TL, Tan KE. The role of magnetic resonance tumour regression grade in the prediction of regression and survival of rectal adenocarcinoma after long-course chemoradiotherapy: a cohort study. *Ann Med Surg (Lond)*. 2023 Apr 3;85(4):842-848. doi: 10.1097/MS9.0000000000000441. PMID: 37113901; PMCID: PMC10129100.
187. Shi L, Zhang Y, Hu J, Zhou W, Hu X, Cui T, Yue NJ, Sun X, Nie K. Radiomics for the Prediction of Pathological Complete Response to Neoadjuvant Chemoradiation in Locally Advanced Rectal Cancer: A Prospective Observational Trial. *Bioengineering (Basel)*. 2023 May 24;10(6):634. doi: 10.3390/bioengineering10060634. PMID: 37370565; PMCID: PMC10295574.
188. Suzuki C, Halperin SK, Nilsson PJ, Martling A, Holm T. Initial magnetic resonance imaging tumour regression grade (mrTRG) as response evaluation after neoadjuvant treatment predicts sustained complete response in patients with rectal cancer. *Eur J Surg Oncol*. 2022 Jul;48(7):1643-1649. doi: 10.1016/j.ejso.2022.02.012. Epub 2022 Feb 17. PMID: 35272899.
189. Yang Y, Luo D, Zhang R, Cai S, Li Q, Li X. Tumor Regression Grade as a Prognostic Factor in Metastatic Colon Cancer Following Preoperative Chemotherapy. *Clin Colorectal Cancer*. 2022 Jun;21(2):96-106. doi: 10.1016/j.clcc.2021.10.006. PMID: 34895989.

LIST OF SCIENTIFIC PUBLICATIONS

Publications related to the results of the dissertation:

1. **Pikūnienė I**, Strakšytė V, Basevičius A, Žilinskas J, Ambrazienė R, Jančiauskienė R, Saladžinskas Ž. Prognostic Value of Tumor Volume, Tumor Volume Reduction Rate and Magnetic Resonance Tumor Regression Grade in Rectal Cancer. *Medicina (Kaunas)*. 2023 Dec 18;59(12):2194. doi: 10.3390/medicina59122194.
2. **Pikūnienė I**, Saladžinskas Ž, Basevičius A, Strakšytė V, Žilinskas J, Ambrazienė R. MRI Evaluation of Rectal Cancer Lymph Node Staging Using Apparent Diffusion Coefficient. *Cureus*. 2023 Sep 10;15(9):e45002. doi: 10.7759/cureus.45002. eCollection 2023 Sep.

Other publications:

1. Saha A, Bosma JS, Twilt JJ, van Ginneken B, Bjartell A, Padhani AR, Bonekamp D, Villeirs G, Salomon G, Giannarini G, Kalpathy-Cramer J, Barentsz J, Maier-Hein KH, Rusu M, Rouvière O, van den Bergh R, Panebianco V, Kasivisvanathan V, Obuchowski NA, Yakar D, Elschot M, Veltman J, Fütterer JJ, de Rooij M, Huisman H; PI-CAI consortium (**Pikūnienė I**, et al). „Artificial intelligence and radiologists in prostate cancer detection on MRI (PI-CAI): an international, paired, non-inferiority, confirmatory study,.. *Lancet Oncol*. 2024 Jul;25(7):879-887. doi: 10.1016/S1470-2045(24)00220-1. Epub 2024 Jun 11. PMID: 38876123
2. Greijdanus NG, Wienholts K, Ubels S, Talboom K, Hannink G, Wolthuis A, de Lacy FB, Lefevre JH, Solomon M, Frasson M, Rotholtz N, Denost Q, Perez RO, Konishi T, Panis Y, Rutegård M, Hompes R, Rosman C, van Workum F, Tanis PJ, de Wilt JHW; TENTACLE-Rectum Collaborative Group (**Pikūnienė I**, et al). Stoma-free survival after rectal cancer resection with anastomotic leakage: development and validation of a prediction model in a large international cohort. *Ann Surg*. 2023 Nov 1;278(5):772-780. doi: 10.1097/SLA.0000000000006043. Epub 2023 Jul 27.
3. Greijdanus NG, Wienholts K, Ubels S, Talboom K, Hannink G, Žilinskas J, **Pikūnienė I**, Wolthuis A, et al. Stoma-free survival after anastomotic leak following rectal cancer resection: worldwide cohort of 2470 patients. *Br J Surg*. 2023;110(12). doi: 10.1093/bjs/znad311. PMID: 37819790; PMCID: PMC10638542.
4. Sondaitė, M; Atstupėnaitė, V; **Pikūnienė, I**. „Primary fallopian tube carcinoma: a case report of rare disease“. *European Journal of Trans-*

lational and Clinical Medicine : 28TH International Student Scientific Conference (ISSC) in Gdańsk, 1315 April 2023.

5. Nekrosius D, Zilinskas J, Petkevicius V, **Pikuniene I**, Tamelis A. Perirectal Abscess and Fistula Secondary to a Fecalith in Rectal Pouch Occurring 51 Years After Duhamel Operation for Hirschsprung's Disease: Minimally Invasive Treatment. *J Surg.* 2022;7:1585.
6. **Pikūnienė, Ingrida**; Viršilas, Matas; Gleiznienė, Rymantė. Kraujagyslinė demencija = : Vascular dementia // *Medicinos teorija ir praktika = Theory and Practice in medicine.* , 2015, t.21, Nr. 4.1, p. 487-495, ISSN 1392-1312. Prieiga per internetą: <<https://hdl.handle.net/20.500.12512/16648>>. Index Copernicus. [S4] [M.kr.: M001]

LIST OF PRESENTATIONS IN SCIENTIFIC CONFERENCES

The results of the dissertation were presented in the scientific conferences:

1. Ambrazienė, Rita; Pužauskienė, Lina; Kairevičė, Laura; Tamelis, Algimantas; Latkauskas, Tadas; Paužas, Henrikas; Lizdenis, Paulius; Švagždys, Saulius; **Pikūnienė, Ingrida**; Gineikienė, Irina; Butnoriūtė, Eglė; Jacevičiūtė, Emilija; Jaruševičius, Laimonas; Jančiauskas, Dainius; Navickis, Tomas; Jančiauskienė, Rasa. Changing Clinical Characteristics and Management of Local Rectal Cancer During Recent Decades // 9th Kaunas / Lithuania International Hematology / Oncology Colloquium : 24 May 2024 : Online Poster Abstract Book/ Editor Elona Juozaitytė, p. 3 - 4, ISBN 978-609-8343-00-7. Prieiga per internetą: <<https://hdl.handle.net/20.500.12512/244784>>. [T1e] [M.kr.: M001]
2. Ambrazienė, Rita; Chlebopaševienė, Greta; Malonytė, Rasa; Muduraitė, Rasa; Jaruševičius, Laimonas; **Pikūnienė, Ingrida**; Tamelis, Algimantas; Latkauskas, Tadas; Jančiauskienė, Rasa. Neoadjuvant intensified chemotherapy vs Standard Therapy in Locally Advanced Rectal Cancer // Baltic Congress of Oncologists and Surgeons 2023 : Program and Abstract Book : 07-08.09.2023, Tallinn, Estonia / Estonian Society of Oncologist. Estonian Association of Surgeons, p. 48 - 49, ISBN 978-9916-4-1920-5. Prieiga per internetą:<<https://foto.piletid.eu/konverents/events/2023-bcos/Baltic-Congress-of-Oncologists-and-Surgeons-2023-ebook.pdf>> <<https://hdl.handle.net/20.500.12512/239657>>. [T2] [M.kr.:M001]
3. Ambrazienė, Rita; Chlebopaševienė, Greta; Malonytė, Rasa; Muduraitė, Rasa; Kupčinskaitė-Noreikienė, Rita; Trumpaitienė, Danguolė; Jaruševičius, Laimonas; **Pikūnienė, Ingrida**; Tamelis, Algimantas; Latkauskas, Tadas; Jančiauskienė, Rasa. Neoadjuvant intensified chemotherapy vs Standard Therapy in Locally Advanced Rectal Cancer // 7th Kaunas / Lithuania International Hematology / Oncology Colloquium : 26 May 2022, Kaunas, Lithuania : Online Poster Abstract Book / Editor Elona Juozaitytė ; Abstracts' Reviewers Rolandas Gerbutavičius, Arturas Inčiūra, Dietger Niederwieser, Domas Vaitiekus ; Kaunas Region Society of Oncologists, Hematologists and Transfusiologists. Kaunas : Eventas, 2022. ISBN 9786099616759, p. 3-4, ISBN 9786099616759. Prieiga per internetą: <<https://hdl.handle.net/20.500.12512/115386>>. [T1e] [M.kr.: M001]

4. **Pikūnienē, Ingrida.** Role of MRI in locally advanced rectal cancer // 8th Baltic Congress of Radiology - BCR : 6-8 October, 2022, Tallinn, Estonia : abstract book / Estonian Society of Radiology [et al.]. Tallinn : PCO Conference Expert, 2022, p. 1-1. Prieiga per internetu: <<https://hdl.handle.net/20.500.12512/115791>>. [T2] [M.kr.: M001]

APPENDICES

Appendix 1

UICC TNM staging (8th edition) classification for colon and rectal cancer.

C TNM staging (8th edition) classification for colon and rectal cancer.

TNM Clinical Classification	
T - Primary tumour	
TX	Primary tumour cannot be assessed
T0	No evidence of primary tumour
Tis	Carcinoma in situ: invasion of lamina propria
T1	Tumour invades submucosa
T2	Tumour invades muscularis propria
T3	Tumour invades subserosa or into non-peritonealised pericolic or perirectal tissues
T4	Tumour directly invades other organs or structures ^{b,c,d} and/or perforates visceral peritoneum
T4a	Tumour perforates visceral peritoneum
T4b	Tumour directly invades other organs or structures
N - Regional lymph nodes	
NX	Regional lymph nodes cannot be assessed
N0	No regional lymph node metastasis
N1	Metastasis in 1–3 regional lymph nodes
N1a	Metastasis in 1 regional lymph node
N1b	Metastasis in 2–3 regional lymph nodes
N1c	Tumour deposit(s), i.e. satellites, ^c in the subserosa, or in non-peritonealised pericolic or perirectal soft tissue without regional lymph node metastasis
N2	Metastasis in 4 or more regional lymph nodes
N2a	Metastasis in 4–6 regional lymph nodes
N2b	Metastasis in 7 or more regional lymph nodes
M – Distant metastasis	
M0	No distant metastasis
M1	Distant metastasis
M1a	Metastasis confined to one organ (liver, lung, ovary, non-regional lymph node(s)) without peritoneal metastases
M1b	Metastasis in more than one organ
M1c	Metastasis to the peritoneum with or without other organ involvement
<p>^a Tis includes cancer cells confined within the mucosal lamina propria (intramucosal) with no extension through the muscularis mucosae into the submucosa.</p> <p>^b Invades through to visceral peritoneum to involve the surface.</p> <p>^c Direct invasion in T4b includes invasion of other organs or segments of the colorectum by way of the serosa, as confirmed on microscopic examination, or for tumours in a retroperitoneal or subperitoneal location, direct invasion of other organs or structures by virtue of extension beyond the muscularis propria.</p> <p>^d Tumour that is adherent to other organs or structures, macroscopically, is classified cT4b. However, if no tumour is present in the adhesion, microscopically, the classification should be pT1–3, depending on the anatomical depth of wall invasion.</p> <p>^e Tumor deposits (satellites) are discrete macroscopic or microscopic nodules of cancer in the pericorectal adipose tissue's lymph drainage area of a primary carcinoma that are discontinuous from the primary and without histological evidence of residual lymph node or identifiable vascular or neural structures. If a vessel wall is identifiable on H&E, elastic or other stains, it should be classified as venous invasion (V1/2) or lymphatic invasion (L1).</p> <p>Similarly, if neural structures are identifiable, the lesion should be classified as perineural invasion (Pn1). The presence of tumour deposits does not change the primary tumour T category, but changes the node status (N) to pN1c if all regional lymph nodes are negative on pathological examination.</p>	

Subclassification of T3 rectal cancer.

Classification of T3 rectal cancer.

	Depth of invasion beyond the muscularis propria (in mm)
T3a ^a	<1
T3b	1-5
T3c	5-15
T3d	>15

^aThis sub-classification based upon an evaluation using MRI before treatment decision is clinically valuable and is used in these recommendations. It can be used also in the histopathological classification.

Stage grouping of colon and rectal cancer

TNM Pathological Classification			
The pT and pN categories correspond to the T and N categories.			
pN0 Histological examination of a regional lymphadenectomy specimen will ordinarily include 12 or more lymph nodes. If the lymph nodes are negative, but the number ordinarily examined is not met, classify as pN0.			
Stage			
Stage 0	Tis	N0	M0
Stage I	T1, T2	N0	M0
Stage II	T3, T4	N0	M0
Stage IIA	T3	N0	M0
Stage IIB	T4a	N0	M0
Stage IIC	T4b	N0	M0
Stage III	Any T	N1, N2	M0
Stage IIIA	T1, T2	N1	M0
	T1	N2a	M0
Stage IIIB	T1, T2	N2b	M0
	T2, T3	N2a	M0
	T3, T4a	N1	M0
Stage IIIC	T3, T4a	N2b	M0
	T4a	N2a	M0
	T4b	N1, N2	M0
Stage IV	Any T	Any N	M1
Stage IVA	Any T	Any N	M1a
Stage IVB	Any T	Any N	M1b
Stage IVC	Any T	Any N	M1c
TNM, tumor, node, metastasis.			

Structured MRI report template. Primary staging [6]

Structured MRI report template primary staging

Local tumour status

- Morphology: Solid - polypoid
 Solid - (semi-)annular: from to o'clock
 Mucinous: from to o'clock
- Distance from the anorectal junction to the lower pole of the tumour: cm
 - Tumour length: cm
- T-stage: T1-2
 T3 → T3a or T3b (≤5 mm extramural growth)
 T3c or T3d (>5 mm extramural growth)
 T4, based on growth into:
- Sphincter invasion: No
 Internal sphincter only
 " + intersphincteric plane
 " + external sphincter
- } upper middle distal 1/3 of anal canal

Mesorectal fascia (and peritoneal) involvement

- Shortest distance between tumour and MRF: mm → free (> 2 mm)
 threatened/involved (≤2 mm)
- Location of the shortest distance between tumour and MRF: o'clock
 - Relation to anterior peritoneal reflection: below (MRF invasion) above

Lymph nodes and tumour deposits

- N-stage: N0 N+
- Total number of lymph nodes:
- Number of suspicious lymph nodes: (..... mesorectal nodes; extramesorectal nodes)
 nodes with short axis diameter ≥ 9 mm
 nodes with short axis diameter 5-8 mm AND at least 2 morphologic criteria*
 nodes with short axis diameter < 5 mm AND all 3 morphologic criteria*
- *N.B. Morphologic suspicious criteria: [1] round shape, [2] irregular border, [3] heterogenous signal
- Are there any tumour deposits within the mesorectum: no,
 yes, (number of deposits)

Extramural vascular invasion

- Yes No

Structured MRI report template. Restaging after neoadjuvant treatment
[6]

Structured MRI report template
restaging after neoadjuvant treatment

Local tumour status

- Residual tumour mass: No, completely normalised rectal wall (complete response)
- No, fibrotic wall thickening without clear residual mass (complete or near complete response)
- Yes, residual mass (and/or focal high signal on DWI):
 - yT-stage: yT1-2
 - yT3 → yT3a or yT3b (≤5 mm extramural growth)
 - yT3c or yT3d (>5 mm extramural growth)
 - yT4, based on growth into:

- Distance from the anorectal junction to the lower pole of the tumour: cm
- Tumour length: cm

- Sphincter invasion: No
 - Internal sphincter only
 - " + intersphincteric plane
 - " + external sphincter
- } upper middle distal 1/3 of anal canal

Mesorectal fascia (and peritoneal) involvement

- Shortest distance between tumour and MRF: mm → free (> 2 mm)
- threatened/involved (≤2 mm)
- Location of the shortest distance between tumour and MRF: o'clock
- Relation to anterior peritoneal reflection: below (MRF invasion) above

Lymph nodes and tumour deposits

- Lymph nodes yN0 = no remaining nodes or only nodes < 5 mm
- yN+, = presence of any nodes with a short axis diameter ≥ 5 mm
- Number of residual suspicious (≥ 5 mm) mesorectal lymph nodes:
- Number of residual suspicious (≥ 5 mm) extramesorectal lymph nodes:
- Are there any remaining tumour deposits within the mesorectum: no
- yes, (number of deposits)

Extramural vascular invasion

- Yes No

Paciento apklausos forma magnetinio rezonanso tomografijai atlikti

PATVIRTINTA
Kauno klinikų generalinio direktoriaus
2014 m. vasario 25 d. įsakymu Nr. V-192
Priedas Nr. 7

**PACIENTO APKLAUSOS FORMA
MAGNETINIO REZONANSO TOMOGRAFIJAI ATLIKTI**

Pacientas _____ Gimimo data _____ Svoris _____ Ūgis _____
(Vardas, Pavardė)

Ar Jūsų kūne yra kuris nors iš žemiau išvardytų prietaisų, protezų ar svetimkūnių?	TAIP	NE
Širdies stimulatorius ar poodinis širdies defibriliatorius		
Smegenų kraujagyslių kabutės ir metalinės plokštelės po neurochirurginės operacijos, smegenų skysčio drenas		
Dirbtiniai širdies vožtuvai		
Kraujagyslių implantai (stentai, filtrai, kateteriai)		
Elektroniniai ar mechaniniai implantai (neurostimulatorius, vaistų pompa – ne intraveninis kateteris)		
Metalinės kabutės kitose kūno vietose		
Kitoks stimulatorius		
Akių, ausų implantai		
Sąnarių, galūnių protezai, kaulų fiksatoriai		
Dantų protezai ar „sidabro“ plombos, metalo keramikos karūnėlės, breketai, kabės		
Kitokie, aukščiau nepaminėti protezai		
Metaliniai implantai naudojami kaulų lūžiams gydyti		
Metaliniai implantai po stuburo operacijos		
Buitiniai metalo svetimkūniai (kulkos, metalinės atplaišos ir skeveldros)		
Bet koks kitas aukščiau nepaminėtas elektroninis, mechaninis ar magnetinis implantatas, protezas		
Medicininiai pleistai		
Tatuiruotės, permanentinis (ilgalaikis) makiažas		
Ar jūs naudojate:	TAIP	NE
Klausos aparatą		
Akių kontaktinius lęšius		
Insulino, morfijaus ar kitų vaistų pompą (ne intraveninis kateteris)		

Bendri klausimai:	TAIP	NE
Ar jums kada buvo atlikta neurochirurginė operacija?		
Ar jums kada nors buvo atlikta laparoskopinė (neatveriant pilvo ertmės) operacija?		
Ar jums kada nors buvo metalinėmis skeveldromis sužeistos akys?		
Ar bijote uždarytų patalpų?		
Ar sate jautrus(i) vaistams ar kontrastinėms medžiagoms?		
Ar sergate bronchine astma, alerginėmis ligomis, epilepsija, inkstų ligomis ar cukriniu diabetu?		
(Tik moterims) Spiratė		
(Tik moterims) Ar jūs esate nėščia arba manote esanti nėščia?		
(Tik moterims) Ar jūs maitinate kūdikį?		

Aš perskaičiau ir suprata visa anketos tekstą. Tvirtinu, kad visus aukščiau pateiktus klausimus atsakiau teisingai ir kiek galima tiksliau.

Paciento (jo atstovo) parašas _____

Data _____

CURRICULUM VITAE

Name, Surname: Ingrida Pikūnienė
Address: Department of Radiology, Hospital of Lithuanian University of Health Sciences Kauno klinikos. Eivenių 2, LT-50009 Kaunas, Lithuania
E-mail: ingrida.pikuniene@lsmu.lt

Workplace:
from 2011 till present Radiologist, Department of Radiology, Hospital of Lithuanian University of Health Sciences Kauno klinikos

Education:
August 2015 – October 2023 PhD Student, Lithuanian University of Health Sciences
September 2010 – June 2015 Medical Resident Officer, Hospital of Lithuanian University of Health Sciences Kauno klinikos
September 2004 – June 2010 Kaunas University of Medicine, Lithuania
Master Degree in Medicine

Membership at professional societies:
Lithuanian Radiologists' Association
Kaunas Region Radiologists' Association
European Society of Radiology
European Society of Gastrointestinal and Abdominal Radiology

PADĖKA

Pirmiausiai noriu padėkoti disertacinio darbo vadovui prof. dr. Žilvinui Saladžinskui už darbo idėją ir pagalbą pradiniam etape.

Labai dėkoju doc. dr. Vestinai Strakšytei už suteiktus vertingus patarimus, visapusišką pagalbą bei rūpestį rengiant publikacijas ir disertaciją.

Nuoširdus Ačiū prof. dr. Algidui Basevičiui už patarimus rengiant publikacijas, už palaikymą ir supratingumą.

Noriu išreikšti dėkingumą gyd. Ritai Ambrazienei, kartu einančiai bendros studijos keliu ir besidalinančiai aktualia informacija, taip pat prof. dr. Rasai Jančiauskienei įtraukusiai mane į studiją.

Dėkoju savo pirmoms mokytojoms doc. dr. Irinai Gineikienei ir prof. dr. Kristinai Žvinienei už žinias, pritaikytas šio mokslo kelyje bei paramą nelengvose gyvenimiškose situacijose.

Nuoširdžiai dėkoju savo vyrui Gintarui, vaikams Justinui ir Laurynui, už palaikymą, supratimą ir kantrybę disertacijos rašymo periodu.

Taip pat didžiausią Ačiū siunčiu savo mamytei Laimai, už jos tikėjimą manimi, kuris suteikė motyvacijos įveikti šį neįkainojamos patirties kupiną etapą.

Dėkoju visiems asmeniškai neįvardintiems, už palaikymą ir padrąšinimus per visą doktorantūros kelionę.